Київський національний університет технологій та дизайну

ТЕХНОЛОГІЇ ТА ІНЖИНІРИНГ

Науковий журнал

Том 26, № 3, 2025

Київ
2025

ISSN 2786-5371
e-ISSN 2786-538X

Засновник журналу:
Київський національний університет технологій та дизайну

Рік заснування: 1999 р.

Періодичність випуску: 6 разів на рік

*Рекомендовано до друку та поширення
через мережу Інтернет Вченою Радою
Київського національного університету технологій та дизайну
(протокол № 4 від 25 червня 2025 р.)*

Державна реєстрація:
Ідентифікатор медіа: R30-05423
Рішення Національної ради України з питань телебачення і радіомовлення № 2520,
протокол № 22 від 8 серпня 2024 року

Журнал внесено до категорії «Б» Переліку наукових фахових видань України,
відповідно до якого можуть публікуватися результати дисертаційних робіт на здобуття наукових ступенів доктора та кандидата наук зі спеціальностей:
технічні (наказ Міністерства освіти і науки України № 735 від 29 червня 2021 р.):
122 – Комп'ютерні науки, 131 – Прикладна механіка, 133 – Галузеве машинобудування,
151 – Автоматизація та комп'ютерно-інтегровані технології, 161 – Хімічні технології та інженерія,
132 – Матеріалознавство, 182 – Технології легкої промисловості, 141 – Електроенергетика,
електротехніка та електромеханіка, 144 – Теплоенергетика, 171 – Електроніка.

Журнал представлено у міжнародних наукометричних базах даних,
репозитаріях та пошукових системах: Національна бібліотека України імені В. І. Вернадського,
Crossref, Google Scholar, Litmaps, OUCI, Фахові видання України, EBSCO, Dimensions, UCSB Library,
University of Oslo Library, University of Hull Library, BASE, Ulrichsweb Global Serials Directory

Адреса редакції:
Київський національний університет технологій та дизайну
01011, вул. Мала Шияновська, 2, м. Київ, Україна
тел/факс: +38 (044) 256-84-27
E-mail: info@technologies-engineering.com.ua
https://technologies-engineering.com.ua/uk

Kyiv National University of Technologies and Design

TECHNOLOGIES AND ENGINEERING

Scientific Journal

Vol. 26, No. 3, 2025

Kyiv
2025

ISSN 2786-5371
e-ISSN 2786-538X

Founder:
Kyiv National University of Technologies and Design

Year of foundation: 1999

Frequency: 6 issues per year

*Recommended for printing and distribution
via the Internet by the Academic Council
of Kyiv National University of Technologies and Design
(Minutes No. 4 June 25, 2025)*

State registration:
Media identifier: R30-05423
Decision of the National Council of Television and Radio Broadcasting of Ukraine No. 2520,
Minutes No. 22 dated 08.08.2024

The journal is included in category "B" of the List of scientific professional publications of Ukraine, in which the results of dissertations for the degree of doctor and candidate of sciences can be published in the following specialties: technical (Order of the Ministry of Education and Science of Ukraine No. 735 dated 29.06.2021): 0612 – Database and network design and administration, 0715 – Mechanics and metal trades, 0714 – Electronics and automation, 0711 – Chemical engineering and processes, 0588 – Inter-disciplinary programmes and qualifications involving engineering, manufacturing and construction, 0723 – Textiles (clothes, footwear and leather), 0713 – Electricity and energy, 0714 – Electronics and automation

The journal is presented in the international scientometric databases, repositories and scientific systems: Vernadsky National Library of Ukraine, Crossref, Google Scholar, Litmaps, OUCI, Professional Publications of Ukraine, EBSCO, Dimensions, UCSB Library, University of Oslo Library, University of Hull Library, BASE, Ulrichsweb Global Serials Directory

Editors office address:

Kyiv National University of Technologies and Design
01011, 2 Mala Shyianovska Str., Kyiv, Ukraine
tel/fax: +38 (044) 256-84-27
E-mail: info@technologies-engineering.com.ua
https://technologies-engineering.com.ua/en

Редакційна колегія

Редакційна колегія

Editorial Board

Editorial Board

ЗМІСТ

CONTENTS

TECHNOLOGIES AND ENGINEERING

Journal homepage: https://technologies-engineering.com.ua/en
Vol. 26, No. 3, 2025

Received: 03.02.2025
Revised: 21.05.2025
Accepted: 25.06.2025

UDC 621.372.8:004.7

DOI: 10.30857/2786-5371.2025.3.1

Ultra-wideband transmission lines for next-generation digital systems: Modelling and analysis

Serhii Boichenko*

Postgraduate Student
Kharkiv National University of Radio Electronics
61000, 14 Nauky Ave., Kharkiv, Ukraine
https://orcid.org/0009-0008-6118-8314

Abstract. The study aimed to theoretically analyse the modelling of pulse transmission in ultra-wide bandwidth media with consideration of losses, dispersion and phase shifts. A comprehensive approach was used, combining mathematical modelling and analysis of electromagnetic processes in various transmission line topologies, such as coaxial, stripline, microstrip, and structures based on metamaterials and superconductors. The study determined that the dispersion, frequency-dependent losses caused by the surface resistance, which increased proportionally to the root of the frequency, and dielectric losses with a frequency-dependent tangent caused distortion of pulses with delays of 10-100 picoseconds and phase shifts of up to 20 degrees. For pulses with a duration of 0.5 nanoseconds, the spectral width was about 2 GHz, which confirmed the dependence between the pulse duration and the frequency range. Modelling using the telegraphic equations, the Fourier transform and numerical methods such as finite difference time domain and finite element analysis quantified losses of up to 3-6 decibels per 10 cm and the critical line length, which depended on geometric inhomogeneities. The advantages of superconducting structures with losses of less than 0.01 decibels per metre up to 100 GHz and coplanar lines for transmission speeds of 25-50 Gbps were revealed. The frequency-dependent performance criteria were formulated for a reasonable choice of the line type depending on the requirements for minimising phase shifts and pulse attenuation. The practical significance of the results is determined by the possibility of their use by specialists in the design of telecommunications and sensor systems to improve the reliability and accuracy of data transmission in real-world conditions

Keywords: dispersion; surface resistance; pulse signal; frequency-dependent losses; metamaterials; superconductors; phase stability

Introduction

The development of digital technologies in the 21st century, including 5G and 6G communication systems, high-speed networks, and an increase in the amount of data transmitted, necessitates fundamentally new solutions in the field of signal transmission lines. One of the most promising areas is Ultra-Wideband Transmission Line (UWB-TL), which provides high bandwidth, low power consumption and the ability to operate in conditions of strong spectral noise. Their implementation is important for applications such as wireless power transmission, ultrafast data communications, microwave photonics, high-precision positioning systems and edge computing. In the scientific literature, there is an increasing interest in research on modelling UWB systems. They focus on solutions that can adapt to changing environmental conditions and minimise losses. At the level of system architecture, attention is focused on the impact of antenna configuration and combining networks on the efficiency of power transmission.

In the context of a wide frequency range, it is worth citing the study by S. Roy *et al.* (2023), which demonstrated that phased array antennas provide higher resistance to spectral interference compared to traditional combining networks, indicating their suitability for conditions with variable radio-frequency (RF) characteristics. The obtained results demonstrated the relevance of using UWB components in environments with a high level of RF disturbances.

Suggested Citation:
Boichenko, S. (2025). Ultra-wideband transmission lines for next-generation digital systems: Modelling and analysis. *Technologies and Engineering,* 26(3), 11-23. doi: 10.30857/2786-5371.2025.3.1.

*Corresponding author

A separate area is the miniaturisation of components while maintaining effective alignment. The study by S.-Z. Liu *et al.* (2025) presented a ferrite circulator optimised for UWB operation. The authors showed that the appropriate selection of materials and geometric parameters can achieve compactness while maintaining key performance characteristics, which is important for the integration of such components into multifunctional digital platforms. Improving the efficiency of impedance matching in UWB structures is also associated with the development of compact filters capable of operating in a wide frequency range with high selectivity. A. Kayalvizhi *et al.* (2025) considered the design of a bandpass filter based on an open loop with a discontinuity intended for use in wireless devices. Numerical modelling and verification of the layout were conducted to establish the stability of transmission characteristics in the ultra-wideband mode, with effective impedance matching and low losses within a given frequency band. The proposed circuitry solution provided the necessary conditions for the functioning of components in digital systems operating in a wide frequency range.

The development of switching structures has formed a separate branch of research. A. Fisher *et al.* (2025) demonstrated the potential of using silicon plasma as an active element of an ultrafast switch with low losses. This approach has opened new perspectives for building adaptive paths in UWB systems, where switching time and stability of signal parameters are of key importance. Regarding physical transitions between line types, for example, from coplanar to microstrip, the study by G.H. Lee *et al.* (2021) is notable. The study proposed compact transitions from coplanar lines to microstrip lines using a curved structure on a two-layer substrate. These transitions provide high efficiency in a wide frequency range from 2 to 17 GHz and minimal transition losses of up to 2 dB. Good performance has been demonstrated, making them useful for high-density microelectronic component applications where compactness and precise parameter matching are important. This confirmed the importance of developing efficient solutions for UWB links in high-speed digital paths. Digital distortion compensation is another critical area that is also gaining importance. The deep Sequence-to-Sequence neural architectures for modelling fibre-optic media presented by M. Shi *et al.* (2025) have a high level of dispersion and nonlinearities. Despite the different physical nature of the systems, their analytical principles and results demonstrate high relevance to UWB environments. The study proved that digital signal processing based on artificial intelligence can significantly improve transmission accuracy even in difficult conditions.

Ukraine is also developing ultra-wideband technologies in applied and fundamental research, in particular, the development and improvement of antennas, transmission lines and pulsed UWB systems. The modelling and analysis of broadband transceiver structures is also being addressed with increasing intensity. D.O. Batrakov *et al.* (2024) proposed a system for detecting subsurface cracks in non-rigid pavement using ultra-wideband GPR. The use of two receiving antennas with orthogonal polarisation made it possible to record cross-polarisation components of the signal. Experimental studies conducted on motorways in Ukraine have confirmed the effectiveness of the approach in a complex environment. The work is an example of the use of UWB transmission lines in a complex heterogeneous environment, which is of high practical importance.

Additionally, F.F. Dubrovka *et al.* (2023) presented the development of an ultra-compact biconical antenna for unmanned aerial vehicles with support for various types of polarisations (circular, horizontal, vertical and tilted). The antenna was modelled, fabricated and measured in the range of 2-18 GHz. The revealed effect of multiple resonant reflections was used to analyse the influence of geometry on the voltage standing wave ratio and gain, which is important for the development of UWB technologies in avionics. Pulsed UWB signals received by a ferrite antenna with a two-turn helix were analysed in the time and energy domains using Finite-Difference Time-Domain (FDTD) modelling in T. Ogurtsova *et al.* (2023). The results showed the dependence of the signal characteristics on the load and geometry, which highlighted the theoretical aspects of modelling UWB lines in receiving systems.

Despite a significant number of theoretical and applied developments in UWB-TL modelling, an integrated approach to considering electromagnetic, thermal and nonlinear effects used in chips and adapting numerical methods (moments, FDTD) for the complex geometry of ultrawideband structures remains insufficiently developed. Therefore, the study aimed to theoretically substantiate the principles of modelling and analysing the processes of pulse signal transmission in ultra-wideband lines to ensure their efficiency in digital systems, considering dispersion, frequency-dependent losses and phase stability. To achieve this goal, the following objectives were set: to systematise the physical mechanisms of pulse signal distortion in UWB-TL, to analyse mathematical models of UWB signal transmission lines, to conduct a comparative analysis of typical transmission line configurations, and to formulate recommendations for selecting and optimising UWB lines for phase stability and loss minimisation.

Materials and Methods

The study involved a theoretical modelling and analysis of the processes of pulse signal transmission via UWB-TL, combining theoretical, numerical and analytical methods for modelling dispersion, losses and nonlinear effects in UWB transmission lines. The choice of methods was based on their ability to reflect the diverse line structures and practical applications in 21st-century technologies. Seven types of UWB transmission lines were selected for analysis: coaxial, stripline, microstrip, Coplanar Stripline (CPS), Coplanar Waveguide (CPW), metamaterial and superconducting structures. Their choice was based on a wide range of technical characteristics and application scenarios in broadband transmission technologies. The selected configurations are discussed in terms of their electromagnetic properties, limitations, and typical applications.

In addition, standardised numerical modelling methods and mathematical models were used to analyse and evaluate the behaviour of transmission lines under real operational loads. To quantitatively described electromagnetic processes, the RLGC-line model (a generalised representation of the distributed longitudinal distributed parameters of a transmission line that describes electromagnetic processes in telegraphic equations) was used. It is characterised by four parameters per unit length: R – ohmic resistance of conductors, which takes into account conduction losses, in particular the surface effect in the UWB mode, L – inductance, which models the accumulation of magnetic field energy around conductors, G – conductivity between conductors, which describes losses in the dielectric, C – capacitance between conductors, which determines the accumulation of electric field energy), which described transmission lines as a linear system with distributed parameters (1, 2):

$$\frac{\partial V(x,t)}{\partial x} = -L\frac{\partial I(x,t)}{\partial t} - RI(x,t), \tag{1}$$

$$\frac{\partial I(x,t)}{\partial x} = -C\frac{\partial V(x,t)}{\partial t} - GV(x,t), \tag{2}$$

where V(x,t) – voltage at point x at time t; I(x,t) – current at point x at time t. These equations define the transmission function of a transmission line as a function of frequency H(f), incorporating Z_0(f) and α(f).

The losses in conductive materials during signal propagation were described through the surface resistance, which depends on the frequency (3):

$$R_s(f) = \sqrt{\frac{\pi f \mu_O \rho}{2}}, \tag{3}$$

where f – frequency of the electromagnetic signal; – magnetic permeability of the vacuum (physical constant established by the International System of Units $4\pi \times 10^{-7}$.

Any pulse signal x(t) can be represented as a direct Fourier transform (4) (Oppenheim *et al.*, 1997):

$$X(f) = \int_{-\infty}^{\infty} x(t)e^{-j2\pi ft}dt, \tag{4}$$

where X(f) – complex spectral amplitude of the signal at frequency f determines the frequency component of the signal x(t) in the form of a complex number containing both amplitude and phase information; $\int_{-\infty}^{\infty}$ – an integral over the entire time domain, which provides full coverage of the signal (this means that the analysis was performed considering all time points from minus to plus infinity); $e^{-j2\pi ft}$ – the original signal in the time domain that is subject to spectral analysis (this is a real- or complex-time function that describes the signal amplitude at each time point t, dt – a complex exponent that acts as the base transformation function. In this case, $e^{-j2\pi ft}$ – an analyser function that "extracts" the frequency component f from the signal x(t), j – imaginary unit (j^2=-1 is used in engineering instead of i to avoid confusion with electric current), 2πft – phase shift that depends on time and frequency, dt – differential of the integration variable t, indicating that integration was performed on the time variable.

Given a known frequency response of the transmission line H(f), the spectrum of the signal after passing through the line is (5):

$$Y(f) = H(f) \cdot X(f). \tag{5}$$

This corresponds to the convolution of the signal with the impulse response of the line in the time domain. The inverse Fourier transform restores the signal in the time domain (6):

$$y(t) = \int_{-\infty}^{\infty} Y(f)e^{j2\pi ft}df, \tag{6}$$

where y(t) – restored signal in the time domain; Y(f) – spectral function obtained as a result of the direct Fourier transform; df – frequency differential that defines the integration variable in the spectral domain.

In applied engineering problems, the analytical Fourier transform is implemented in a discrete form. For this purpose, a discrete Fourier transform is used, which grounds calculations based on a finite number of signal samples (7):

$$X[k] = \sum_{n=0}^{N-1} x[n] \cdot e^{-j\frac{2\pi kn}{N}}, \tag{7}$$

where X[k] – complex spectral value at the kth harmonic; x[n] – signal value in the time domain at the nth discrete step; $e^{-j\frac{2\pi kn}{N}}$ – basic exponential function corresponding to the kkkth harmonic; k – frequency index (from 0 to N-1); N – total number of points or samples (signal length). This transformation converts the signal from the time domain to the frequency domain, where each X[k] represents the amplitude and phase of the corresponding frequency component.

The inverse Fourier transform (8) (Küpfmüller, 1928) is used to recover the signal from its spectrum:

$$x[n] = \frac{1}{N}\sum_{k=)}^{N-1} X[k] \cdot e^{-j\frac{2\pi kn}{N}}, \tag{8}$$

where x[n] – restored signal value in the time domain at a discrete step nnn; $\frac{1}{N}$ – normalisation factor that ensures the preservation of signal energy when moving from the frequency domain back to the time domain.

Based on the literature data by M.-J. Kim *et al.* (2024), B.-C. Min *et al.* (2024) and Y. Weng *et al.* (2025) summarised UWB-TL modelling methods by their implementation and examples of application in real systems. To analyse the behaviour of UWB transmission lines in real conditions, numerical methods, such as FDTD and finite element method (FEM), system identification methods were considered to more accurately assess the behaviour of lines in real conditions. This approach optimised the UWB-TL parameters to minimise losses and distortion in a wide frequency range. Additionally, the parameters that affect the distortion of pulse signals in UWB transmission lines were investigated: time delay of the edge, maximum amplitude offset, integrated loss energy, optimisation of transmission line design, loss and distortion analysis, and sensitivity to transmission line topology. The parameters were evaluated concerning real-world conditions and applied to numerical models to analyse and optimise transmission line performance, ensuring minimal pulse distortion in UWB systems.

The types of UWB transmission lines and their applications in electronic systems of the Internet of Things (IoT) and Wireless Body Area Network (WBAN), ultrafast digital interfaces, 5G/6G systems, superconducting and MicroElectroMechanical Systems (MEMS) technologies, sensitivity to geometry and operating conditions are analysed to describe in detail the technical parameters of UWB-TL, assess their effectiveness in real applications and compare different transmission line designs for applications in various electronic and telecommunication systems. The choice of UWB transmission line types was made based on their ability to meet the specific requirements of different systems: for IoT and WBAN, accuracy and resistance to fluctuations are important, for 5G/6G, transmission speed and low losses, for superconducting technologies, minimal losses and phase stability. Based on the analysis of the results, practical recommendations were formulated for the further development of UWB-TL technologies.

The Zotero bibliographic manager was used to process the literature sources, which ensured the systematisation of scientific publications and their thematic classification. For the theoretical analysis of the electromagnetic characteristics of UWB-TL, the Ansys High-Frequency Structure Simulator (HFSS) software was used to assess the influence of frequency-dependent parameters and geometric characteristics on the behaviour of signals in various UWB-TL structures. Ansys HFSS was chosen because of its ability to accurately simulate electromagnetic processes in broadband systems, which estimated the frequency-dependent loss, dispersion, and phase stability of UWB-TL.

Results and Discussion

The term UWB-TL refers to structures that provide stable electromagnetic signal transmission over a wide frequency range. UWB systems cover a frequency band of more than 500 MHz or at least 20% of the centre frequency. In the context of transmission lines, this means the ability to provide a uniform transmission characteristic (in particular, in phase and amplitude) over the frequency range required to transmit pulses on a nanosecond or picosecond scale. Such structures include coaxial, strip, microstrip, and metamaterial-based topologies and MEMS technologies. UWB-TLs are widely used in digital signal processing systems, wireless data transmission, pulse radar, and IoT devices (Kim *et al.*, 2024). A classical digital pulse is a time-limited signal containing a set of harmonic components in its spectral structure. According to the Fourier uncertainty principle, the shorter the pulse in the time domain, the wider the spectrum of its frequency representation (Küpfmüller, 1928). This is quantitatively expressed as (9):

$$\Delta f \geq \frac{1}{t}, \tag{9}$$

where Δf – spectrum width (working frequency band); t – spectrum width (working frequency band); effective pulse duration.

For pulses with a duration of 0.5 ns, a frequency band of approximately 2 GHz is typical. In such conditions, traditional transmission lines become unsuitable due to increased losses, dispersion and nonlinear effects. In broadband conductive media, the electromagnetic wave undergoes significant deformation due to dispersion and loss effects. Dispersion causes different phase and group velocities for individual spectral components of the signal, which leads to a distortion of its time form. Frequency-dependent losses, mainly caused by an increase in the surface resistance of conductors $R_s \sim \sqrt{f}$ and dielectric losses in insulating materials, further degrade signal integrity. Spatial inhomogeneities in the medium cause partial reflections and variations in group delay, which also affect the quality of pulse transmission. Even with a relatively short transmission line length (10-20 cm), a picosecond pulse is subject to significant distortion (Oppenheim *et al.*, 1997). Therefore, modelling such distortions and taking them into account at the design stage is critical to ensure reliable transmission of ultra-wideband signals. Transmission of pulses with an ultra-wide spectrum requires the use of transmission line structures that provide minimal losses, stable phase and amplitude response over a wide frequency range. Classical solutions include coaxial, stripline, and planar lines, but modern technologies also use metamaterial and superconducting approaches (Table 1).

Table 1. *Classification of transmission lines by the principle of implementation and area of use*

Structure type	Characteristics and features	Application examples
Coaxial lines	Symmetrical design with a central conductor and shield to minimise electromagnetic radiation and sensitivity to external disturbances. Provide stable wave impedance ($Z_0(f)$) in the range up to 20-30 GHz due to the choice of dielectric (e.g., silicon substrates) and precise conductor design. Limitations: high production costs for ultra-high frequencies.	MEMS-based coaxial line array for IoT devices with broadband signal transmission.
Strip lines	A planar structure with a conductor between two grounded layers, which enables high integration with digital and RF components. Supports frequencies up to 10 GHz and above, but is sensitive to dielectric substrate inhomogeneities that cause phase distortion and loss.	Vertical junctions in stripline structures for ultra-high-speed digital interfaces.
Microstrip lines	Conductor on a dielectric substrate with a ground at the bottom for easy manufacturing and compatibility with multilayer boards. Sensitive to dielectric losses and surface resistance ($R_s \sim \sqrt{f}$), which limits their effectiveness at frequencies above 15 GHz.	Filters with defective ground structure for mm-waves in multilayer boards.

Table 1. Continued

Structure type	Characteristics and features	Application examples
CPS	Two parallel conductors on a single dielectric layer, providing high integration with planar circuits and low losses at frequencies up to 10 GHz. Supports autonomous phase balancing, but requires precise geometry control to minimise parasitic effects.	CPS structures in data transmission systems with autonomous phase balancing.
CPW	A central conductor with grounded planes on each side on a single layer, combining the advantages of microstripes (simplicity) and symmetrical lines (broadband). Provides effective adaptation to planar antennas at frequencies up to 20 GHz, but is sensitive to substrate inhomogeneities.	UWB antennas for high-bandwidth wireless networks.
Metamaterials	Structures with non-standard electromagnetic properties (e.g. negative dielectric constant) that enable miniaturisation and bandwidth expansion up to 30 GHz and beyond. Require complex design and precision manufacturing.	Metasurface UWB antennas for WBAN with improved gain and bandwidth.
Superconducting structures	Superconducting materials are used to reduce surface resistance $R_s(f)$, providing almost zero losses up to 100 GHz. Provide high efficiency but require cryogenic cooling, which complicates practical application.	Magic-T structure for mm/submm cameras in the 6-14 GHz range, pulsed sensor systems and quantum electronics.

Source: *compiled by the author based on M.-J. Kim et al. (2024), B.-C. Min et al. (2024), Y. Zhu et al. (2024), S. Inoue et al. (2024), Y. Weng et al. (2025), X. Li et al. (2025)*

UWB-TL is represented by a variety of structures, each of which has specific characteristics that determine its application in high-speed systems. Coaxial lines provide stability and minimal loss at high frequencies but are expensive to manufacture. Planar structures, such as stripline, microstrip, CPS and CPW, are easy to integrate with digital and RF components, but their performance is limited by their sensitivity to inhomogeneities and dielectric losses. Metamaterials open opportunities for miniaturisation and bandwidth expansion, while superconducting structures provide minimal losses in the millimetre range but require sophisticated cryogenic support. Superconducting materials can significantly reduce the surface resistance, which, accordingly, minimises power losses during the propagation of high-frequency pulses. In such structures, the impedance becomes complex (10):

$$Z_s(f) = R_s(f) + jX_s(f), \tag{10}$$

where $R_s(f)$ – frequency-dependent active (ohmic) resistance, which is mainly due to the surface current effect (surface effect); $X_s(f)$ – the reactive component, which describes the inductive properties of the surface layer. The choice of a specific structure depends on frequency range requirements, technological integration, and economic feasibility, which underlines the importance of further research to optimise UWB-TL in modern telecommunications systems. For the quantitative description and modelling of broadband transmission lines, the following frequency-dependent functions are used as the basis for modelling pulse distortion. $Z_O(f)$ – wave (characteristic) impedance; $\alpha(f)$ – attenuation coefficient, including losses in the conductor and dielectric; $\beta(f)$ – phase constant (rad/m) associated with group delay; $R_s(f)$ – surface resistance of the conductor, which increases with frequency as $\sqrt{f}$.

Effective UWB-TL design requires the use of mathematical models capable of adequately describing both the frequency and time behaviour of signals during their propagation in an electromagnetic medium. The main task of such modelling is to quantify the changes in the pulse signal caused by the combined effect of losses, dispersion phenomena and distortions caused by the geometry of the conductive structure, electrophysical properties of materials, as well as boundary conditions that form the configuration of the transmission line. The RLGC line model describes transmission lines as a linear system with distributed parameters (formula 1-2). Losses in conductive materials during signal propagation are described through the surface impedance, which depends on the frequency (formula 3). The dependence $R_s(f) \propto \sqrt{f}$ means that high-frequency components of the signal suffer greater losses than low-frequency components. This leads to an uneven attenuation of the pulse spectrum to a decrease in the amplitude of peak values, blurring of signal edges, and asymmetry in the pulse waveform after passing the transmission line. Such effects are critical in UWB-TL systems, where time distortion directly affects the localisation accuracy or data reception quality. To compensate for them, loss modelling is required at the transmission line design stage.

Any impulse signal x(t) can be represented as a direct Fourier transform (formula 4). According to Fourier's theorem, any limited signal can be represented as a combination of such exponents. Given a known frequency response of the transmission line H(f), the spectrum of the signal after passing through the line is determined by the formula (formula 5): This corresponds to the convolution of the signal with the impulse response of the line in the time domain. The inverse Fourier transform restores the signal in the time domain (formula 6): In applied engineering problems, the analytical Fourier transform is implemented in a discrete form. For this purpose, a discrete Fourier transform is used, which grounds calculations based on a finite number of signal samples (formula 7). This transformation converts the signal from the time domain to the frequency domain, where each X[k] represents the amplitude and phase of the corresponding frequency component. To restore the signal from its spectrum, the inverse Fourier transform is used (formula 8).

The forward and inverse Fourier transform, as well as their discrete implementation, are fundamental tools for analysing and modelling signals in ultra-wideband transmission lines. These methods were used to accurately describe the change in the spectral structure of the signal during its propagation and calculate the impulse response of the line in terms of real losses and dispersion. Table 2 showed examples of UWB-TL modelling methods used to optimise pulse transmission, minimise losses and preserve signal integrity in high-frequency digital paths and wireless interfaces.

Table 2. *Real-world examples of UWB-TL modelling methods*

Method	Implementation
RLGC model	The RLGC model is used to simulate stripline vertical transitions in high-speed digital interfaces (up to 10 GHz). The R, L, G, C parameters are used to analyse the loss through and dielectric losses, which can be used for optimising transitions to reduce phase distortion and preserve the integrity of picosecond pulses.
Frequency-dependent parameters (Z_0(f), α(f))	They are used for designing mm-wave multilayer UWB filters with a defective ground structure. The simulation addresses frequency-dependent losses in microstrip lines caused by and the dielectric, providing stable signal filtering in the 30-40 GHz range for telecommunications systems.
Phase constant β(f)	Used to analyse CPS structures in high-speed digital transmission systems. Phase stability modelling compensates for the dispersion that occurs when transmitting picosecond pulses, providing accurate phase balancing for frequencies up to 10 GHz in digital circuits.
Surface resistance Rs(f)	Modelled for MEMS-based coaxial lines in IoT devices. Surface impedance loss analysis enables optimised array design for broadband signal transmission (up to 20 GHz), reducing pulse asymmetry and increasing data transmission efficiency.
Fourier transformation	Used to analyse the spectral and temporal behaviour of UWB signals in wireless networks. The forward and inverse transforms are used to estimate the impulse response, which can be used for predicting signal distortion due to dispersion and losses in real communication channels (up to 15 GHz).

Source: *compiled by the author based on M.-J. Kim et al. (2024), B.-C. Min et al. (2024), Y. Zhu et al. (2024), Y. Weng et al. (2025), P. Poggiolini & Y. Jiang (2025)*

The results of the study confirmed the feasibility of using the RLGC model with consideration of frequency-dependent parameters and the phase constant to analyse the impulse distortion in UWB-TL. This is consistent with a study by Y. Zhang *et al.* (2023), which developed a method for broadband extraction of RLGC parameters for multi-conductor lines using an advanced mode tracking algorithm. The proposed solution ensured high accuracy in determining the frequency-dependent values of resistance, inductance, conductivity, and capacitance (R, L, G, C) in a wide frequency range, which is important for high-frequency modelling.

The evaluation of the influence of frequency-dependent characteristics, such as impedance Z_0(f) and attenuation α(f), on the efficiency of pulse transmission in a high-frequency environment is confirmed by the work of M.-J. Kim *et al*. (2024). The authors implemented an ultra-wideband vertical transition in a coplanar ribbon line for next-generation digital interfaces with an operating range of up to 110 GHz. Although the technical implementation is different from the approaches used in the current study, both approaches emphasise modelling the behaviour of the transmission medium concerning frequency-dependent losses and impedance parameters. In both studies, the line characteristics are matched, which is critical for reducing dispersion-induced phase distortion and ensuring reliable reproduction of the pulse waveform.

K. Mao *et al*. (2022) proposed a new methodology for modelling broadband channels using a continuous frequency response and inverse/direct Fourier transform. As part of this work, the time structure of signals up to 15 GHz was studied, and the characteristic forms of impulse distortion in real conditions were established. The generalised conclusions showed the effectiveness of using frequency analysis to reproduce the dynamics of pulse signals, which corresponded to the results of this study on modelling UWB transmission lines. In the process of modelling UWB transmission lines and antenna structures in the context of WBAN systems, numerical and experimental methods are used. Table 3 provided a comparative overview of common modelling methods, their characteristics, and applications in the field of ultra-wideband technologies.

Table 3. *Methods of modelling UWB transmission lines and their parameters*

Method	Characteristic	Application examples
FDTD	Numerical method for simulating the spatial and temporal evolution of electromagnetic waves in real time. Uses space and time discretisation to solve Maxwell's equations, effective for broadband signals and complex structures.	Modelling of UWB antennas (e.g., Vivaldi) to analyse the propagation of pulsed signals in the range of 3-10 GHz, incorporating dispersion and losses.
FEM	A method for analysing complex geometries and heterogeneous media by breaking down the structure into finite elements. Suitable for modelling UWB structures with irregular shapes,such as metamaterials.	Designing metasurface UWB antennas for WBAN, considering complex metamaterial geometries and dielectric properties for up to 30 GHz.
System identification	Based on experimental impulse or frequency responses to create models of system behaviour. Used to predict signal distortion in real-world conditions	Analysis of the impulse response of UWB wireless network systems to estimate distortions due to dispersion and losses in communication channels (up to 15 GHz).

Source: *compiled by the author based on S.M. Kameli et al. (2024), X. Li et al. (2025), P. Poggiolini & Y. Jiang (2025)*

The FDTD method is effective for modelling the spatial and temporal propagation of signals in complex environments. FEM provides high accuracy when analysing structures with complex geometries, such as metasurface antennas. System identification methods, in turn, describe the behaviour of real systems based on empirical data. The choice of a particular approach depends on the problem formulation, accuracy requirements, and the availability of experimental information. In UWB-TL, the shape of a pulse signal changes due to the nonlinear interaction of its spectral components with the amplitude-phase response of the transmission line. This process can be described as a convolution of the signal spectrum with the frequency response of the transmission line, which leads to distortions in the time waveform. Quantifying such distortions is critical to ensure accurate transmission of short-term pulses in high-bandwidth systems such as wireless networks, IoT devices, or high-speed digital interfaces (Min *et al.*, 2024).

The main parameters that characterise pulse distortion include the time delay of the front and back pulse expansion fronts in the time domain caused by dispersion and frequency-dependent losses α(f). This phenomenon reduces the synchronisation accuracy in UWB systems, which is especially critical for picosecond pulses, the shift of the maximum amplitude of the pulse amplitude peak relative to its initial position due to the uneven phase response β(f) of the transmission line, integral energy loss is the total loss of pulse energy caused by frequency-dependent attenuation (α(f)) due to $R_s(f)\propto\sqrt{f}$ and dielectric losses and dielectric losses. This reduces the signal amplitude, making it difficult to detect. To ensure minimal distortion of pulse signals, it is necessary to optimise the design of the transmission line, its geometry, materials and length. One of the criteria is to limit the length of the transmission line, which should not exceed the critical distortion length, the maximum distance at which dispersion and losses do not lead to significant changes in the pulse shape. This length depends on the frequency range of the signal, the parameters of the RLGC model (R, L, G, C) and the electrophysical properties of the medium. In microstrip lines, the critical length decreases due to dielectric losses, while in coaxial structures, it can be longer due to the stable $Z_0(f)$. One of the problems with UWB-TL is signal loss and associated distortion. To transmit pulses of nanosecond or picosecond duration, the frequency-dependent characteristics of the medium that lead to selective attenuation of spectral components are critical (Table 4).

Table 4. *Types of losses and distortions and their impact on UWB-TL performance*

Influence type	Source	Nature of the impact	Change the signal characteristic	Application examples
Losses	Surface resistance $R_s(f)\propto\sqrt{f}$	Ohmic losses due to skin effect	Attenuation of RF components, reduction of amplitude	Analysis $R_s(f)$ and dielectric losses in microstrip filters for mm-waves (30-40 GHz)
	Dielectric losses tan δ(f)↑	Energy absorption in dielectrics	Reduction of the energy efficiency of the pulse	IoT structures with thin film substrates
	Radiation $\alpha_{rad} \propto f^2$	Energy leakage in unshielded structures	Deterioration of coherence, reduction of power	Microstrip lines
	Impedance heterogeneities $Z_0(f)$	Occurrence of signal reflection $\Gamma \neq 0$	Waveform distortion, multi-path	Stripline transitions up to 10 GHz
Distortion (dispersion)	Frequency variance β(f)	Out-of-sync spectral components	Pulse duration lengthening (), maximum shift	Superconducting Magic-T structures (6-14 GHz)
Distortion (amplitude)	Frequency-dependent attenuation α(f)	Uneven spectrum attenuation	Shape asymmetry, loss of pulse integrity (up to 6 dB per 10 cm)	MEMS arrays for IoT (up to 20 GHz)
Temperature sensitivity	Temperature variation ΔT\Delta TΔT in CPW (co-planar waveguide)	Variations of the phase constant Δβ(f)	Phase instability up to ±10%	CPW structures at ΔT = 50°C
Material sensitivity	Growth of tan δ at f > 20 GHz	Increased dielectric losses	Reduced amplitude, increased attenuation	Coaxial arrays for IoT
Impedance sensitivity	Reactive component in $Z_0(f)$ superconductors	Variability of phase velocity	Violation of phase stability, decomposition	Superconducting lines in quantum electronics

Source: *compiled by the author based on M.-J. Kim et al. (2024), B.-C. Min et al. (2024), S. Inoue et al. (2024), Y. Zhu et al. (2024), Y. Weng et al. (2025), X. Li et al. (2025)*

The sources of losses, distortion, and sensitivity to topological parameters of UWB transmission lines indicate the complex nature of pulse signal degradation over a wide frequency range. The ohmic, dielectric, and radiation losses increase with frequency, which necessitates an accurate consideration of $R_s(f)$, tanδ and in the modelling process. Dispersion effects, reflected in β(f) and phase velocity changes, create signal distortion, which is critical for picosecond pulses. In addition, the efficiency of the line depends largely on its topology; coaxial and superconducting configurations have the potential to minimise losses but require special attention to phase stability. When designing UWB systems, it is necessary to apply multi-parameter models capable of reflecting the frequency-dependent behaviour of losses, dispersion and the effect of thermal or geometric fluctuations.

The results obtained in this study on the influence of frequency-dependent losses, dispersion, and phase instability in UWB-TL are confirmed by several studies. V. Monebhurrun *et al*. (2023) considered the fifth generation new radio frequency range 1 UWB antenna as a reference structure for the development of the Recommended Practice for Evaluating the Performance of Consumer Wireless Devices Regarding Human Exposure to Radio Frequency Fields P2816 standard. The emphasis is placed on ensuring stable radiation and phase characteristics, which correlate with the influence of radiation losses $\alpha_{rad} \propto f_2$ identified in this study and the need to control phase shifts during pulse transmission.

Among the approaches to reducing losses in coplanar structures, the implementation of an inverted microstrip transmission line with an integrated EBG filter based on the Gap Waveguide principle, which was studied by L. Inclán-Sánchez (2022), attracts attention. In this structure, the electric field is concentrated in an air gap above a continuous metal layer, which significantly reduces dielectric losses due to reduced interaction with the substrate. In addition, the periodic geometry provides a forbidden band for parasitic modes and at the same time supports broadband transmission with controlled phase characteristics. This confirms the relevance of modelling the losses associated with the dielectric loss tangent tanδ and phase fluctuations in CPW structures analysed in the current study.

The challenges faced in modelling broadband transmission systems include frequency impedance inhomogeneity, phase instability and the need for accurate matching of elements in the high-frequency range. These aspects are discussed in detail in study A. Richter *et al.* (2022), which analyses broadband lines with pronounced inter-element interaction and complex frequency dependence of characteristics. Comparison with the present study confirms the relevance of the chosen methodology for the analysis of distortions caused by variations $Z_O(f)$ and reflections ($\Gamma \neq 0$) in CPW, coaxial and superconducting UWB transmission line configurations. The current study not only supports the existing theoretical approaches but also complements them with practical evaluations in the high-frequency regime. UWB-TLs are used in electronic systems due to their ability to transmit ultra-short pulses with minimal distortion, stable phase characteristics and low losses. Applications include sensor networks, high-speed digital interfaces, millimetre-wave communications (5G/6G), and superconducting and MEMS technologies. Table 5 summarised the areas of UWB-TL application that demonstrate the effectiveness of these structures in the face of increased requirements for signal reliability and accuracy.

Table 5. *Application and technical parameters of UWB-TL in electronic systems*

Application/ technology	Characteristic	Examples of implementation
IoT and WBAN	Metasurface UWB-TLs operating in the pulse transmission mode (UWB-IR, 3-10.6 GHz) provide ultra-short pulses with a duration of 0.1-0.5 ns without distortion. Provide high spatial resolution (<10 cm), which is critical for accurate positioning in medical sensor systems. The structures demonstrate resistance to temperature (up to ±40°C), mechanical (~1 cm), and humidity (ε change <5%) fluctuations, and are easily integrated into flexible wearable devices (LP size <5 mm).	Metasurface UWB antennas for WBAN (3-10 GHz) with >5 dB gain and >7 GHz bandwidth for wireless heart rate/respiration monitoring.
Ultra-fast digital interfaces	UWB-TL in the form of coplanar structures (CPS, CPW) on printed circuit boards is capable of transmitting signals at 25-50 Gbps. Dispersion compensation is achieved due to precise impedance matching (Z_0 = 50±5 Ohm) and geometric optimisation (conductor width ~0.1 mm). Pulse edge preservation is guaranteed by a time distortion of <10 ps.	Phase-balanced CPS structures for digital interfaces (up to 10 GHz) transmitting picosecond pulses with <2 dB loss per 10 cm.
5G/6G systems	UWB-TLs are used as transmission paths in FR2/FR3 systems (24-52 GHz), between TX-ANT, ANT-RX and in filters (BPF, LPF). Provides a bandwidth of >10 GHz, loss <0.5 dB/cm, and low reflection coefficient (Γ<0.1). The design uses striplines or microstrip tracts with materials having a very low loss tangent (tanδ 0.005).	UWB mm-wave filters with a defective ground structure (30-40 GHz) for 5G/6G, with a 12 GHz bandwidth and <1 dB loss.
Superconducting and MEMS technologies	Superconducting UWB-TLs ($R_s \approx 0$ to 100 GHz) provide extremely low losses (<0.01 dB/m) and phase stability (φ<1°), which are critical for quantum sensors and submillimetre systems. MEMS elements enable dynamic change of impedance and phase ($Z_0(f)$, $\beta(f)$) at microsecond rates for adaptive systems.	Superconducting Magic-T structures (6-14 GHz) for mm/submm cameras with <0.1 dB loss; MEMS coaxial arrays for IoT (up to 20 GHz) with tunable bandwidth.

Source: *compiled by the author based on M.-J. Kim et al. (2024), B.-C. Min et al. (2024), Y. Zhu et al. (2024), S. Inoue et al. (2024), Y. Weng et al. (2025), X. Li et al. (2025)*

UWB-TLs have proven to be highly flexible in terms of design and functionality, enabling them to be effectively integrated into a wide range of applications: from medical WBAN systems and ultrafast digital interfaces to 5G/6G components, MEMS and superconducting electronics. UWB-TLs provide high signal transmission characteristics (low loss, phase stability, broadband) that are critical for modern adaptive and sensor systems. At the same time, their effectiveness largely depends on manufacturing accuracy, material stability and operating conditions. UWB-TLs are a priority technology in high-frequency communication systems, provided that geometric and temperature factors affecting the phase and amplitude characteristics of the lines are addressed. Figure 1 illustrated the practical integration of UWB-TL.

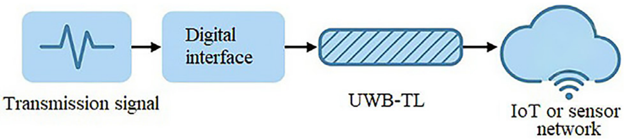

Figure 1. *Block diagram of UWB-TL integration into digital interfaces and sensor networks*
Source: *compiled by the author*

To ensure the effective functioning of UWB-TL in digital systems, it was advisable to formulate several recommendations, the comprehensive implementation of which creates the basis for improving the accuracy, reliability and adaptability of transmission lines. The main factors of influence, including frequency-dependent losses, phase instabilities, and design features of the environment, are addressed. The application of such recommendations helps to reduce signal distortion, improve component matching and ensure high transmission quality even in difficult operating conditions. Table 6 summarised technical approaches that can improve the efficiency of UWB-TL in electronic and sensor platforms.

Table 6. *Engineering and theoretical vectors of UWB-TL improvement*

Recommendation	Description
Extending models for complex environments	Development of analytical and numerical models (FDTD, FEM) to account for inhomogeneities (Δe_r ~ 5-10%), angular rotations (θ ~ 45-90^0), transient elements (ΔZ_0 5-10 Ω) and dispersion ($\beta(f) \propto f$). Integration of the temperature dependence of the surface resistivity ($R_s(f, T) = R_s(f)\cdot[1+\alpha_T (T - T_0)]$) for superconductors (T < 100K) and dielectrics (tanδ (T) 0.001-0.01) in the range of 1-40 GHz.
Modelling nonlinear and adaptive structures	Theoretical justification for MEMS and tunnelled transmission lines with adjustable impedance (ΔZ_0 ~ 5-10 Ω) and phase response ($\Delta\beta(f)$ ~ 0.1 - 0.5 rad/m via control signals (voltage 1-10 V, switching time <1 μs). Nonlinear effects analysis ($\Delta\phi$ ~ 5-20°), (ΔA ~ 0.5 - 2 dB) under dynamic geometry change in real time for IoT and 5G/6G (up to 20 GHz).
Digital distortion compensation	Optimisation of digital inverse filters ($H^{-1}(f)$) based on the impulse response (h(t)) of the transmission line, taking into account frequency-dependent losses ($\alpha(f) \propto \sqrt{f}$, surface impedance ($R_s(f) \propto \sqrt{f}$) and phase dispersion ($\Delta\beta(f)$ ~ 0.01-0.1rad/GHz). Creation of open databases for microstrip, CPS and coaxial LPs (1-40 GHz) for testing AI (Artificial Intelligence)/DSP (Digital Signal Processing) algorithms.
Investigation of UWB lines in the THz band	UWB-TL modelling for 6G front ends (100-1000 GHz), considering micro-/nano-scale effects (λ ~ 0.3-3 mm), reflections (G < 0.05) and interactions with antennas. Analysis of bioengineered media for WBAN (e_r ~ 10-50, tanδ ~ 0.1) and biosensors with picosecond pulses (τ ~ 1 - 10 пс).
Interdisciplinary research	Integration of mathematical physics (solving Maxwell's equations for waveguides), materials science (models e_r, tanδ), superconductors with $R_s(f) \rightarrow 0$, computer engineering (DSP, deep learning for h(t) and biomedical engineering (biocompatible dielectrics, WBAN). Orientation to real conditions – temperature fluctuations (ΔT ~ 20 - 70°, humidity up to 80%, (Δe_r ~ 5%)).

Note: *α_T – temperature coefficient of change of surface resistance, reflects the sensitivity of a material to temperature changes, T – current temperature, Kelvin (or °C in case of appropriate conversion), T_0 – usually a fixed reference temperature at which the base temperature is measured $R_s(f)$, THz-range (terahertz frequency range) frequency range from 0.1 to 10 THz (100-10000 GHz), occupying an intermediate position between the microwave and infrared spectra*
Source: *compiled by the author based on B.-C. Min et al. (2024), Y. Zhu et al. (2024), A.M. Elbir et al. (2024), X. Li et al. (2025), S.U. Rehman et al. (2025), Y. Siraj et al. (2025)*

The results of the study showed that one of the areas of development is the adaptation of models to complex real-world conditions considering the terahertz range, temperature dependencies and nonlinear behaviour. S. Iwamatsu *et al.* (2023) demonstrated the prospect of a multiband planar interconnect line capable of efficient operation in the range of 60-340 GHz. The authors focused on reducing reflection and considering geometric inhomogeneities, which correlates with the current study on modelling UWB-TL in the terahertz band for 6G. The data provided by the authors on the response of the system in a microscale waveguide structure is also consistent with the assumptions of the current study on the influence of λ- and Γ-parameters in media with high dielectric contrast.

One of the areas that finds its practical reflection in the scientific literature is the modelling of adaptive UWB structures with the ability to control impedance and phase characteristics. For instance, A. Rajput & B. Mukherjee (2023) demonstrated the implementation of an electronically controlled varicap notch filter capable of changing the characteristic impedance in the range of $\Delta Z_0 \approx 5 - 10$ Ohm and the phase constant $\Delta\beta(f) \approx 0.1 - 0.5$ rad/m in real time. These parameters are confirmed by the engineering vector formulated in the current study, which justifies the need for theoretical modelling of nonlinear effects and controlled signal transmission in adaptive environments. Common to both approaches is the emphasis on switching speed, sensitivity to geometry, and the ability of the structure to maintain transmission stability over a wide frequency range of up to 20 GHz.

This study proposed to address the temperature dependence of the surface resistance $R_s(f, T)$ as one of the factors affecting the phase instability in UWB-TL, for superconducting and dielectric media in the range up to 40 GHz. This approach involved the integration of temperature parameters into dispersion and loss models, which is important for accurate prediction of phase shift and pulse attenuation under conditions of environmental changes. F. Defrance *et al.* (2024) confirmed the validity of this approach: the authors experimentally investigated losses in amorphous silicon at low temperatures and quantified the behaviour of the dielectric loss tangent tan δ at $T \rightarrow 0$ K. The study emphasised the need to consider temperature dependencies in ultrahigh-frequency superconducting systems, which directly supported the position formulated in the current results.

Approaches to digital distortion compensation in transmission lines are actively developing both in the radio frequency and optical ranges. In the study by V. Bajaj *et al.* (2022), devoted to linear and nonlinear distortions in fibre-optic systems, the use of deep neural networks in combination with inverse $H^{-1}(f)$ filters, which provide signal recovery by compensating for amplitude- and phase-dependent losses, proved to be effective. This approach demonstrated the relevance of the method for ultra-wideband environments, where the frequency-dependent parameters $\alpha(f)$, $R_s(f)$ and $\beta(f)$ also cause critical pulse distortion. The digital compensation vector formulated in the current study suggests a similar strategy for constructing a correction filter based on the h(t) characteristic of the medium, considering statistical models of losses and dispersion. This alignment emphasised the versatility of the inverse filtering principle in the tasks of restoring the integrity of a broadband signal. Similar principles of signal optimisation and input data filtering have also proven effective in related fields, particularly in the study by O. Turchyn (2024), where the use of combined neural networks for processing dynamometric signals improved the accuracy of technical diagnostics in complex equipment operating conditions.

Furthermore, the results of the study showed that the adaptation of numerical methods to the conditions of variable dispersion $\beta(f)$, temperature effects on the surface impedance $R_s(f, T)$ and inhomogeneous characteristics of the medium ΔZ_0 can significantly improve the accuracy of modelling pulse transmission in UWB lines. A similar approach was implemented in a study by J. Sarkis *et al.* (2024), where an algorithm was proposed to quickly calculate the spatial power profile in inverse Raman amplification systems, which also addresses frequency-dependent effects and medium inhomogeneities. This solution provided up to 30 times faster computations with high accuracy (<0.05 dBm) and can be adapted to the tasks of modelling UWB structures with complex losses, which was fully consistent with the current study.

Thus, an interdisciplinary approach combining mathematical physics, materials science, computer science, and biomedical engineering ensured realistic modelling and optimisation of UWB-TL in conditions of variable temperature, humidity, and bioelectrical properties of the environment. This approach is important for war-torn Ukraine, as reliable UWB systems can become the basis for restoring critical infrastructure and ensuring stable signal transmission in difficult conditions (communication disruption and power outages). A holistic solution to these challenges will bring the high-frequency signal transmission infrastructure to the level of meeting the challenges of the digital age of the 21st century.

Conclusions

The results of the study showed that UWB-TLs can provide efficient transmission of ultrashort pulse signals with a wide frequency range (over 500 MHz) in telecommunication and sensor systems. It was found that the metamaterial UWB-TLs for WBAN support pulses with a duration of 0.1-0.5 ns without distortion, providing high spatial resolution (<10cm). Coaxial, stripline, microstrip, coplanar (CPS, CPW), and superconducting structures can transmit short pulses, but suffer from distortion due to frequency-dependent losses (surface resistance $R_s(f) \propto \sqrt{f}$, tan $\delta(f)$ and dispersion ($\beta(f)$), which leads to pulse lengthening and amplitude reduction. The RLGC, FDTD, and FEM models revealed that the geometric inhomogeneities of the transient elements caused phase shifts and multipath reflections that distorted the waveform. It was found that such distortions could be significantly reduced by precise impedance matching and digital compensation in the presence of high-frequency losses. Superconducting lines showed losses of <0.01 dB/m up to 100 GHz, making them effective for quantum and submillimetre systems. The coplanar structures provided data transmission at 25-50 Gbps with time-distortion.

The metamaterial antennas for WBAN provided >5 dB gain and >7 GHz bandwidth, which was essential for accurate positioning in medical systems. The temperature dependence of the surface resistance $R_s(f, T)$ was modelled, which demonstrated the effect of temperature changes on the characteristics of transmission lines. This effect was typical for superconducting and dielectric structures operating in a wide frequency range. Particular attention was also paid to the modelling of variations in the wave impedance (ΔZ_0) and phase constant ($\Delta\beta(f)$), which revealed a significant impact on the pulse transmission parameters. For practical implementation in IoT systems, it is recommended to use MEMS structures with adjustable impedance and phase parameters, for 5G microstrip filters with low losses and wide bandwidth, for WBAN metamaterial UWB antennas with high gain and stable spatial accuracy in the face of environmental fluctuations.

The study was limited to partial consideration of noise and the influence of complex operational factors, such as humidity and micro-/nano-effects in the THz range (100-1,000 GHz). The temperature dependence and material inhomogeneities were partially analysed, but required further improvement to more accurately reproduce real-world conditions. Further research should focus on the development of digital distortion compensation methods using AI and deep learning, as well as the development of temperature-stable materials for UWB systems for use in telecommunications, biosensor technologies, and 6G networks.

Acknowledgements

None.

Funding

None.

Conflict of Interest

None.

References

[1] Bajaj, V., Buchali, F., Chagnon, M., Wahls, S., & Aref, V. (2022). Deep neural network-based digital pre-distortion for high baudrate optical coherent transmission. *Journal of Lightwave Technology*, 40(3), 597-606. doi: 10.1109/JLT.2021.3122161.

[2] Batrakov, D.O., Antyufeyeva, M.S., Batrakova, A.G., & Ruban, V.P. (2024). Ground penetrating radar application for positioning cracks in non-rigid road pavements. In A.K. Nagar, D.S. Jat, D. Mishra & A. Joshi (Eds.), *Intelligent sustainable systems* (pp. 453-464). Singapore: Springer. doi: 10.1007/978-981-99-7569-3_37.

[3] Defrance, F., Beyer, A.D., Shu, S., Sayers, J., & Golwala, S.R. (2024). Characterization of the low electric field and zerotemperature twolevelsystem loss in hydrogenated amorphous silicon. *Physical Review Materials*, 8, article number 035602. doi: 10.1103/PhysRevMaterials.8.035602.

[4] Dubrovka, F.F., Piltyay, S., Movchan, M., & Zakharchuk, I. (2023). Ultrawideband compact lightweight biconical antenna with capability of various polarizations reception for modern UAV applications. *IEEE Transactions on Antennas and Propagation*, 71(4), 2922-2929. doi: 10.1109/TAP.2023.3247145.

[5] Elbir, A.M., Mishra, K.V., Chatzinotas, S., & Bennis, M. (2024). Terahertz-band integrated sensing and communications: Challenges and opportunities. *IEEE Aerospace and Electronic Systems Magazine*, 39(12), 38-49. doi: 10.1109/MAES.2024.3476228.

[6] Fisher, A., Jones, T.R., & Peroulis, D. (2025). Ultra-wideband silicon plasma switches. *IEEE Journal of Microwaves*, 5(3), 677-686. doi: 10.1109/JMW.2025.3559499.

[7] Inclán-Sánchez, L. (2022). Inverted microstrip gap waveguide coplanar EBG filter for antenna applications. *Electronics*, 11(18), article number 2951. doi: 10.3390/electronics11182951.

[8] Inoue, S., Chin, K.W., Uno, S., Kohno, K., Niwa, Y., Naganuma, T., Yamamura, R., Watanabe, K., Takekoshi, T., & Oshima, T. (2024). A design method of an ultra-wideband and easy-to-array magic-T: A 6-14 GHz scaled model for a mm/submm camera. *Journal of Low Temperature Physics*, 216(1-2), 378-385. doi: 10.1007/s10909-024-03150-w.

[9] Iwamatsu, S., Ali, M., Fernández-Estévez, J.L., Tebart, J., Kumar, A., Makhlouf, S., Carpintero, G., & Stöhr, A. (2023). Ultra-wideband multi-octave planar interconnect for multi-band THz communications. *Journal of Infrared, Millimeter, and Terahertz Waves*, 44, 532-550. doi: 10.1007/s10762-023-00926-1.

[10] Kameli, S.M., Refaat, S.S., Abu-Rub, H., Darwish, A., Ghrayeb, A., & Olesz, M. (2024). Ultrawideband Vivaldi antenna with an integrated noise-rejecting parasitic notch filter for online partial discharge detection. *IEEE Transactions on Instrumentation and Measurement*, 73, article number 8001610. doi: 10.1109/TIM.2024.3353284.

[11] Kayalvizhi, A., Sankara Malliga, G., & Seetharaman, R. (2025). Compact inverted E-shaped open-circuited impedance matching stub bandpass filter for wireless applications. *Analog Integrated Circuits and Signal Processing*, 123(1), article number 14. doi: 10.1007/s10470-025-02357-5.

[12] Kim, M.-J., Lee, J.-S., Min, B.-C., Choi, J.-S., Kumar, S., Choi, H.-C., & Kim, K.-W. (2024). Ultra-wideband vertical transition in coplanar stripline for ultra-high-speed digital interfaces. *Sensors*, 24(10), article number 3233. doi: 10.3390/s24103233.

[13] Küpfmüller, K. (1928). On the dynamics of automatic gain controllers. *Electrical Communications Engineering*, 5(11), 459-467.

[14] Lee, G.H., Mohyuddin, W., Kumar, S., Choi, H.C., & Kim, K.W. (2021). Compact wideband coplanar stripline-to-microstrip line transition using a bended structure on a two-layered substrate. *Electronics*, 10(11), article number 1272. doi: 10.3390/electronics10111272.

[15] Li, X., Zhou, Z., Wang, K., Yang, Y., Pang, Z., Zhou, X., Tang, W., Huang, Z., & Lan, D. (2025). UWB metasurface antenna with improved gain and bandwidth for WBAN application. *IEEE Transactions on Consumer Electronics*, 71(2), 5465-5474. doi: 10.1109/TCE.2025.3552597.

[16] Liu, S.-Z., Liu, R., Li, L.-Y., Meng, F.-Y., Xu, S., & Ding, C. (2025). Investigation of miniaturized ultra-wideband circulator based on composite ferrite. *Journal of Physics D: Applied Physics*, 58, article number 205001. doi: 10.1088/1361-6463/adcbb7.

[17] Mao, K., Zhu, Q., Ye, X., Feng, R., Duan, F., Miao, Y., & Song, M. (2022). UWB channel modeling and simulation with continuous frequency response. *China Communications*, 19(11), 88-98. doi: 10.23919/JCC.2022.11.007.

[18] Min, B.-C., Choi, J.-S., Choi, H.-C., & Kim, K.-W. (2024). Ultra-wideband common-mode rejection structure with autonomous phase balancing for ultra-high-speed digital transmission. *Sensors*, 24(19), article number 6180. doi: 10.3390/s24196180.

[19] Monebhurrun, V., Chakrabarti, S., & Quoi, R. (2023). A 5G NR FR1 UWB antenna as benchmark for the development of IEEE standard P2816. In *Proceedings of the 45th annual meeting and symposium of the antenna measurement techniques association* (pp. 1-2). Renton: IEEE. doi: 10.23919/AMTA58553.2023.10293360.

[20] Ogurtsova, T., Blinova, N., Pochanin, G., Nesterenko, M., & Pochanina, I. (2023). Reception of UWB pulsed electromagnetic fields: Ferrite antenna with a two-turns coil. In *Proceedings of the international seminar/workshop on direct and inverse problems of electromagnetic and acoustic wave theory* (pp. 84-89). Tbilisi: IEEE. doi: 10.1109/DIPED59408.2023.10269503.

[21] Oppenheim, A.V., Willsky, A.S., & Nawab, S.H. (1997). *Signals and systems*. Upper Saddle River: Prentice-Hall.
[22] Poggiolini, P., & Jiang, Y. (2025). *Recent advances in real-time models for UWB transmission systems*. doi: 10.48550/arXiv.2504.03873.
[23] Rajput, A., & Mukherjee, B. (2023). Electronically tunable UWB band stop filter using varactor diode. *AEÜ – International Journal of Electronics and Communications*, 164, article number 154610. doi: 10.1016/j.aeue.2023.154610.
[24] Rehman, S.U., Alkanhal, M.A., Ahmad, M., Malik, W.A., Abdulkawi, W.M., Salim, A., & Sheta, A.-F. (2025). Mathematical modeling development and synthesis of tapered transmission line resonators and filters. *Physica Scripta*, 100, article number 015511. doi: 10.1088/1402-4896/ad96e6.
[25] Richter, A., Di Rosa, G., & Koltchanov, I. (2022). Challenges in modeling wideband transmission systems. In J. Leuthold, C. Harder, B. Offrein & H. Limberger (Eds.), *Proceedings of the European conference on optical communication* (article number We1A.1). Basel: Optica Publishing Group.
[26] Roy, S., Mahin, R., & Mahbub, I. (2023). A comparative analysis of UWB phased arrays with combining network for wireless-power-transfer applications. *IEEE Transactions on Antennas and Propagation*, 71(4), 3204-3215. doi: 10.1109/TAP.2023.3243852.
[27] Sarkis, J., Jiang, Y., & Poggiolini, P. (2024). *An algorithm to speed up the spatial power profile calculation in backward Raman amplified systems*. doi: 10.48550/arXiv.2411.12688.
[28] Shi, M., Niu, Z., Yang, H., Xiao, J., Zeng, C., Zhang, Y., Zheng, Z., Hu, W., & Yi, L. (2025). Fast and accurate waveform modeling based on sequence-to-sequence framework for multi-channel and high-rate optical fiber transmission. *Optics Letters*, 50(7), 2286-2289. doi: 10.1364/OL.555880.
[29] Siraj, Y., Khardioui, Y., Alaoui, K.S., & Foshi, J. (2025). High-performance terahertz patch antenna with metamaterials for advanced 6G and biomedical technologies. *Scientific African*, 28, article number e02716. doi: 10.1016/j.sciaf.2025.e02716.
[30] Turchyn, O. (2024). Optimisation of dynamometric data collection and processing to improve the efficiency of neural network diagnostics of a sucker-rod pump. *Bulletin of Cherkasy State Technological University,* 29(3), 55-64. doi: 10.62660/bcstu/3.2024.55.
[31] Weng, Y., Feng, W., Shi, Y., Shen, G., Cao, Y., Tang, Y., Zhu, H., Wu, L.-S., Che, W., & Xue, Q. (2025). Millimeter-wave multilayer ultrawideband common-mode filters using defected ground structure. *IEEE Transactions on Components, Packaging and Manufacturing Technology*, 15(4), 800-809. doi: 10.1109/TCPMT.2024.3517734.
[32] Zhang, Y., Liu, P., Xia, B., Wei, G., Song, Y., & Xu, W. (2023). A new wideband RLGC extraction method for multiconductor transmission lines using improved mode tracking algorithm. *IEEE Transactions on Electromagnetic Compatibility*, 66(1), 293-301. doi: 10.1109/TEMC.2023.3331031.
[33] Zhu, Y., Li, X., & Mao, J. (2024). An ultra-wideband substrate integrated coaxial line array based on silicon-based MEMS process. *Journal of Circuits, Systems and Computers*, 33(18), article number 2550016. doi: 10.1142/S0218126625500161.

Надширокосмугові лінії передачі для цифрових систем нового покоління: моделювання та аналіз

Сергій Бойченко

Аспірант
Харківський національний університет радіоелектроніки
61000, просп. Науки, 14, м. Харків, Україна
https://orcid.org/0009-0008-6118-8314

Анотація. Метою дослідження був теоретичний аналіз моделювання імпульсної передачі у середовищах з надширокою смугою пропускання із врахуванням втрат, дисперсії та фазових зсувів. Використано комплексний підхід, що поєднував математичне моделювання та аналіз електромагнітних процесів у різних топологіях ліній передачі, таких як коаксіальні, стриплайнові, мікросмужкові, а також структури на основі метаматеріалів і надпровідників. Встановлено, що дисперсія, частотозалежні втрати, зумовлені поверхневим опором, який зростав пропорційно кореню частоти, і діелектричними втратами з тангенсом, що залежали від частоти, спричиняли спотворення імпульсів із затримками 10-100 пікосекунд і фазовими зсувами до 20 градусів. Для імпульсів тривалістю 0,5 наносекунди ширина спектру становила близько 2 ГГц, що підтверджувало залежність між тривалістю імпульсу та частотним діапазоном. Моделювання за допомогою телеграфних рівнянь, перетворення Фур'є та чисельних методів, таких як скінченних різниць у часовій області та скінченних елементів, дозволило кількісно оцінити втрати до 3-6 децибел на 10 см і критичну довжину ліній, що залежало від геометричних неоднорідностей. Виявлено переваги надпровідних структур із втратами менше 0,01 децибел на метр до 100 ГГц і копланарних ліній для швидкості передачі 25-50 Гбіт/с. Сформульовано частотно-залежні критерії ефективності, які дозволили обґрунтовано обирати тип лінії залежно від вимог до мінімізації фазових зсувів та затухання імпульсу. Практична значимість результатів полягала в можливості їх використання фахівцями з проєктування телекомунікаційних і сенсорних систем для підвищення надійності та точності передачі даних у реальних умовах експлуатації

Ключові слова: дисперсія; поверхневий опір; імпульсний сигнал; частотозалежні втрати; метаматеріали; надпровідники; фазова стабільність

TECHNOLOGIES AND ENGINEERING

Journal homepage: https://technologies-engineering.com.ua/en
Vol. 26, No. 3, 2025

Received: 21.01.2025
Revised: 09.05.2025
Accepted: 25.06.2025

UDC 552.576.1:661.183.03:554.723.2
DOI: 10.30857/2786-5371.2025.3.2

Adsorbents derived from nitric acid-oxidised coal and activated with potassium hydroxide

Volodymyr Kucherenko

Doctor of Chemical Sciences, Senior Researcher
L.M. Litvinenko Institute of Physical-Organic and Coal Chemistry
of the National Academy of Sciences of Ukraine
02155, 50 Kharkivske Hwy., Kyiv, Ukraine
https://orcid.org/0000-0001-7234-947X

Yuliia Tamarkina*

PhD in Chemical Sciences, Senior Researcher
L.M. Litvinenko Institute of Physical-Organic and Coal Chemistry
of the National Academy of Sciences of Ukraine
02155, 50 Kharkivske Hwy., Kyiv, Ukraine
https://orcid.org/0000-0002-8747-4481

Anastasiia Redko

Leading Engineer
L.M. Litvinenko Institute of Physical-Organic and Coal Chemistry
of the National Academy of Sciences of Ukraine
02155, 50 Kharkivske Hwy., Kyiv, Ukraine
https://orcid.org/0000-0001-9768-4020

Iryna Frolova

PhD in Chemical Sciences, Researcher
L.M. Litvinenko Institute of Physical-Organic and Coal Chemistry
of the National Academy of Sciences of Ukraine
02155, 50 Kharkivske Hwy., Kyiv, Ukraine
https://orcid.org/0000-0001-9660-5474

Abstract. Alkaline activation is the most effective method for producing carbon-based adsorbents with a highly developed surface area (⩾1,000 m^2/g). However, its major drawback – the requirement for large quantities of alkali – necessitates research aimed at improving the process. This study aimed to quantitatively assess the effect of nitric acid oxidation of long-flame coal on the porous structure and adsorption properties of adsorbents produced by alkaline activation at a low KOH-to-coal ratio (⩽1 g/g). Experimental, analytical and comparative scientific methods were employed. The properties of the adsorbents were characterised using infrared spectroscopy, porometry, and the kinetics and isotherms of 4-chlorophenol, methylene blue dye, and lead cation adsorption from aqueous solutions (at 25°C). It was found that pre-oxidation of the coal with nitric acid introduces ether, ester, phenolic, carboxylic, and nitro groups into the carbon matrix, resulting in a mass increase of up to 16% and significantly influencing the formation of the adsorbents. Increasing the HNO_3-to-carbon ratio from 0 to 1.0 mol/mol reduces the adsorbent yield (from 50.2% to 33.85%), increases the specific surface area (from 1,685 m^2/g to 2,216 m^2/g), and improves adsorption properties by 25%-51%. The dominant portion (~80%) of the effect occurs within the range of ⩽0.4 mol/mol. A comparison of the porous structure characteristics of the adsorbents revealed that oxidation primarily promotes the formation of subnanopores and mesopores with diameters of 2-5 nm. A comparison of adsorption properties showed that adsorbents derived from oxidised coal adsorb greater

Suggested Citation:
Kucherenko, V., Tamarkina, Yu., Redko, A., Frolova, I. (2025). Adsorbents derived from nitric acid-oxidised coal and activated with potassium hydroxide. *Technologies and Engineering,* 26(3), 24-37. doi: 10.30857/2786-5371.2025.3.2.

*Corresponding author

quantities of adsorbates (by a factor of 1.20-1.43) and with a higher initial rate (by a factor of 1.2-4.0). This property is particularly important for the rapid removal of highly toxic compounds from water. The adsorbent produced from oxidised coal possesses a more developed surface and a subnanoporous structure, and it exhibits greater adsorption activity than the material derived from non-oxidised coal. Pre-oxidation significantly enhances the adsorption capacity of activated carbon in capturing ecotoxicants from aqueous environments

Keywords: oxicarbon; alkaline thermochemolysis; porous carbon material; pore structure; ecotoxicant adsorption

Introduction

Activated carbon (AC) derived from fossil coal represents a broad group of promising adsorptive materials, characterised by well-developed nanoporous structures, high specific surface area, chemical stability, and electrical conductivity. The combination of these properties enables their application in hydrogen, natural gas, and energy storage (e.g. in supercapacitors), as well as in the removal of pollutants from air and water environments. As of 2025, the most widely used method for producing AC is alkaline activation – thermolysis (700°C-900°C) of the precursor material with potassium hydroxide. This is the only method capable of yielding carbon materials with an extremely high specific surface area (approximately 4,000 m^2/g or more). However, it requires high KOH-to-precursor mass ratios ($R_{KOH} \geqslant 3$ g/g), which represents the main drawback of the process and significantly limits its industrial viability. Consequently, research into producing AC using lower (preferably catalytic) amounts of alkali remains highly relevant.

Global studies of alkaline activation have revealed a general trend: the higher the oxygen content in the precursor, the more developed the porous structure of the resulting AC – particularly at lower R_{KOH} ratios. In other words, a high content of structural oxygen is a key prerequisite for producing AC with a well-developed nanoporous structure using reduced quantities of KOH as the activating agent. Two main approaches exist in this context. The first involves selecting raw materials from the category of solid substances with high oxygen content and strong chemical reactivity towards KOH – typically, certain types of biomass. For example, D. Bergna *et al*. (2022) converted hydrolysis lignin with an oxygen content of [O] = 31.9% into AC with a specific surface area of 928 m^2/g under the following alkaline activation conditions: R_{KOH} = 1.0 g/g, 800°C, 1 hour. Under precisely the same activation conditions, M. Li *et al.* (2022) obtained AC with a surface area of 1,225 m^2/g from kraft lignin ([O] = 29.41%), while L.S. Queiroz *et al.* (2020) synthesised AC with a well-developed porous structure (1,462 m^2/g) from biomass ([O] = 47.6%). Perhaps the most impressive result achieved via this approach was the production of AC with a surface area of 2,276 m^2/g from sodium lignosulphonate at R_{KOH} = 0.4 g/g (Zhu *et al*., 2024), which exhibited rapid adsorption of organic dyes.

The second approach involves the immobilisation of structural oxygen in the precursor through pre-oxidation using various reagents, most commonly hydrogen peroxide or nitric acid. S.M. Lee *et al*. (2022) demonstrated that pre-oxidising petroleum coke with hydrogen peroxide increased its oxygen content from 1.4% to 12.4% and enhanced the specific surface area of the resulting AC from 874 m^2/g to 3,159 m^2/g. These results were obtained using a high quantity of activator (R_{KOH} = 3.0 g/g) under more severe process conditions (850°C, 1.5 hours). The effectiveness of peroxide oxidation at low KOH-to-precursor ratios ($R_{KOH} \leqslant 1.0$ g/g) remains unexplored, and it is therefore still unclear to what extent pre-oxidation can compensate for the reduced amount of activator. There is also a lack of systematic data on the effect of pre-oxidation with nitric acid on the ability of fossil coal to form AC with a well-developed porous structure when using small amounts of activator ($R_{KOH} \leqslant 1.0$ g/g). Using anthracite as an example, S.-Yi. Lee & R.L. Mahajan (2021) found that HNO_3 oxidatively cleaves aliphatic bonds between crystallites and transforms graphene fragments into graphene oxides, increasing the oxygen content and introducing structural nitrogen, which participates in the formation of the threedimensional AC framework during activation. In a study on the alkaline activation of bituminous coal at different stages of metamorphism, Yu.V. Tamarkina *et al*. (2022) showed that the higher the oxygen content in the raw coal, the greater the development of porosity during activation. In particular, long-flame coal produced AC with the highest specific surface area (1,547 m^2/g) and the greatest adsorption activity for removing ecotoxicants from water (Tamarkina *et al*., 2020).

This led to the task of assessing the extent to which nitric acid oxidation affects the porous structure and adsorption properties of AC derived from long-flame coal. A review of the literature revealed no available data on this subject. The aim of the present study was to determine how pre-oxidation of longflame coal with nitric acid influences the development of the porous structure and adsorption characteristics of carbon materials synthesised by alkaline thermochemolysis under low KOH-to-coal mass ratio conditions (1 g/g).

Materials and Methods

The study used a sample of long-flame coal (grade D according to the Ukrainian fossil coal classification system, DSTU 3472-96, 2009) with a particle size of 0.16-0.25 mm. The sample was characterised by a moisture content of 10.9%, ash content of 1.8%, and volatile matter yield of 44.8%. The elemental composition of the organic coal matter (% daf) was as follows: C – 80.0; H – 5.3; N – 1.9; S – 1.0; O – 11.8 (by difference), where daf (dry ash-free basis) refers to the mass of coal calculated on a dry, ash-free basis. Oxidation of the coal was performed using an aqueous solution of HNO_3 (50%) following the procedure outlined below. A 10 g sample was dried (120 ± 5°C, ⩾ 2 hours), cooled, and mixed with the reagent at a HNO_3-to-carbon ratio (R_{OX}) ranging from 0.1 to 1.0 mol/mol (OX = HNO_3). The mixture was left to stand for 24 hours at room temperature. The oxidised coal product was then filtered and dried to constant weight in a heated oven (120 ± 5°C). The coal mass increase (Δm, %) was determined by comparing the weights before and after oxidation, and the oxidised samples were designated as D_{OX}. The coal was treated with potassium hydroxide by three-stage impregnation: mixing of 10 g of dried coal with 33.3 g of a 30% aqueous KOH solution to achieve a mass ratio of KOH-tocoal (R_{KOH} = 1.0 g/g); holding the mixture for 24 hours at 20°C-30°C; removal of the aqueous phase at 90°C-100°C, followed by drying to constant weight at 120 ± 10°C for at least 2 hours.

The AC samples were obtained by thermoprogrammed alkaline activation, which involved heating the impregnated coal (~40 g) in an argon atmosphere at a rate of 4°C/min to 800°C, maintaining the isothermal condition for 1 hour, and then cooling in an argon flow to a temperature of ⩽50°C. The resulting carbon product was washed to remove potassium compounds (KOH, $KHCO_3$, K_2CO_3) using water, a 0.1 M HCl solution, and water again until no chloride ions were detected (confirmed by $AgNO_3$ test). The samples were then dried at 120 ± 5°C to constant weight. The yield of AC (Y, %) was determined with an accuracy of ±2%. Samples synthesised from raw coal are denoted as AC(D), and those from oxidised coal as AC(D_{OX}).

Infrared (IR) spectra of the coal samples were obtained using pellets made from mixtures of 5% sample and 95% KBr, with 16 scans recorded in the range of 4,000-400 cm^{-1} (PerkinElmer Spectrum RX I FT-IR System). Band assignments were made based on IR spectra of individual organic compounds (Bellamy, 1975). The porous structure characteristics of the AC were determined from nitrogen adsorption-desorption isotherms at low temperature (77 K) using a Micromeritics ASAP 2020 instrument. Prior to measurement, AC samples were degassed for 20 hours at 260°C. The total pore volume, V_t (cm^3/g), was calculated from the volume of N_2 adsorbed at a relative pressure of p/p_0 ~1.0. The specific surface area, S_{BET}, was calculated using the BET method at $p/p_0 \leqslant 0.12$. Integral and differential pore surface area (S_{DFT}, m^2/g) and pore volume (V, cm^3/g) distributions as functions of average pore diameter (D, nm) were calculated using the 2D-NLDFT-HS method (2-Dimensional Nonlocal Density Functional Theory for Heterogeneous Surfaces) in the SAIEUS software (Jagiello *et al.*, 2020). From the integral curves "V – D" and "S_{DFT} – D", the volumes of ultramicropores (V_{umi}), supermicropores (V_{smi}), subnanopores (V_{1nm}), and micropores (V_{mi}) were determined, where $V_{mi} = V_{umi} + V_{smi}$. The combined volume of mesopores and macropores was calculated as $V_{me+ma} = V_t - V_{mi}$. The margin of error in pore volume determination was ±0.01 cm^3/g. In a similar manner, the specific surface areas of ultramicropores (S_{um}), supermicropores (S_{smi}), subnanopores (S_{1nm}), and micropores (S_{mi}) were determined, as well as the total surface area of mesopores and macropores (S_{me+ma}). The measurement error for specific surface area was ±5%. The classification of pores and their average diameters was adopted according to IUPAC recommendations (Thommes *et al.*, 2015): ultramicropores ($D \leqslant 0.7$ nm), supermicropores (D = 0.7-2.0 nm), micropores ($D \leqslant 2.0$ nm). The above categories are collectively referred to as nanopores, with an upper size limit of $D \leqslant 100$ nm. Additionally, the volume fractions (P_V, %) of different pore types in the total adsorptive pore volume, and the surface fractions (P_S, %) of pore types in the total specific surface area (S_{DFT}) of the AC samples were calculated.

Adsorption capacity for selected adsorbates, denoted as A_{AD} (mmol/g), where AD refers to 4chlorophenol (CP), methylene blue dye (MB), or lead(II) cations from a $Pb(NO_3)_2$ solution, was determined as follows. A precisely weighed sample (m = 0.100 g) of the AC sample, dried at 120 ± 10°C, was introduced into 100 cm^3 of aqueous adsorbate solution at a predefined initial concentration ($C_{AD(0)}$, mmol/L), and shaken at 25 ± 0.5°C (150 rpm) using a MAXTURDY-45 shaker bath (Daihan). The concentration of AC in the adsorbate solution was kept constant at 1 g/L. After the designated contact time, the mixture was filtered, and either the current concentration, C_{AD} (for adsorption kinetics) or the equilibrium concentration, $C_{AD(e)}$ (for adsorption isotherms), was measured. The concentrations of CP and MB were determined by comparison with calibration curves based on the optical density of the solution, measured using a PerkinElmer Lambda 20 spectrophotometer at wavelengths of 280 nm and 665 nm, respectively (Tamarkina *et al.*, 2022). The concentration of Pb(II) cations was determined by titration with a solution of Trilon B in the presence of xylenol orange as an indicator. The adsorption capacity A_{AD} was calculated using the following formula:

$$A_{AD} = (C_{AD(0)} - C_{AD}) \cdot V/m. \quad (1)$$

Adsorption kinetics data were fitted using the pseudo-first-order (2), pseudo-second-order (3), and intraparticle diffusion (4) models:

$$A_{AD} = A_{AD(e)}[1 - \exp(-k_1\tau)], \quad (2)$$

where k_1 is the rate constant, τ is the adsorption time (Revellame *et al.*, 2020; Wang & Guo, 2022).

$$A_{AD} = k_2 A^2_{AD(e)}\tau / (1 + k_2 A_{AD(e)}\tau), \quad (3)$$

where k_2 is the rate constant, τ is the adsorption time.

$$A_{AD} = k_d \tau^{0.5} + C, \quad (4)$$

where k_d is the rate constant, τ is the adsorption time.
The initial adsorption rate was calculated using the following formula:

$$R_{AD(0)} = k_2 A^2_{AD(e)}. \quad (5)$$

Adsorption isotherms were fitted using the Langmuir (6) and Freundlich (7) models:

$$A_{AD(e)} = A_{AD(L)} k_{AD(L)} C_{AD(e)} / (1 + k_{AD(L)} C_{AD(e)}), \quad (6)$$

where $A_{AD(L)}$ is the monolayer adsorption capacity, $k_{AD(L)}$ is the Langmuir constant.

$$A_{AD(e)} = k_{AD(F)} \cdot C_{AD(e)}^{1/n}, \quad (7)$$

where $k_{AD(F)}$ and n are Freundlich constants (Al-Ghouti & Da'ana, 2020).

Additionally, the specific adsorption capacity $A_{AD(S)}$ was calculated as: $A_{AD(S)}$= 1,000 · $A_{AD(L)}$ / S_{BET}(μmol/m²), which is proportional to the surface concentration of adsorption centres (ACs) on the activated carbon.

Results and Discussion

With increasing contact time with HNO_3 solution at room temperature, long-flame coal exhibited a weight gain, denoted as Δm. This gain reached its maximum after approximately 24 hours, after which it either remained constant or gradually declined. In subsequent experiments, a standard nitric acid oxidation time of 24 hours was adopted for all values of R_{OX}. The weight gain Δm exhibited a pronounced dependence on the R_{OX} ratio (Fig. 1), reaching a maximum value of 16% at R_{OX} = 0.4 mol/mol. The decline beyond this point is attributed to low-temperature combustion of the coal's organic matter as a result of oxidative degradation reactions producing CO and CO_2. Based solely on Δm values, the R_{OX} range of 0.4-1.0 mol/mol is considered suboptimal. Nitric acid dissociates to form the nitronium cation, which acts as an electron acceptor. When interacting with coal polyarenes, it produces cation-radical or cationic fragments within the carbon matrix. This significantly enhances the reactivity of the coal and initiates numerous secondary reactions leading to the formation of oxygen-containing functional groups. The nitronium cation also functions as a nitrating agent, converting polyarenes into nitropolyarenes. Structural changes in coal upon interaction with HNO_3 are illustrated by the IR spectra of the original coal sample *D* and the oxidised sample D_{OX} obtained at R_{OX} = 0.4 mol/mol (Fig. 2).

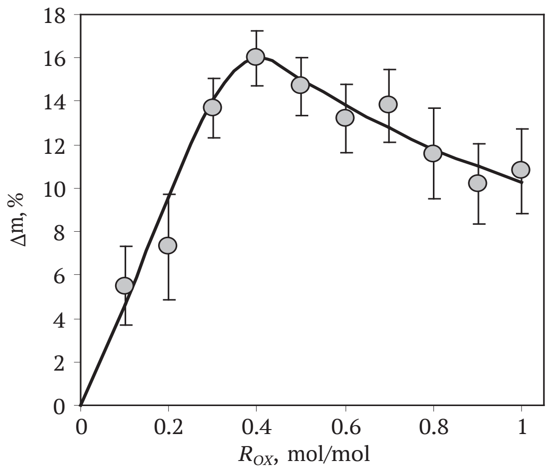

Figure 1. *Weight gain of long-flame coal upon interaction with nitric acid*
Source: *compiled by the authors based on experimental data*

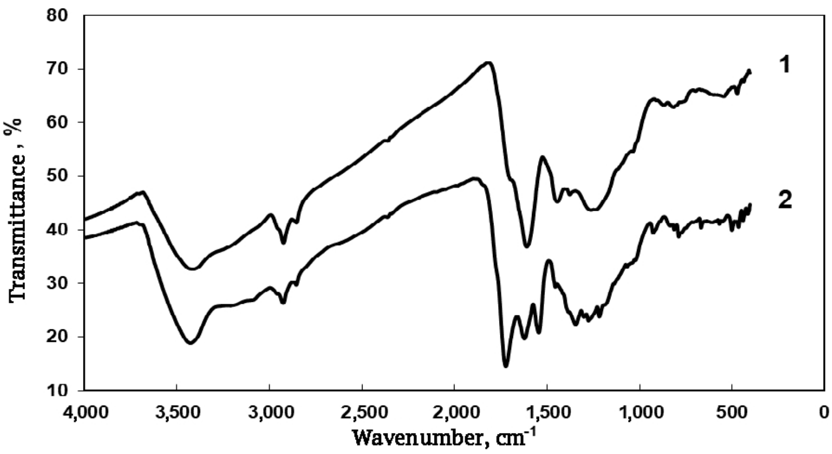

Figure 2. *IR spectra of coal D and oxidised coal* D_{OX}
Note: *1 – coal D, 2 – oxidised coal* D_{OX}
Source: *compiled by the authors based on experimental data*

Both samples contain aromatic fragments, identified by the absorption band corresponding to skeletal vibrations of $C_{ar} = C_{ar}$ bonds at 1,618 cm^{-1}. In the spectrum of coal *D*, bands are observed for isolated hydrogen atoms (868 cm^{-1}), two and three adjacent hydrogen atoms (814 cm^{-1}), and four adjacent hydrogen atoms (755-770 cm^{-1}) within the aromatic ring. The corresponding region for oxidised coal D(A) is considerably more complex. Absorption bands appear at 926 cm^{-1} and 668 cm^{-1} with uncertain assignments, along with absorptions of Car-H bond vibrations at 833 cm^{-1} and 811 cm^{-1} (two adjacent hydrogen atoms) and 787 cm^{-1} (three adjacent hydrogen atoms). Vibrations of Car-H bonds in polynuclear nitroarenes (833 cm^{-1}) and deformation vibrations of NO_2 groups (787 cm^{-1}) were identified. The D_{OX} sample contains carbonyl groups, evidenced by bands at 1,718 cm^{-1} (COOH groups) and a shoulder at 1,760-1,780 cm^{-1} (esters and lactones). Chemolysis with nitric acid introduces nitro groups into the coal, identifiable by absorption bands at 1,540 cm^{-1} and 1,342 cm^{-1}. The nature of substituents in coal arenes changes significantly under nitric acid oxidation due to electrophilic aromatic substitution reactions (ArH → Ar-NO_2), oxidation of arene fragments (ArH → Ar-OH), oxidation of methyl groups (Ar-CH_3 → Ar-COOH), and the formation of ethers and esters. This fully aligns with the conclusions drawn by L. Giraldo *et al*. (2020). Coal samples oxidised at various R_{OX} ratios were converted into ACs under identical alkaline activation conditions. The characteristics of these ACs are presented in Table 1.

Table 1. *Yield and properties of AC(D) and AC(D_{OX}) samples*

Sample	R_{OX}, mol/mol	Y, %	S_{BET} m²/g	$A_{CP(e)}$ mmol/g	$A_{CP(S)}$ μmol/m²	$A_{MB(e)}$ mmol/g	$A_{MB(S)}$ μmol/m²	$A_{Pb(e)}$ mmol/g	$A_{Pb(S)}$ μmol/m²
AC(D)	0	50.2	1,685	3.66	2.17	0.72	0.43	0.71	0.42
AC(D_{OX})	0.2	43.9	1,888	4.25	2.25	0.83	0.44	0.92	0.49
	0.4	40.4	2,108	4.43	2.10	0.91	0.43	1.02	0.48
	0.6	39.1	2,100	4.43	2.11	0.90	0.43	1.03	0.49
	0.8	37.7	2,216	4.60	2.08	0.97	0.44	1.11	0.50
	1.0	33.8	2,157	4.59	2.13	1.09	0.51	1.12	0.52

Note: *$A_{CP(e)}$, $A_{MB(e)}$, $A_{Pb(e)}$ are the equilibrium adsorption capacities for 4-chlorophenol, methylene blue, and lead cations, respectively; $A_{CP(S)}$, $A_{MB(S)}$, and $A_{Pb(S)}$ are the specific adsorption capacities for the same adsorbates*
Source: *compiled by the authors based on experimental data*

An increase in the R_{OX} ratio results in an almost linear decrease in AC yield (Fig. 3, Line 1), described by the correlation equation $Y = 48.13 - 14.56 \cdot R_{OX}$ (R_2 = 0.929). The reduction in yield is accompanied by further development of the AC surface area (Fig. 3, Line 2). The S_{BET} value increases by a factor of 1.44, with approximately 80% of this surface growth occurring within the R_{OX} range ≤0.4 mol/mol.

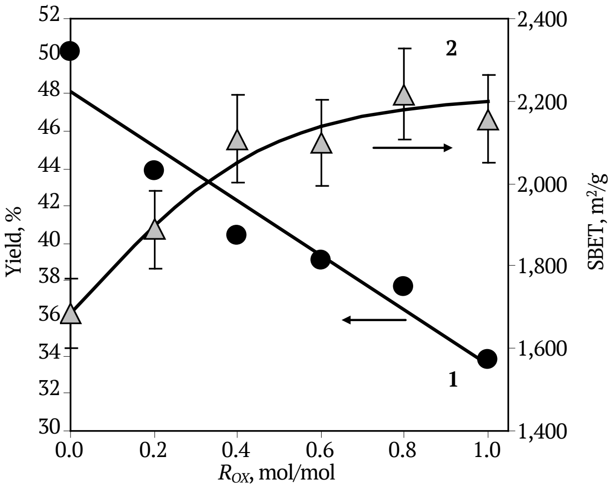

Figure 3. *Yields and specific surface areas (S_{BET}) of AC(D) and AC(D_{OX}) samples* produced at different HNO_3-to-carbon ratios
Note: *1 – yields, 2 – specific surface area (S_{BET})*
Source: *compiled by the authors based on experimental data*

For the AC(D) and AC(D_{OX}) samples, the equilibrium adsorption capacities for CP, MB, and Pb(II) cations from aqueous solutions (25°C, initial adsorbate concentration $C_{AD(0)}$ = 5 mmol/L, contact time – 4 hours, AC content – 1 g/L) were measured and are presented in Table 1. With an increase in the R_{OX} ratio, the capacities for CP and Pb(II) increase (Fig. 4), in line with the growth of the specific surface area (S_{BET}). The adsorption capacity for MB also increases and is described by the correlation equation: A_{MB} = 0.697 – 0.323[HNO_3/C] + 0.742 (R^2 = 0.932), with values ranging from 0.72 to 1.09 mmol/g. The specific adsorption capacity, which reflects the surface concentration of adsorption centres, changes little with increasing R_{OX} ratio (Table 1). The values of $A_{MB(S)}$ and $A_{Pb(S)}$ are similar, ranging from 0.42 to 0.52 μmol/m². The values of $A_{CP(S)}$ are 4-5 times higher and remain nearly constant.

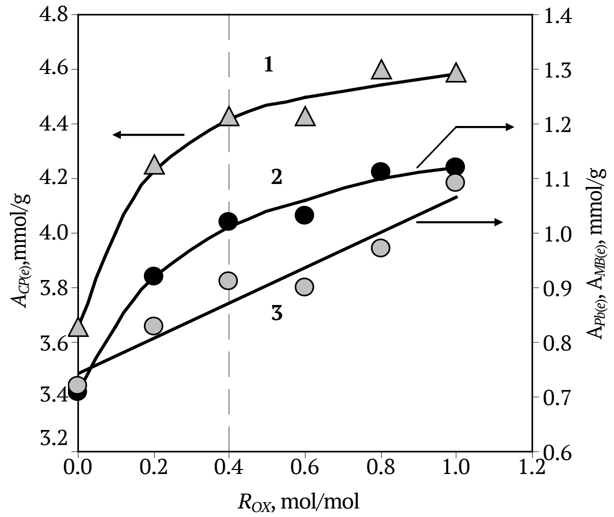

Figure 4. *Adsorption capacities for CP, Pb(II) cations, and MB of AC(D) and AC(D_{ox}) samples produced at different HNO_3-to-carbon ratio*
Note: *1 – adsorption capacity for CP, 2 – adsorption capacity for Pb(II), 3 – adsorption capacity for MB*
Source: *compiled by the authors based on experimental data*

The data obtained showed that nitric acid pre-oxidation of the carbon significantly influences the yield, specific surface area, and adsorption properties of the AC. The primary effect is observed at R_{OX} ratios ⩽ 0.4 mol/mol and manifests in increases in the S_{BET} value (from 1,685 m^2/g to 2,108 m^2/g) and the adsorption capacities for A_{CP} (from 3.66 mmol/g to 4.59 mmol/g), A_{MB} (from 0.72 mmol/g to 1.09 mmol/g), and A_{Pb} (from 0.71 mmol/g to 1.12 mmol/g). However, oxidation has virtually no effect on the surface concentration of ACs. Owing to the marked positive effect of nitric acid oxidation, it was considered appropriate to carry out a more detailed comparison of the properties of two AC samples, namely AC(D) derived from the raw carbon, and AC(D_{OX}), obtained at an R_{OX} ratio of 0.4 mol/mol. The nitrogen adsorption-desorption isotherms at low temperature for these two ACs are shown in Figure 5. At low relative pressures (p/p_0), a sharp increase in the amount of adsorbed nitrogen is observed, which in itself indicates the dominance of microporosity. According to the IUPAC classification (Thommes *et al.,* 2015), these isotherms correspond to type II with H4-type hysteresis, which arises due to the presence of narrow slit-shaped pores and capillary condensation within mesopores.

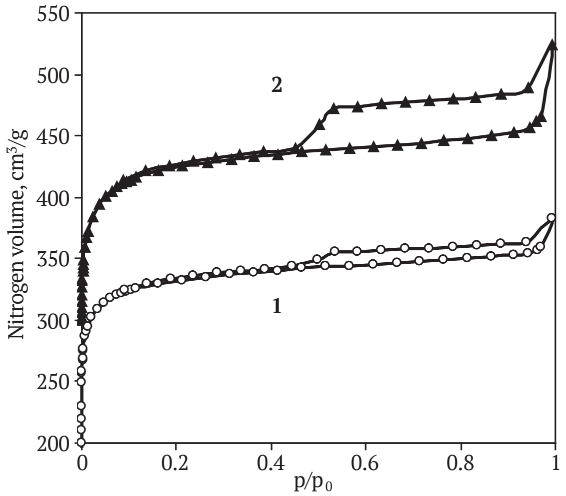

Figure 5. *Nitrogen adsorption-desorption isotherms for AC(D) and AC(D_{OX}) samples*
Note: *1 – sample AC(D), 2 – sample AC(D_{OX})*
Source: *compiled by the authors based on experimental data*

Integral pore volume versus average pore diameter (*D*) relationships, calculated using the 2D-NLDFT method (Fig. 6), showed the following. Alkaline activation primarily produces microporosity, with the majority of the total pore volume attributed to pores with $D \leqslant 5$ nm. Both samples lack pores with diameters in the range $D = 5$-15 nm, but contain mesopores with $D \geqslant 15$ nm. A comparison of the V_t vs *D* relationships and pore size distributions (Fig. 7) indicates that nitric acid oxidation primarily promotes the additional formation of micropores and mesopores with diameters of $D = 2$-5 nm, while having virtually no effect on the development of pores of other sizes. The S_{DFT} vs *D* dependencies exhibit similar trends.

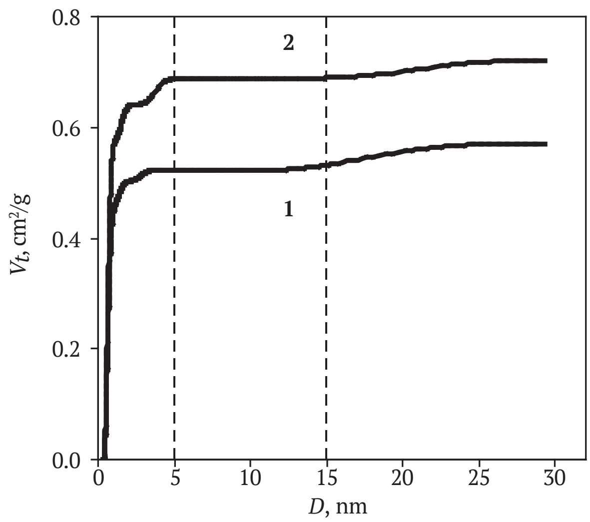

Figure 6. *Integral pore volume as a function of pore diameter for AC(D) and AC(D_{OX}) samples*
Note: *1 – sample AC(D), 2 – sample AC(D_{OX})*
Source: *compiled by the authors based on experimental data*

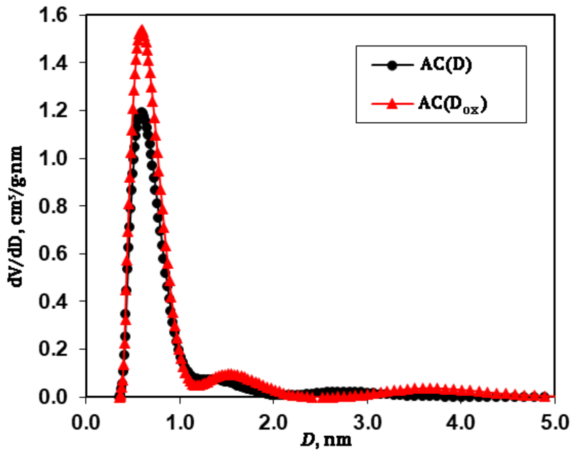

Figure 7. *Pore size distribution of AC(D) and AC(D_{OX}) samples*
Source: *compiled by the authors based on experimental data*

A comparison of the pore volumes and specific surface areas of various pore types in the two AC samples (Table 2) reveals the following. Preliminary nitric acid oxidation results in a 37% increase in total pore volume, a 29% increase in ultramicropore volume, a 27% increase in supermicropore and subnanopore volumes, and a 28% increase in micropore volume. The most substantial increase (88%) is observed in the combined volume of meso- and macropores. The specific surface area S_{DFT} increases by 27%, and S_{me+ma} increases by 50%. The specific surface areas of the other pore types grow proportionally with their volume increases.

Table 2. *Pore volumes and specific surface areas of various pores in AC(D) and AC(D_{OX}) samples*

Sample	Pore volume, cm³/g					
	V_t	V_{umi}	V_{smi}	V_{1nm}	V_{mi}	V_{me+ma}
AC(D)	0.59	0.28	0.22	0.44	0.50	0.09
AC(D_{OX})	0.81	0.36	0.28	0.56	0.64	0.17
Sample	**Specific surface area, m²/g**					
	S_{DFT}	S_{umi}	S_{umi}	S_{1nm}	S_{mi}	S_{me+ma}
AC(D)	1,510	980	510	1,400	1,490	20
AC(D_{OX})	1,920	1,270	620	1,780	1,890	30

Note: *explanations of the designations used for pore volume and specific surface area are provided in the Materials and Methods section*
Source: *compiled by the authors based on experimental data*

Oxidation reduces the proportion of micropore volume ($P_{V(mi)}$) due to an increase in the proportion of meso- and macropores (Table 3). This effect is most pronounced in the subnanopore volume fraction ($P_{V(1nm)}$). However, the proportion of specific surface area attributed to these pores ($P_{S(1nm)}$) remains largely unchanged. Both samples exhibit a high proportion of micropore surface area, amounting to no less than 98%. This indicates that the resulting ACs can be classified as microporous materials, with a predominance of ultramicroporosity.

Table 3. *Pore volumes and specific surface area fractions of various pore types in AC(D) and AC(D_{OX}) samples*

Sample	Pore volume fractions, %				
	$P_{V(umi)}$	$P_{V(smi)}$	$P_{V(1nm)}$	$P_{V(mi)}$	$P_{V(me+ma)}$
AC(D)	47	37	75	85	15
AC(D_{OX})	44	35	69	79	21
Sample	**Specific surface area fractions, %**				
	$P_{S(umi)}$	$P_{S(smi)}$	$P_{S(1nm)}$	$P_{S(mi)}$	$P_{S(me+ma)}$
AC(D)	65	34	93	99	1
AC(D_{OX})	66	32	93	98	2

Note: *explanations of the designations used for pore volume and specific surface area are provided in the Materials and Methods section*
Source: *compiled by the authors based on experimental data*

The adsorption kinetics of CP, MB, and Pb(II) cations were measured at an identical initial concentration of $C_{AD(0)}$ = 5 mmol/L. Adsorption equilibrium was reached within 2-4 hours, depending on the nature of the adsorbate, as illustrated in Figure 8 for the AC(D_{OX}) sample.

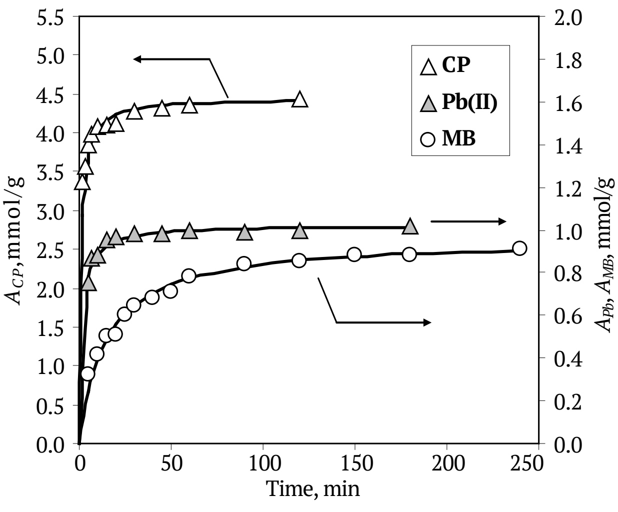

Figure 8. *Adsorption kinetics for the AC(D_{OX}) sample*
Source: *compiled by the authors based on experimental data*

Kinetic curves of a similar shape were also observed for the AC(D) sample. The kinetic model parameters are presented in Table 4. The adsorption kinetics of CP and Pb(II) are poorly approximated by the pseudo-first-order model ($R^2 \leqslant 0.912$), whereas this model is more suitable for the adsorption of MB ($R^2 \geqslant 0.963$). A better fit for describing the kinetics is provided by the pseudo-second-order model, which was used to calculate the solid lines shown in Figure 8. This model suggests that the rate of adsorption is limited by the interaction between the adsorbate and the AC surface (Revellame *et al.*, 2020), rather than by diffusion into the porous structure of the AC. The highest adsorption capacities were observed for CP. The values of $A_{AD(e)}$ differ by a factor of 4.4 to 5.2 depending on the adsorbate, while the k_2 values vary by a factor of 6.1 for AC(D) and 8.8 for AC(D_{OX}). The highest initial adsorption rate is recorded for CP, and the lowest for MB. The differences in $R_{AD(0)}$ rate between the adsorbates are substantial – up to 105-fold for AC(D) and 65-fold for AC(D_{OX}). Oxidation with nitric acid promotes the formation of ACs with enhanced adsorption rates – 1.2 times faster for CP, 1.9 times for MB, and 4.1 times for Pb(II) cations. This indicates a significant improvement in the efficiency of ACs for rapid water purification applications. The amount of adsorbate taken up during the initial stage of adsorption can be estimated using the adsorption capacity $A_{AD(1)}$, calculated for the first minute of the process. Accordingly, the ratio $A_{AD(1)}/A_{AD(e)}$ reflects the efficiency of adsorbate uptake by the AC samples during the early phase. Data from Table 4 show that the lowest efficiency is observed during the adsorption of MB (0.65%-1.24%), while the highest is recorded for CP: approximately half of the maximum amount of 4-chlorophenol is adsorbed within the first minute. This property of the adsorbent is particularly important for the rapid removal of highly toxic compounds from water. The kinetic data were additionally approximated using the intraparticle diffusion model, as illustrated for the AC(D_{OX}) sample in Figure 9.

Table 4. *Parameters of kinetic models of adsorption by samples AC(D) and AC(D_{OX})*

Sample	Model	Parameter	Adsorbate		
			CP	MB	Pb(II)
AC(D)	Pseudo-first-order	$A_{AD(exp)}$, mmol/g	3.66	0.72	0.71
		$k_1 \cdot 10^2$, min^{-1}	7.65	2.42	0.25
		R^2	0.824	0.985	0.715
	Pseudo-second-order	$A_{AD(e)}$, mmol/g	3.70	0.82	0.72
		k_2, g/mmol·min	0.26	0.051	0.31
		$R_{AD(0)}$, mmol/g·min	3.56	0.034	0.16
		$A_{AD(1)}$, mmol/g	1.81	0.033	0.13
		$A_{AD(1)}/A_{AD(e)}$, %	36	0.65	2.6
		R^2	0.998	0.997	0.998
AC(D_{OX})	Pseudo-first-order	$A_{AD(exp)}$, mmol/g	4.43	0.91	1.02
		$k_1 \cdot 10^2$, min^{-1}	4.18	1.83	1.84
		R^2	0.912	0.963	0.651
	Pseudo-second-order	$A_{AD(e)}$, mmol/g	4.45	0.96	1.03
		k_2, g/mmol·min	0.22	0.072	0.63
		$R_{AD(0)}$, mmol/g·min	4.29	0.066	0.65
		$A_{AD(1)}$, mmol/g	2.19	0.062	0.40
		$A_{AD(1)}/A_{AD(e)}$, %	44	1.24	8.0
		R^2	0.997	0.998	0.998

Note: *explanations of the designations used for adsorption kinetic parameters are provided in the Materials and Methods section*
Source: *compiled by the authors based on experimental data*

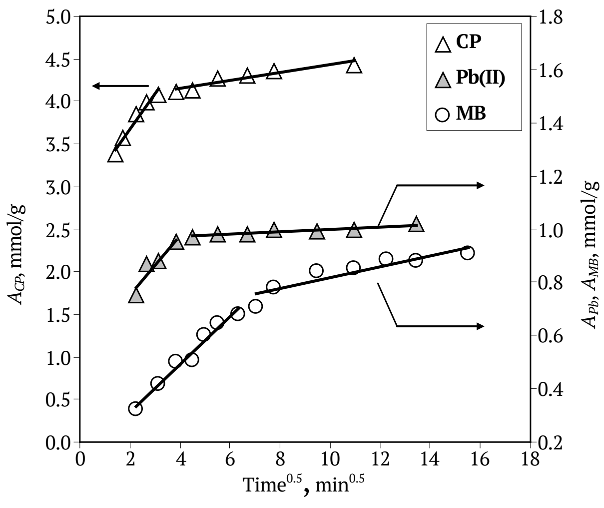

Figure 9. *Application of the intraparticle diffusion model to adsorption by AC(D_{OX}) sample*
Source: *compiled by the authors based on experimental data*

A similar pattern was observed for AC(D_{OX}), and the coefficients of the equations are presented in Table 5. This model implies the following: 1) the presence of several linear segments indicates that multiple adsorption mechanisms are involved; 2) diffusion is the rate-limiting step if the dependence of A_{AD} versus $\tau^{0.5}$ passes through the origin (C_{d1} = 0) (Wang & Guo, 2022). For both AC samples, the A_{AD} versus $\tau^{0.5}$ dependencies exhibit two linear regions, indicating the involvement of at least two adsorption mechanisms. This is observed for all adsorbates, albeit within different time intervals. For CP adsorption, the first mechanism dominates during the initial ~10 minutes; for Pb(II) cations, during 15-20 minutes; and for MB, during 40-50 minutes. The adsorption of MB by AC(D) sample is characterised by a low C_{d1} value (−0.05 mmol/g), suggesting that the rate of adsorption is limited by diffusion. Additionally, MB molecules are significantly larger than the other adsorbates, which hinders their transport into the microporous structure of AC. However, this limitation is mitigated in the case of AC derived from oxidised coal. In the remaining cases, the initial segments do not pass through the origin (C_{d1} > 0), indicating the absence of diffusion constraints during the early stage of adsorption. This finding is consistent with the better applicability of the pseudo-second-order model, which also assumes no diffusion limitation. The adsorption isotherms for AC(D) and AC(D_{OX}) samples are presented in Figures 10 and 11, respectively. The data were approximated using the Langmuir and Freundlich models, which are the most commonly applied to describe the adsorption of the selected adsorbates from aqueous media.

Table 5. *Parameters of the intraparticle diffusion model for adsorption by AC(D) and AC(DOX) samples*

Sample	Adsorbate	Parameters					
		k_{d1}, mmol/g·min$^{0.5}$	kd2, mmol/g·min$^{0.5}$	C_{d1}, mmol/g	C_{d2}, mmol/g	R^2_{d1}	R^2_{d2}
AC(D)	CP	0.535	0.017	1.660	3.497	0.937	0.526
	MB	0.091	0.015	−0.05	0.506	0.964	0.865
	Pb(II)	0.060	0.011	0.322	0.571	0.950	0.994
AC(D_{OX})	CP	0.410	0.046	2.854	3.965	0.956	0.871
	MB	0.091	0.021	0.130	0.606	0.975	0.840
	Pb(II)	0.109	0.005	0.539	0.951	0.854	0.859

Note: *k_{d1} and k_{d2} are the rate constants of the intraparticle diffusion model for the first and second linear regions shown in Figure 9; C_{d1} and C_{d2} are the intercepts; R^2_{d1} and R^2_{d2} are the determination coefficients for the approximations of the first and second regions*
Source: *compiled by the authors based on experimental data*

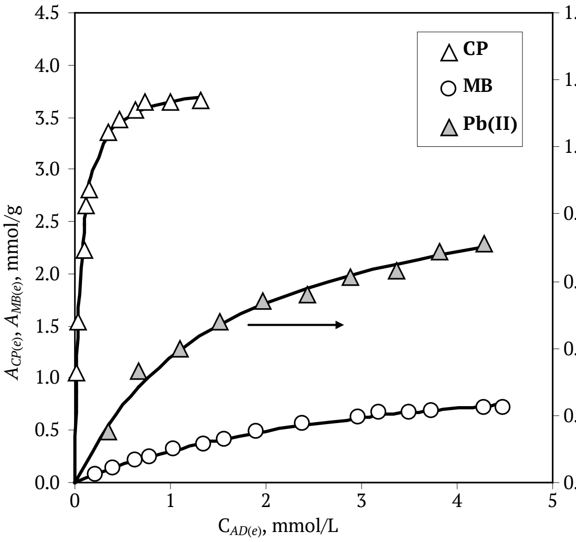

Figure 10. *Adsorption isotherms for the AC(D) sample*
Source: *compiled by the authors based on experimental data*

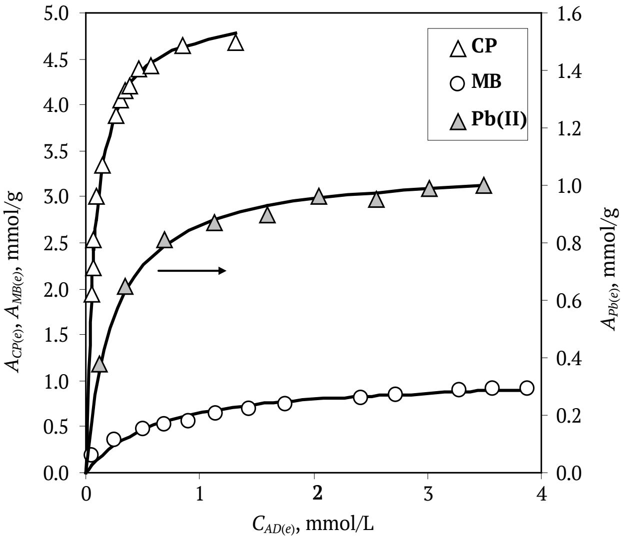

Figure 11. *Adsorption isotherms for the AC(D_{OX}) sample*
Source: *compiled by the authors based on experimental data*

From the linearised forms of these models, the parameters of the Langmuir (using the coordinates "$C_{AD(e)}/A_{AD(e)}) - C_{AD(e")}$ and Freundlich (using "$lnA_{AD(e)}) - ln$-$C_{AD(e)}$") equations were calculated, and the results are presented in Table 6. The Langmuir model assumes a chemically homogeneous surface of the AC and that the maximum adsorption capacity corresponds to a saturated monolayer of adsorbate, denoted as $A_{AD(L)}$. In contrast, the Freundlich model describes multilayer adsorption on a chemically heterogeneous surface containing adsorption sites with varying activity. The *1/n* coefficient accounts for surface heterogeneity, reflected in the range of interaction energies between ACs and adsorbate molecules. Adsorption is considered favourable when 0 < *1/n* < 1, while values of *1/n* > 1 indicate an unfavourable process (Al-Ghouti & Da'ana, 2020).

Table 6. *Adsorption isotherm parameters for the AC(D) and AC(D_{OX}) samples*

Sample	Model	Parameter	Adsorbate		
			CP	MB	Pb(II)
AC(D)	Langmuir	$A_{AD(L)}$, mmol/g	3.834	1.282	0.960
		$k_{AD(L)}$, L/mmol	19.38	0.311	0.622
		$A_{AD(S)}$, μmol/m^2	2.54	0.85	0.64
		R^2	0.998	0.991	0.984
	Freundlich	$k_{AD(F)}$, (mmol/g)(L/mmol)$^{1/n}$	4.042	0.282	0.343
		1/n	0.276	0.734	0.556
		R^2	0.915	0.987	0.931

Table 6. Continued

Sample	Model	Parameter	Adsorbate		
			CP	MB	Pb(II)
$AC(D_{OX})$	Langmuir	$A_{AD(L)}$, mmol/g	5.043	1.037	1.069
		$k_{AD(L)}$, L/mmol	13.398	1.674	4.097
		$A_{AD(S)}$, μmol/m^2	2.63	0.54	0.56
		R^2	0.998	0.992	0.998
	Freundlich	$k_{AD(F)}$, (mmol/g)(L/mmol)$^{1/n}$	5.788	0.582	0.774
		$1/n$	0.325	0.365	0.256
		R^2	0.936	0.991	0.904

Source: *compiled by the authors based on experimental data*

According to the determination coefficients, the Langmuir model provides a better fit to the isotherm data. The values of the saturated monolayer capacity $A_{AD(L)}$ differ by a factor of 4.0-4.9 across the adsorbates and, for the AC(D) sample, increase in the order: Pb(II) < MB < CP. For the $AC(D_{OX})$ sample, the sequence differs: MB < Pb(II) < CP, although the $A_{AD(L)}$ values for Pb(II) and MB are nearly identical. The numerical values of $A_{AD(L)}$ (Table 6) are within the commonly reported range. According to the literature, the adsorption capacity of most ACs for CP generally ranges from 0.33 to 2.52 mmol/g (Chen *et al.*, 2017), and for Pb(II) cations from 0.029 to 1.42 mmol/g (Ghorbani *et al.*, 2020). The capacity for MB typically varies between 0.021 and 2.58 mmol/g (Oladoye *et al.*, 2022; Jasri *et al.*, 2023), although significantly higher values of $A_{MB(L)}$ = 5.50-7.04 mmol/g have also been reported (Li *et al.*, 2021). Comparison of the obtained results with published data indicates that both AC(D) and $AC(D_{OX})$ samples exhibit acceptable capacities for MB and Pb(II) cations, as well as high adsorption capacities for 4-chlorophenol. The adsorption constants $k_{AD(L)}$ for AC(D) vary by a factor of 62 across the different adsorbates, whereas for $AC(D_{OX})$ the variation is only eightfold. This suggests that preoxidation of the coal makes the AC significantly less sensitive to the adsorbate's nature, thereby reducing adsorption selectivity.

A comparison of the adsorption parameters for the two AC samples yields the following observations. The $AC(D_{OX})$ sample adsorbs greater quantities of all adsorbates (Table 4): 1.20 times more CP, 1.17 times more MB, and 1.43 times more Pb(II) cations. For Pb(II) and MB, the specific adsorption capacities $A_{AD(S)}$ of $AC(D_{OX})$ are lower than those of AC(D), while for CP, the $A_{AD(S)}$ value is higher, although not substantially so. The lower surface concentrations of adsorbed Pb(II) and MB suggest that treatment with HNO_3 negatively affects the formation of ACs under alkaline activation conditions. The AC(D) and $AC(D_{OX})$ samples exhibit significantly higher surface concentrations of ACs – 4 to 5 times greater – that are active exclusively towards CP. This may be attributed to structural features, including differences in the number of functional groups and the presence of graphene fragments within the spatial framework of the AC. The initial adsorption rate of CP is high for both materials (Table 4), although it is 1.2 times higher for the $AC(D_{OX})$ sample. Other adsorbates are also absorbed more rapidly by this sample: MB at twice the rate, and Pb(II) cations at four times the rate. Furthermore, the oxidised carbon material possesses a more developed total surface area and a subnanoporous structure. Consequently, the $AC(D_{OX})$ sample is a more effective adsorbent than the AC(D) material derived from unoxidised long-flame coal.

Overall, nitric acid oxidation has a pronounced impact on the properties of AC. In the study by Y. Gokce & Z. Aktas (2014), it was demonstrated that treating AC with an HNO_3 solution at 90°C damages the porous structure. As the concentration of nitric acid increases to 80%, the pore volume decreases from 1.18 cm^3/g to 0.02 cm^3/g, while the specific surface area decreases from 1,398 m^2/g to 49 m^2/g. This substantial reduction in S_{BET} (by a factor of 28.5) and V_t (by a factor of 59) was attributed to the destruction of pore walls due to oxidative degradation, which transforms micro- and mesopores into macropores.in the process. These trends are qualitatively supported by the findings of I. Demiral *et al.* (2021) investigated the oxidation of AC with nitric acid (⩽ 69%) under similar conditions (90°C). Increasing the HNO_3 concentration to 69% led to a 16.1-fold reduction in V_t (from 0.680 cm^3/g to 0.042 cm^3/g) and a 93.3-fold decrease in S_{BET} (from 1,399 m^2/g to 15 m^2/g). According to W. Somyanonthanakun *et al.* (2023), oxidation of biomass-derived AC under milder conditions (4 hours, 80°C, $[HNO_3]$ = 4-10 M) resulted in less severe degradation of the porous structure, with S_{BET} decreasing by a factor of 1.8 (from 767 m^2/g to 418 m^2/g) and V_t by a factor of 3.7 (from 0.78 cm^3/g to 0.21 cm^3/g). A deterioration of pore structure parameters – typically by factors of 2 to 6 – as a result of nitric acid oxidation was also reported by L. Giraldo *et al.* (2020) for lignocellulosic-based AC, by E. Wolak & A. Orzechowska-Zięba (2024) for industrial AC, and by L.S. Queiroz *et al.* (2020) for a series of ACs prepared via alkaline activation of biomass with various KOH ratios (R_{KOH} = 1-5 g/g). Analysis of the aforementioned studies indicates that pore structure degradation occurs in all cases. However, the extent of this degradation depends both on the oxidation conditions and the type of AC used, with no clear patterns identified to date.

A more complex picture emerges when oxidation with nitric acid is carried out at room temperature. According to H.-K. Kim *et al.* (2024), treating AC at 25 °C for 24 hours in solutions with HNO_3 concentrations ⩽3 M reduced the specific surface area from 1,027 m^2/g to 746 m^2/g, whereas a concentration of 5 M resulted in an increase to 793 m^2/g.

This effect was attributed to oxidative destruction that opens previously closed internal pores of AC – an effect not observed in the studies by Y. Gokce & Z. Aktas (2014), I. Demiral *et al.* (2021), or W. Somyanonthanakun *et al.* (2023). An opposite trend was reported by X. Jiang *et al.* (2019) for coke-derived AC under similar oxidation conditions (25°C, 4 hours): increasing the HNO_3 concentration to 3 M increased the S_{BET} from 642 m^2/g to 802 m^2/g, but further increasing it to 4 M reduced it to 689 m^2/g. Overall, the negative effect of oxidation on AC porosity is mitigated at lower HNO_3 concentrations and lower temperatures, though the outcome varies depending on the carbon precursor material. An unusual effect was first identified in a study by R. Pietrzak *et al.* (2009): while nitric acid oxidation of AC reduced the specific surface area from 2,876 m^2/g to 359 m^2/g – consistent with other studies – oxidising the precursor material (orthocoke fossil coal) increased the surface area to 3,087 m^2/g. This effect was confirmed by data from J.H. Kim *et al.* (2019) for wood-derived AC: contact with an HNO_3 solution (5%, 80°C, 12 hours) reduced the S_{BET} from 1,485 m^2/g to 833 m^2/g, while subsequent alkaline activation increased it to 2,027 m^2/g. A similar trend is observed in the present study when oxidising the precursor – long-flame coal (Table 1).

Nitric acid oxidation also affects the adsorption properties of AC, although systematic data remain limited. Y. Gokce & Z. Aktas (2014) found that AC oxidation increased the adsorption capacity for MB by a factor of 1.6 – from 1.34 mmol/g to 2.14 mmol/g – despite a substantial 28.5-fold reduction in specific surface area. This indicates an increase in the surface concentration of the adsorbed dye from 0.75 μmol/m^2 to 2.55 μmol/m^2. An even greater increase in MB capacity was reported by D.H. Nguyen *et al.* (2019) following nitric acid oxidation of biomass carbonisate: the $A_{MB(L)}$ value increased 4.5-fold (from 0.17 mmol/g to 0.77 mmol/g), while the specific surface area changed only slightly (decreasing from 7.33 m^2/g to 4.49 m^2/g). Of particular note is that oxidation significantly improved the adsorption performance of a carbon material with a poorly developed surface (S_{BET} = 4.49 m^2/g), corresponding to a specific capacity of $A_{MB(S)}$ = 170 μmol/m^2. In the present study, oxidation also increases the $A_{MB(e)}$ value, although the specific capacity changes only slightly and remains within the range $A_{MB(S)}$ = 0.430.51 μmol/m^2 (Table 1). A comparison of the MB adsorption data suggests that oxidation of the precursor affects the adsorption properties of AC differently from the oxidation of the AC itself. The iodine adsorption capacity varies in parallel with changes in specific surface area following nitric acid oxidation, as reported by R. Pietrzak *et al*. (2009) and X. Jiang *et al.* (2019). However, a strict proportionality between the I2 capacity and S_{BET} is not maintained.

The most pronounced effect of HNO_3 treatment is the enhancement of the adsorption activity of AC with respect to lead cations. This is attributed to the increased content of hydroxyl and acidic functional groups in oxidised carbon materials (Rudenko *et al*., 2021). For instance, according to W. Somyanonthanakun *et al.* (2023), AC oxidation increases the Pb(II) adsorption capacity 3.5-fold (from 0.29 mmol/g to 1.02 mmol/g), even though the specific surface area decreases from 767 cm^2/g to 418 cm^2/g. The adsorption kinetics are better described by the pseudo-second-order equation, and the adsorption isotherms fit the Langmuir model, which aligns with the present study's findings (Tables 4 and 6). The $k_{Pb(L)}$ values range from 6.22 to 103 L/mol, and k_2 values fall within 1.24-9.53 g/mmol·min, showing little dependence on HNO_3 concentration. In this case, the rate constants are significantly lower, although the Pb(II) adsorption capacities are of the same order of magnitude.

Analysis of the presented data reveals fundamentally different outcomes of nitric acid oxidation applied to the precursor and the resulting activated carbon. Oxidation of AC reduces its specific surface area and pore volume, transforms its microporous structure into a macroporous one, and partially destroys the carbon spatial framework. In contrast, oxidation of the precursor enhances its chemical reactivity during activation, increases the specific surface area of the resulting AC, and promotes micropore formation. Nitric acid oxidation of the precursor is thus an independent and equally important method of influencing the porous structure and adsorption properties of activated carbon.

Conclusions

For the first time, the porous structure and properties of AC samples derived from long-flame coal through a combination of nitric acid oxidation and alkaline activation at a low KOH-to-coal ratio (1 g/g) have been investigated. Interaction with a 50% HNO_3 solution immobilises structural oxygen and nitrogen within the coal via the formation of phenolic, carboxylic and nitro groups, as well as ethers and esters. This is accompanied by an increase in coal mass, which exhibits a pronounced dependence on the HNO_3-to-carbon ratio in the range R_{OX} = 0.1-1.0 mol/mol, with a maximum increase (16%) observed at R_{OX} = 0.4 mol/mol. Coal samples oxidised at various R_{OX} ratios were converted into AC under identical alkaline activation conditions. It was found that increasing the R_{OX} ratio from 0 to 1.0 mol/mol reduces the AC yield (from 50.2% to 33.85%) but increases the specific surface area (from 1,685 m^2/g to 2,216 m^2/g). The dominant portion (~80%) of the effect occurs within the range of $R_{OX} \leqslant 0.4$ mol/mol. The adsorption capacities of the AC for 4-chlorophenol (CP), methylene blue (MB), and Pb(II) cations also increase with rising R_{OX}. The obtained results demonstrate that preliminary nitric acid oxidation of coal has a significant effect on the yield, specific surface area, and adsorption properties of the AC. The most pronounced influence is observed at $R_{OX} \leqslant 0.4$ mol/mol. A detailed comparison was made between two samples: AC(D), derived from untreated coal, and AC(D_{OX}), obtained from coal oxidised at R_{OX} = 0.4 mol/mol. The nitrogen adsorption–desorption isotherms at low temperature correspond to type II with an H4-type hysteresis loop, according to the IUPAC classification. Analysis of the pore volume and surface area as a function of pore diameter (*D*) revealed that nitric acid oxidation most significantly promotes the additional formation of micropores and mesopores with D = 2-5 nm, while it has little effect on the development of pores of other sizes. Both samples exhibit a high proportion (98%) of micropore surface area, indicating that the AC is microporous in nature, with a predominance of ultramicroporosity.

Kinetic measurements of CP, MB, and Pb(II) adsorption showed that equilibrium is reached within 2-4 hours, depending on the nature of the adsorbate. The kinetic curves are better described by the pseudo-second-order model, suggesting that the adsorption rate is limited by interactions between the adsorbate and surface active sites of the AC. This is further supported by the application of the intraparticle diffusion model. The adsorption isotherms are best fitted by the Langmuir model, from which the monolayer adsorption capacities of the adsorbates were calculated. Comparison with published data indicates that both AC(D) and AC(D_{ox}) possess acceptable adsorption capacities for MB and Pb(II) and exhibit high adsorption capacities for CP. The Langmuir constants for AC(D) vary by a factor of 62 across different adsorbates, whereas for AC(D_{ox}), the variation is only by a factor of 8. This suggests that pre-oxidation of oxidised coal renders the AC significantly less sensitive to the nature of the adsorbate and reduces adsorption selectivity. Compared to AC(D), the AC(D_{ox}) sample adsorbs greater quantities of CP (1.20 times more), MB (1.17 times more), and Pb(II) cations (1.43 times more). The initial adsorption rate of CP is high for both materials, but it is 1.2 times faster for AC(D_{ox}). Other adsorbates are also absorbed more rapidly by this sample: MB at twice the rate, and Pb(II) cations at four times the rate. This property is particularly important for the rapid removal of highly toxic compounds from water. Furthermore, the oxidised coal-based material exhibits a more developed overall surface area and a subnanoporous structure. Therefore, AC(D_{ox}) sample is a more effective adsorbent than AC(D), which is derived from non-oxidised long-flame coal. The results obtained provide a positive assessment of the effect of nitric acid oxidation of coal on the adsorption properties of AC produced via alkaline activation. Future research will focus on determining the impact of oxidation on the characteristics of AC derived from highly metamorphosed coals, particularly anthracites, which exhibit low chemical reactivity towards alkalis. Additional studies will also explore further practical applications of the AC, including its use in radionuclide and toxic compound capture and energy storage for supercapacitors.

Acknowledgements

The authors would appreciate to thank Dr. R.D. Mysyk (Basque Research and Technology Alliance, Spain) for his assistance in conducting adsorption measurements and calculations of low-temperature nitrogen adsorption isotherms.

Funding

Financial support for this work was provided by the National Academy of Sciences of Ukraine (State Registration Number: 0117U000022).

Conflict of Interest

None.

References

[1] Al-Ghouti, M.A., & Da'ana, D.A. (2020). Guidelines for the use and interpretation of adsorption isotherm models: A review. *Journal of Hazardous Materials*, 393, article number 122383. doi: 10.1016/j.jhazmat.2020.122383.

[2] Bellamy, L.J. (1975). *The infra-red spectra of complex molecules*. Dordrecht: Springer Dordrecht. doi: 10.1007/978-94-011-6017-9.

[3] Bergna, D., Varila, T., Romar, H., & Lassi, U. (2022). Activated carbon from hydrolysis lignin: Effect of activation method on carbon properties. *Biomass and Bioenergy*, 159, article number 106387. doi: 10.1016/j.biombioe.2022.106387.

[4] Chen, C., Geng, X., & Huang, W.A. (2017). Adsorption of 4-chlorophenol and aniline by nanosized activated carbons. *Chemical Engineering Journal*, 327, 941-952. doi: 10.1016/j.cej.2017.06.183.

[5] Demiral, I., Samdan, C., & Demiral, H. (2021). Enrichment of the surface functional groups of activated carbon by modification method. *Surfaces and Interfaces*, 22, article number 100873. doi: 10.1016/j.surfin.2020.100873.

[6] DSTU 3472-96. (2009). *Lignite, hard coal and anthracite. Classification. With Amendment (IPS No. 9-2003) and Amendment No. 1 (IPS No. 12-2009)*. Retrieved from https://online.budstandart.com/ua/catalog/doc-page.html?id_doc=29353.

[7] Ghorbani, M., Seyedin, O., & Aghamohammadhassan, M. (2020). Adsorptive removal of lead (II) ion from water and wastewater media using carbon-based nanomaterials as unique sorbents: A review. *Journal of Environmental Management*, 254, article number 109814. doi: 10.1016/j.jenvman.2019.109814.

[8] Giraldo, L., Vargas, D.P., & Moreno-Piraján, J.C. (2020). Study of CO_2 adsorption on chemically modified activated carbon with nitric acid and ammonium aqueous. *Frontiers in Chemistry*, 8, article number 543452. doi: 10.3389/fchem.2020.543452.

[9] Gokce, Y., & Aktas, Z. (2014). Nitric acid modification of activated carbon produced from waste tea and adsorption of methylene blue and phenol. *Applied Surface Science*, 313, 352-359. doi: 10.1016/j.apsusc.2014.05.214.

[10] Jagiello, J., Kyotani, T., & Nishihara, H. (2020). Development of a simple NLDFT model for the analysis of adsorption isotherms on zeolite templated carbon (ZTC). *Carbon*, 169, 205-213. doi: 10.1016/j.carbon.2020.06.032.

[11] Jiang, X., Lan, X., Song, Y., & Xing, X. (2019). Adsorption of COD in coking wastewater on nitric acid-modified blue coke activated carbon. *Journal of Chemistry*, 2019(1), article number 8593742. doi: 10.1155/2019/8593742.

[12] Kim, H.-K., Kim, S.-J., Kim, H.-R., & Park, J.-W. (2024). Nitric acid modified powdered activated carbon for simultaneous adsorption of lead and phenol in aqueous solution. *Journal of Environmental Chemical Engineering*, 12(6), article number 114889. doi: 10.1016/j.jece.2024.114889.

[13] Kim, J.H., Hwang, S.Y., Park, J.E., Lee, G.B., Kim, H., Kim, S., & Hong, B.U. (2019). Impact of the oxygen functional group of nitric acid-treated activated carbon on KOH activation reaction. *Carbon Letters*, 29, 281-287. doi: 10.1007/s42823-019-00024-0.

[14] Lee, S.-Yi., & Mahajan, R.L. (2021). A facile method for coal to graphene oxide and its application to a biosensor. *Carbon*, 181, 408-420. doi: 10.1016/j.carbon.2021.05.007.

[15] Lee, S.M., Lee, S.H., Park, S., Yoon, S.-H., & Jung, D.-H. (2022). Preparation of mesoporous activated carbon by preliminary oxidation of petroleum coke with hydrogen peroxide and its application in capacitive deionization. *Desalination*, 539, article number 115901. doi: 10.1016/j.desal.2022.115901.

[16] Li, L., Wu, M., Song, C., Liu, L., Gong, W., Ding, Y., & Yao, J. (2021). Efficient removal of cationic dyes via activated carbon with ultrahigh specific surface derived from vinasse wastes. *Bioresource Technology*, 322, article number 124540. doi: 10.1016/j.biortech.2020.124540.

[17] Li, M., Liu, X., Sun, C., Stevens, L., & Liu, H. (2022). Synthesis and characterization of advanced bio-carbon materials from Kraft lignin with enhanced CO_2 capture properties. *Journal of Environmental Chemical Engineering*, 10(3), article number 107471. doi: 10.1016/j.jece.2022.107471.

[18] Nguyen, D.H., Tran, H.N., Chao, H.-P., & Lin, C.-C. (2019). Effect of nitric acid oxidation on the surface of hydrochars to sorb methylene blue: An adsorption mechanism comparison. *Adsorption Science & Technology*, 37(7-8) 607-622. doi: 10.1177/0263617419867519.

[19] Oladoye, P.O., Ajiboye, T.O., Omotola, E.O., & Oyewola, O.J. (2022). Methylene blue dye: Toxicity and potential elimination technology from wastewater. *Results in Engineering*, 16, article number 100678. doi: 10.1016/j.rineng.2022.100678.

[20] Pietrzak, R., Nowicki, P., & Wachowska, H. (2009). The influence of oxidation with nitric acid on the preparation and properties of active carbon enriched in nitrogen. *Applied Surface Science*, 255(6), 3586-3593. doi: 10.1016/j.apsusc.2008.10.002.

[21] Queiroz, L.S., Souza, L.K.C.D., Thomaz, K.T.C., Lima, E.T.L., Rocha Filho, G.N., Nascimento, L.A.S.D., Oliveira Pires, L.H., Faial, K.D.C.F., & da Costa, C.E.F. (2020). Activated carbon obtained from amazonian biomass tailings (acai seed): Modification, characterization, and use for removal of metal ions from water. *Journal of Environmental Management*, 270, article number 110868. doi: 10.1016/j.jenvman.2020.110868.

[22] Revellame, E.D., Fortela, D.L., Sharp, W., & Zappi, M.E. (2020). Adsorption kinetic modeling using pseudo-first order and pseudo-second order rate laws: A review. *Cleaner Engineering and Technology*, 1, article number 100032. doi: 10.1016/j.clet.2020.100032.

[23] Rudenko, V., Ivanenko, I., Kosogina, I., & Burmak, A. (2021). New efficient carbon adsorbent for water deironing. *Bulletin of Cherkasy State Technological University*, 26(1), 144-154. doi: 10.24025/2306-4412.1.2021.225318.

[24] Somyanonthanakun, W., Ahmed, R., Krongtong, V., & Thongmee, S. (2023). Studies on the adsorption of Pb(II) from aqueous solutions using sugarcane bagasse-based modified activated carbon with nitric acid: Kinetic, isotherm and desorption. *Chemical Physics Impact*, 6, article number 100181. doi: 10.1016/j.chphi.2023.100181.

[25] Tamarkina, Yu.V., Anishchenko, V.M., Redko, A.M., & Kucherenko, V.O. (2020). Adsorption properties of coals activated with potassium hydroxide. Influence of coal rank. *Chemistry, Physics and Technology of Surface*, 11(2), 175-189. doi: 10.15407/hftp11.02.175.

[26] Tamarkina, Yu.V., Anishchenko, V.M., Redko, A.M., & Kucherenko, V.O. (2022). Alkali activated coals. Microporous structure and capability to adsorb phenol compounds. *Chemistry, Physics and Technology of Surface*, 13(1), 111-124. doi: 10.15407/hftp13.01.111.

[27] Thommes, M., Kaneko, K., Neimark, A.V., Olivier, J.P., Rodriguez-Reinoso, F., Rouquerol, J., & Sing, K.S.W. (2015). Physisorption of gases, with special reference to the evaluation of surface area and pore size distribution (IUPAC Technical Report). *Pure and Applied Chemistry*, 87(9-10), 1051-1069. doi: 10.1515/pac-2014-1117.

[28] Wang, J., & Guo, X. (2022). Rethinking of the intraparticle diffusion adsorption kinetics model: Interpretation, solving methods and applications. *Chemosphere*, 309(2), article number 136732. doi: 10.1016/j.chemosphere.2022.136732.

[29] Wolak, E., & Orzechowska-Zięba, A. (2024). Change of the surface and structure of activated carbon as a result of HNO_3 modification. *Adsorption*, 30, 121-128. doi: 10.1007/s10450-023-00401-2.

[30] Zhu, S., Xu, J., Xie, J., Zhang, Z., Ding, Q., & Chen, K. (2024). Ultrafast dyeing wastewater purification by high-performance and reusable lignin-derived activated porous carbon filter. *Separation and Purification Technology*, 349, article number 127672. doi: 10.1016/j.seppur.2024.127672.

Адсорбенти з вугілля, окисненого азотною кислотою та активованого гідроксидом калію

Володимир Кучеренко

Доктор хімічних наук, старший науковий співробітник
Інститут фізико-органічної хімії і вуглехімії ім. Л.М. Литвиненка Національної академії наук України
02155, Харківське шосе, 50, м. Київ, Україна
https://orcid.org/0000-0001-7234-947X

Юлія Тамаркіна

Кандидат хімічних наук, старший науковий співробітник
Інститут фізико-органічної хімії і вуглехімії ім. Л.М. Литвиненка Національної академії наук України
02155, Харківське шосе, 50, м. Київ, Україна
https://orcid.org/0000-0002-8747-4481

Анастасія Редько

Провідний інженер
Інститут фізико-органічної хімії і вуглехімії ім. Л.М. Литвиненка Національної академії наук України
02155, Харківське шосе, 50, м. Київ, Україна
https://orcid.org/0000-0001-9768-4020

Ірина Фролова

Кандидат хімічних наук, науковий співробітник
Інститут фізико-органічної хімії і вуглехімії ім. Л.М. Литвиненка Національної академії наук України
02155, Харківське шосе, 50, м. Київ, Україна
https://orcid.org/0000-0001-9660-5474

Анотація. Найбільш ефективним методом отримання вуглецевих адсорбентів з високорозвиненою поверхнею (⩾1 000 м^2/г) є лужна активація. Її головний недолік – необхідність використання великих кількостей лугу – робить актуальним дослідження, спрямовані на удосконалення процесу. Мета роботи – кількісно оцінити вплив азотнокислотного окиснення довгополуменевого вугілля на пористу структуру та адсорбційні властивості адсорбентів, отриманих лужною активацією при невеликому співвідношенні KOH/вугілля (⩽1 г/г). У дослідженні використано експериментальний, аналітичний та порівняльний методи наукового пізнання. Характеристики адсорбентів отримано за даними інфрачервоної спектроскопії, порометрії, кінетики та ізотерм адсорбції 4-хлорфенолу, барвника метиленового блакитного та катіонів свинцю з водних розчинів (25°C). Встановлено, що попереднє окиснення вугілля азотною кислотою утворює у вугільному каркасі етерні, естерні, фенольні, карбоксильні і нітрогрупи, що обумовлює приріст ваги вугілля до 16 % та істотно впливає на формування адсорбентів. Збільшення співвідношення HNO_3/карбон вугілля з 0 до 1,0 моль/моль зменшує вихід адсорбенту (з 50,2 % до 33,85 %), підвищує питому площу поверхні (з 1 685 м^2/г до 2 216 м^2/г) та на 25-51 % покращує адсорбційні властивості. Домінуюча частина (~80 %) впливу відбувається в інтервалі ⩽0,4 моль/моль. Порівнянням характеристик пористої структурі адсорбентів встановлено, що окиснення найбільше сприяє утворенню субнанопор і мезопор з діаметром 2-5 нм. Зіставленням адсорбційних властивостей визначено, що адсорбенти з окисненого вугілля адсорбують більшу кількість адсорбатів (в 1,20-1,43 рази) з більшою початковою швидкістю (в 1,2-4,0 рази). Ця властивість адсорбенту дуже важлива для термінового очищення води від високотоксичних сполук. Адсорбент з окисненого вугілля має розвиненішу поверхню і субнанопористу структуру та є більш адсорбційно активним ніж матеріал з неокисненого вугілля. Попереднє окиснення дозволяє суттєво збільшити адсорбційну здатність активованого вугілля вловлювати екотоксиканти з водних середовищ

Ключові слова: оксивугілля; лужний термохемоліз; пористий вуглецевий матеріал; пориста структура; поглинання екотоксикантів

TECHNOLOGIES AND ENGINEERING

Journal homepage: https://technologies-engineering.com.ua/en
Vol. 26, No. 3, 2025

Received: 08.01.2025
Revised: 14.05.2025
Accepted: 25.06.2025

UDC 536.65:697.9:620.91
DOI: 10.30857/2786-5371.2025.3.3

Analysis of the use of phase change materials to improve building energy efficiency and thermal energy storage

Yevhen Lazariev*

Postgraduate Student
National Technical University of Ukraine "Igor Sikorsky Kyiv Polytechnic Institute"
03056, 37 Beresteiskyi Ave., Kyiv, Ukraine
https://orcid.org/0009-0008-1655-7918

Iryna Sukhodub

PhD in Technical Sciences, Associate Professor
National Technical University of Ukraine "Igor Sikorsky Kyiv Polytechnic Institute"
03056, 37 Beresteiskyi Ave., Kyiv, Ukraine
https://orcid.org/0000-0002-5895-1306

Abstract. The growing demand for energy-efficient buildings and the need to reduce greenhouse gas emissions necessitate the adoption of innovative approaches to thermal energy management in buildings. One such approach involves the use of phase change materials, which enable thermal energy storage and increase the thermal inertia of building structures. This makes them an effective solution for optimising energy efficiency under varying climatic conditions. This article aimed to analyse existing methods of employing phase change materials to enhance the energy efficiency of buildings through thermal energy storage. In particular, the study focused on techniques for incorporating these materials into building envelopes and their application in thermal storage systems. The article applied methods of analysis and synthesis of scientific literature, with particular attention given to studies on the impact of phase change materials on the thermal inertia of building components, their effectiveness in thermal energy storage units, and their influence on overall building energy performance. It has been established that the use of phase change materials significantly increases the thermal inertia of buildings and reduces heat loss. Various methods of incorporating phase change materials into building envelopes and their application in thermal storage systems have been analysed. The main advantages and drawbacks of each method have been identified, along with examples of their practical implementation. Potential uses of thermal storage units for enhancing building energy efficiency have been outlined, particularly their integration into heating and domestic hot water systems. The findings of the study may be applied in the design of energy-efficient buildings and heating and hot water supply systems that utilise phase change materials for thermal energy storage. This contributes to lower energy consumption and improved living comfort

Keywords: phase change materials; paraffin; building envelope; thermal inertia; latent heat

Introduction

High energy consumption in buildings, particularly due to cooling and heating demands, has become one of the most pressing challenges in the field of energy supply over recent decades. Statistics show that energy use in buildings and the associated emissions continue to rise steadily each year (The International Energy Agency, n.d.). As of 2022, building operations accounted for 30% of global energy consumption and 26% of global emissions. In that year alone, energy use in the building sector increased by approximately 1%, and this trend is expected to persist for the foreseeable future. Scientific and technological advancements in energy efficiency are key to accelerating progress in decoupling energy consumption from the rapid growth in total building floor area. It is projected that by 2030 the

Suggested Citation:
Lazariev, Ye., & Sukhodub, I. (2025). Analysis of the use of phase change materials to improve building energy efficiency and thermal energy storage. *Technologies and Engineering,* 26(3), 38-53. doi: 10.30857/2786-5371.2025.3.3.

*Corresponding author

global residential floor area will increase by around 15%, with approximately 80% of this growth occurring in developing countries, including Ukraine.

A substantial body of research has focused on the integration of phase change materials (PCMs) into building walls, aiming to improve energy efficiency and enhance indoor comfort for occupants. In their study, F.S. Bayraktar & R. Köse (2025) demonstrated that, under the climatic conditions of Turkey, placing PCM blocks on the internal surface of walls reduced electricity consumption by 16.6% during the cold season. F. Carlucci *et al.* (2021) conducted simulations of heat exchange processes involving the incorporation of PCM microcapsules into plasterboard mounted on interior wall surfaces, considering the climatic conditions of various European countries. The simulations were carried out for both office and residential buildings. The results indicated an overall reduction in building energy demand of between 2.5% and 5% for active PCM application strategies, as well as a general decrease in discomfort hours of up to 9% for passive strategies. Another study by M. Özdemir & A. Gülten (2024) focused on the impact of PCM integration on the energy loads of heating and cooling systems in buildings. Particular attention was given to the performance of PCM in various wall construction configurations under Turkey's climatic conditions. The authors aimed to determine how the inclusion of PCM in wall assemblies could reduce energy consumption and improve indoor thermal comfort. The findings showed that insulation alone resulted in a substantial 25% reduction in energy use, while the application of PCM by itself led to approximately a 9% decrease. The combined use of both PCMs and insulation materials achieved the most significant results, reducing energy consumption by 30%.

E. Osterman *et al.* (2023) dedicated their study to the application of PCMs for thermal energy storage in the context of "smart" retrofitting of existing buildings. The research forms part of the Horizon 2020 HEART project, which aims to decarbonise the European building sector. The authors explored the integration of PCM-based systems to enhance building energy efficiency and facilitate the use of green energy. As part of the experiment, three thermal storage tanks, each with a volume of 3,000 litres, were used. These tanks were filled with modules in the form of spheres containing liquid PCM. The total PCM volume enabled the accumulation of up to 90 kW of thermal energy. The payback period for the system was estimated at four to five years. A study by M. Jaradat *et al.* (2023) is also worth noting. The authors examined the use of PCM derived from renewable biomass sources, focusing on the effectiveness of its application in building envelopes under the climatic conditions of Romania and Jordan. It was found that the moderate climate of Jordanian cities such as Irbid and Amman is more favourable for PCM use than the colder, more humid climate of Oradea in Romania. The deployment of PCM systems in Amman showed significant benefits, including a potential annual energy saving of 5,476.14 kWh, a possible yearly cost reduction of 1,150 USD, and a decrease in CO_2 emissions equivalent to 2,382.31 kg.

The study by M. Velasco-Carrasco *et al.* (2020) presented an experimental investigation into the potential of integrating PCMs into ceiling panels for thermal energy storage systems under the climatic conditions of Nottingham, United Kingdom. The authors focused on evaluating the effectiveness of such "smart" ceiling panels in regulating indoor temperature and reducing building energy consumption. The research involved measuring the thermal performance of PCMs under conditions simulating real operating scenarios. The results showed that the integration of S23 panels reduced the need for additional heating by increasing the average indoor temperature in the test space. The use of 20 PCM ceiling panels had a significant impact on the indoor microclimate, raising the room temperature by 5°C.

K. Bodarya & V. Kaushal (2025) focused on the future effectiveness of PCM applications in the context of climate change. Their analysis of future climate models demonstrated that PCM efficiency varies considerably by region. In Curitiba (Brazil), which has a mild climate, PCM integration is expected to lead to a marked improvement in energy efficiency, with a projected reduction in annual energy use intensity (EUI) of 8.2% by 2050 and 10% by 2080, compared to the use of resistive insulation alone. In contrast, in the hot climate of Rio de Janeiro, PCM application may have adverse effects, potentially increasing EUI by 12.1% by 2050 and 20.7% by 2080 relative to resistive insulation.

Given the facts, forecasts, and studies presented, it should be noted that the development of innovative solutions in the fields of energy efficiency and energy supply, as well as their optimal practical implementation, are key criteria for achieving a high level of energy performance in buildings. The present study aimed to analyse approaches to improving building energy efficiency through the use of phase change materials capable of storing thermal energy.

The research employed several scientific methods, including analysis, synthesis, classification, and comparison. A total of 40 literature sources, published both in Ukraine and internationally, were reviewed. The selected studies provide a comprehensive overview of the current state of research on the application of PCMs to improve building energy efficiency and develop thermal energy storage systems. The analysed sources include both theoretical materials concerning PCMs, their key properties, and areas of application, as well as the results of various modelling exercises and experimental investigations. The majority of the references consist of academic articles published in specialised scientific journals. This selection enabled a thorough analysis of advances in the application of PCMs in building envelopes and thermal storage units.

Methods of thermal energy storage using pcms

Modern thermal energy storage technologies are based on three main principles: sensible heat storage, latent heat storage, and the use of thermochemical reactions. Sensible heat is stored through changes in the temperature of a material without a phase change. This method is well-researched and widely applied; however, it has the lowest efficiency due to the low specific heat capacity of materials. The most common storage media include water, metals, rocks, and bricks (Kots *et al.*, 2023). The latent heat storage method relies on the phase transition of a substance, which occurs at a constant temperature. This enables a high energy storage density and allows for the development of compact energy storage systems (Nallusamy *et al.,* 2007). Substances used in this method are known as phase change materials (PCMs). The thermochemical method is based on chemical reactions that absorb or release heat through changes in enthalpy (Pfleger *et al.,* 2015).

The present study focused primarily on the latent heat storage method using PCMs, which is considered a promising approach to improving building energy efficiency due to its high energy storage density and the ability to maintain a constant temperature during heat exchange. Phase transitions can occur in several forms: solid-solid, solid-liquid, solid-gas, liquid-gas, and in the reverse direction for each of these transitions. In the case of a solid-solid phase transition, the crystalline structure of the material changes, accompanied by the absorption or release of thermal energy. This type of phase change is characterised by only a slight change in the material's volume and relatively low heat storage capacity. However, it offers advantages such as reduced requirements for the strength and airtightness of the enclosure, providing greater flexibility in construction design.

Solid-gas and liquid-gas phase transitions can achieve higher thermal energy storage density. Nevertheless, the substantial increase in material volume during these processes complicates their application due to the need for airtight containers and more complex system designs. This significantly limits their practical suitability for thermal energy storage systems. The most balanced and practical option in terms of implementation is the solid-liquid phase transition. Although the amount of thermal energy that can be stored is somewhat limited, this method provides sufficient efficiency while allowing for simple engineering solutions. The volumetric expansion of the material usually does not exceed 10% (Sharma *et al.,* 2009), making it possible to design an optimal PCM enclosure and choose from a wide range of construction materials. The graph of temperature dependence on the amount of stored heat, taking into account the aggregate state of the material, is shown in Figure 1.

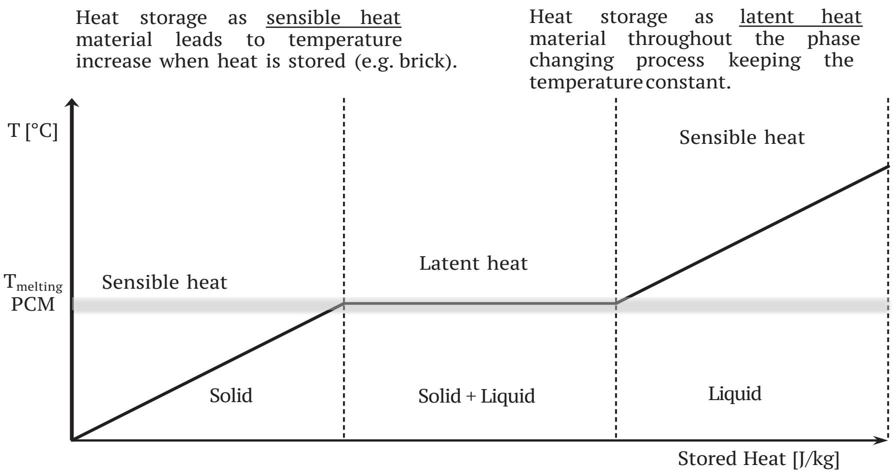

Figure 1. *Phase transition zones of phase change materials*
Source: *developed by the authors based on research by Q. Al-Yasiri & M. Szabó (2021)*

Modern thermal energy storage technologies are based on different physical principles, each with its own advantages and limitations. Among these, the use of phase change materials – which can efficiently store heat during phase transitions – has attracted the greatest practical interest. Of all types of phase transitions, the most common and convenient for building applications is the solid-liquid transition. This approach offers a good balance of energy storage capacity, ease of implementation, and adaptability to various construction systems.

Classification of phase change materials and their properties

Depending on their chemical composition, PCMs are classified into three main groups: organic, inorganic, and eutectic. Each category is characterised by a specific operating temperature range, thermophysical properties, and application features (Kulish *et al.,* 2023). Organic PCMs are divided into paraffins and non-paraffin compounds. They are known for their low corrosiveness, chemical stability, and congruent melting, meaning they can undergo multiple phase changes without decomposing into separate substances or losing their functional properties. These materials also typically crystallise well without supercooling due to active self-nucleation (Sharma *et al*., 2009). Paraffins are the most widely used organic PCMs due to their availability, low cost, predictable behaviour, and broad melting temperature range. Their main disadvantages are flammability and low thermal conductivity, which reduce heat exchange efficiency and can result in the formation of "dead zones" within the material. Nonparaffin PCMs include complex esters, fatty acids, alcohols, and glycols. These often exhibit higher latent heat values but are also associated with toxicity, low ignition temperatures, flammability, and thermal instability at elevated temperatures.

Inorganic PCMs include metals and salt hydrates. Metals (particularly eutectics and low-melting-point alloys) offer high thermal conductivity, reducing the need for additional methods to enhance heat transfer. However, their considerable mass presents complex engineering challenges in the design of metallic thermal storage systems, which limits their practical use. Salt hydrates are crystalline compounds consisting of salts and water. When heated, they undergo a phase change that results in the formation of lower hydrates or anhydrous salts and water. The main drawback is incongruent melting, where part of the salt settles at the bottom of the storage tank, causing material stratification and gradual degradation of performance. Salt hydrates also exhibit low nucleation ability, leading to supercooling and unstable phase transitions (Al-Yasiri & Szabó, 2021). Eutectic PCMs are mixtures of two or more components that melt and solidify simultaneously and congruently, ensuring a homogeneous phase transition without separation. Based on composition, eutectics can be classified as organic (all components organic), inorganic (all components inorganic), or organic-inorganic mixtures. Among organic eutectics, mixtures of fatty acids are the most studied. In contrast, inorganic combinations are less researched, and their properties require further investigation. The main advantage of eutectic PCMs is the ability to precisely select the phase transition temperature. However, their use is limited by high cost and insufficiently understood thermophysical properties (Kulish *et al.,* 2023).

Considering the advantages and limitations of all PCM types, organic materials – especially paraffins – are the most suitable for thermal energy storage systems and enhancing the energy efficiency of buildings. They are environmentally safe, stable, readily available and exhibit low corrosive activity. The main drawback remains their low thermal conductivity; therefore, a significant proportion of research focuses on enhancing heat transfer within paraffin volumes, particularly in building structures or thermal storage units.

Technologies for the integration of pcms in construction

Thermal inertia refers to a building's envelope ability to slow down internal temperature fluctuations in response to changes in external temperature and solar radiation. In summer, building materials absorb excess heat during the day and release it at night, helping to prevent overheating. In winter, they slow the rate of cooling, helping to retain heat indoors. A building envelope typically consists of multiple layers, each serving a distinct purpose: structural (e.g. concrete, reinforced concrete), thermal insulation, decorative, and so on. The composition and structure of the envelope are determined by national construction standards, which account for climatic conditions, energy consumption requirements, and comfort.

One way to improve energy efficiency is to increase the building's thermal inertia through the use of PCMs. For instance, paraffin integrated into walls or ceilings accumulates heat during the day (in summer) or while heating systems are in operation (in winter) as it undergoes a phase change. At night in summer, or after the heating is turned off in winter, the stored energy is released as the paraffin solidifies, helping to stabilise indoor temperatures and reduce the demand on cooling or heating systems. PCMs are most commonly integrated into walls and ceilings, which are the main surfaces exposed to high thermal loads. Incorporation into floors is generally less effective due to the stable temperature of the ground. The use of PCMs in windows is limited owing to the risk of leakage and the potential reduction in glazing transparency. Thus, the application of PCMs in building envelopes contributes to temperature stabilisation, improved energy efficiency and enhanced comfort of the residents. The existing methods for incorporating PCMs into the building envelope, along with their advantages and disadvantages, are presented in Table 1.

Table 1. *Methods for incorporating PCMs into the building envelope*

Method	Description	Advantages	Disadvantages
Mixing with construction materials	Impregnation of porous structural materials with liquid PCM.	Simple implementation; low cost.	Leakage during phase change; reduction in structural strength.
Impregnation of porous structural materials with liquid PCM	Based on capillary absorption of liquid PCM into porous materials.	Relatively simple technology.	Leakage during phase change; potential corrosion of reinforcement due to contact between PCM and metal.
Microencapsulation	PCM is divided into microgranules, each coated with a polymer shell.	High efficiency; prevents leakage.	High cost; may be economically unfeasible; requires complex equipment; some granules may be defective due to limitations in the production process.
Macroencapsulation	PCMs are enclosed in containers of various sizes (tubes, plates, bricks, panels).	Relatively low cost; Easy to implement; no special equipment required.	There is a risk of PCM leakage if the container is damaged or loses integrity.

Table 1. Continued

Method	Description	Advantages	Disadvantages
Incorporation into a supporting matrix	PCM is embedded in a polymer or other supporting structure (e.g. polyethylene or butadiene rubber).	Stable retention of material through repeated phase transitions; improved thermal conductivity throughout the PCM volume; low risk of leakage; high number of phase change cycles without significant degradation of properties.	High cost.
Shape-stabilised method	PCM is absorbed into or embedded within a porous or composite structure (e.g. expanded graphite, polymers, foams).	Simple design; material remains sealed; durability; high number of phase change cycles without significant degradation of properties.	High cost.

Source: *developed by the authors based on research S. Lu et al. (2016), K. Cellat et al. (2017), K. Powała et al. (2022)*

One of the simplest and most widely used methods listed in Table 1 is macroencapsulation, due to its significant advantages and the absence of major drawbacks. Examples of this method in application are shown in Figure 2.

a b c

Figure 2. *Various forms of macroencapsulation used in building structures*
Note: *a – plates; b – tubes; c – spheres*
Source: *developed by the authors based on research P.K.S. Rathore & S.K. Shukla (2020), M. Velasco-Carrasco et al. (2020), E. Osterman et al. (2023)*

The effectiveness of a chosen method depends on numerous factors – material type, enclosure design, temperature fluctuations, cost, and more. Therefore, the integration of PCM must be not only reliable but also an economically justified solution for enhancing a building's energy efficiency. A key thermophysical characteristic of PCM is the optimal temperature at which the phase transition occurs. The optimal phase change temperature must be determined based on the climatic conditions of the specific location where the PCM is intended for use in the building envelope. Primarily, the phase transition temperature should ensure full activation of the melting-crystallisation cycle throughout the entire PCM layer (Lei *et al.*, 2016). This enables the material to be used with maximum efficiency and allows the phase change to occur across the full volume of PCM. On the other hand, the phase change temperature should be as close as possible to the indoor thermal comfort range in order to maintain a comfortable environment for occupants. Several studies have shown that the use of PCM is ineffective if the phase transition temperature is poorly selected (Alshuraiaan, 2022).

The location of the PCM layer within the building envelope also affects the material's efficiency. The number of layers in the building envelope and the materials used depend on construction standards and regulations in a given region. There are two boundary options for positioning PCM to enhance building cooling: on the inner or outer surface of the envelope. Experiments by A. de Gracia (2019), P.K.S. Rathore & S.K. Shukla (2020), and A. Khayyaminejad & A. Fartaj (2024) demonstrated that, in terms of effective cooling, placing the phase change material on the external surface allows it to absorb a substantial amount of heat during the day and undergo a full phase transition (with the proportion of melted PCM approaching 100%). At night, the phase change material cools and crystallises, releasing thermal energy into the surrounding environment. This type of PCM application does not require additional heating or cooling mechanisms and is referred to as a passive system. When the phase change material layer is positioned internally, ventilation systems are needed to enhance night-time cooling and ensure the PCM fully solidifies (Khayyaminejad & Fartaj, 2024). This setup is classified as an active system. Compared to passive systems, active ones are more complex, as they require the installation of additional cooling and ventilation equipment within the building.

The use of PCM in building envelope components offers an effective means of improving energy efficiency and stabilising the indoor microclimate. The most suitable methods of integration are considered to be macroencapsulation and stabilised forms, which combine efficiency with technological simplicity. The selection of the phase change temperature must take into account the local climate and ensure full activation of the material.

Assessing the effectiveness of incorporating a pcm layer into the building envelope

A substantial number of studies focus on assessing the effectiveness of incorporating PCM into building envelopes. Most of them (nearly 60%) are based on the use of organic PCM for passive building cooling, with paraffin being the most commonly used organic PCM (46%). This focus can be attributed to its relatively high melting point, broad compatibility with most envelope materials, and chemical stability. This conclusion aligns with the assertion that chemical instability, supercooling, and high corrosiveness are the main disadvantages of inorganic PCMs. The second most commonly used PCM type is the eutectic variety. Although this category of PCM is expensive, its high latent heat of fusion per unit volume and superior thermal conductivity have made it a promising option for cooling applications (Akeiber *et al.*, 2016). The following section presents the results of several studies.

P. Rathore & S. Shukla (2020) investigated the effectiveness of PCM macroencapsulated within the wall of an experimental cubic chamber (Fig. 3) measuring1.12 m × 1.12 m × 1.12 m under the climatic conditions of Mathura, India.

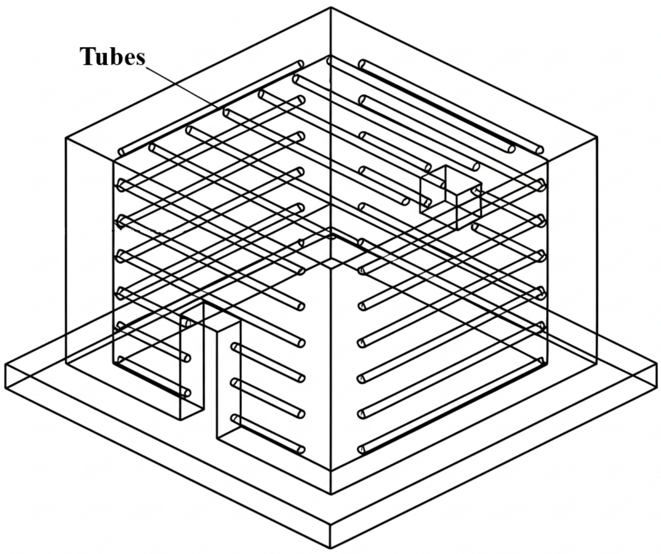

Figure 3. *Schematic diagram of the experimental chamber with macroencapsulated PCM*
Source: *developed by the authors based on research by P.K.S. Rathore & S.K. Shukla (2020)*

Tubes of varying lengths with a diameter of 16.7 mm were used as capsules, positioned horizontally within the building envelope. During the experiment, two identical chambers were constructed: a baseline model and a PCM-enhanced model. The results showed that the incorporation of PCM reduced the heat flux through the envelope wall by 19.41%-41.31% for different components of the structure. Additionally, a 27.32% reduction in overall peak heat flux was achieved. The peak temperature of the PCM-enhanced model was 7.41%-8.08% lower compared to the baseline version. The authors concluded that macroencapsulated PCM integrated into the walls of a building could reduce the cooling load by up to 38.76%.

A. Khayyaminejad & A. Fartaj (2024) examined the effectiveness of placing a PCM layer in three different locations within the envelope of a residential building (Fig. 4) under the climatic conditions of Las Vegas, USA. The baseline wall assembly consisted of brick, wooden siding, insulation, and plasterboard. In the first scenario, the PCM layer was positioned close to the exterior surface of the wall, behind the brick layer and in front of the wooden siding. In the second scenario, the PCM was placed between the wooden siding and the insulation layer. In the third and final scenario, the PCM layer was located near the interior surface of the wall. The results of the study by A. Khayyaminejad & A. Fartaj (2024) demonstrated that integrating a PCM layer into the walls led to a reduction in peak indoor temperature by 1.5 K in scenarios 1 and 2, whereas in scenario 3 the reduction was only 0.5 K. Regarding the percentage of liquid PCM after discharge, in scenarios 1 and 2 the PCM completely melted, with a time difference of 42 minutes (melting occurred earlier in scenario 1). In contrast, in scenario 3, the PCM melted only by 70%. This is due to the greater influence of the indoor temperature. The results indicate that placing the PCM layer near the internal surface of the envelope reduces its effectiveness during summer cooling. Overall, integrating PCM into the building envelope in the most efficient configuration resulted in an additional energy saving of 3.5% over 24 hours and 5% during peak temperature periods.

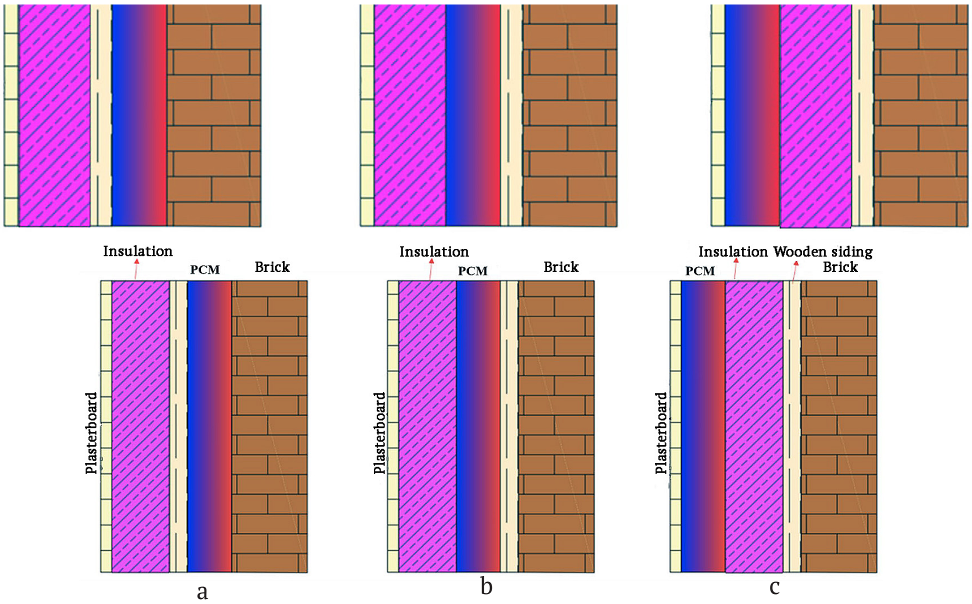

Figure 4. *Investigated configurations of PCM layer placement within the building envelope*
Note: *a – scenario one; b –scenario two; c –scenario three*
Source: *developed by the authors based on research by A. Khayyaminejad & A. Fartaj (2024)*

The study by J. Lei *et al.* (2016) investigated the effectiveness of incorporating a PCM layer into a building envelope under the climatic conditions of Singapore. A simplified cubic model measuring 3 × 3 × 2.8 m was developed, with a 10 mm thick PCM layer applied to the external walls. A reference model without PCM was also simulated as the baseline. A reduction in the peak temperature of the concrete surface located behind the PCM layer reached 3-4°C. Furthermore, the phase-change material contributed to a 21-32% annual reduction in monthly heat gain through the envelope. In the study by K. Powała *et al.* (2022), the authors used a specialised technique to produce gypsum granules containing PCM, which were coated with a protective polymer layer. This encapsulation method was then applied by adding the granules in large quantities to a gypsum mixture, which was subsequently used to manufacture plasterboard panels. After placing the granules into dedicated moulds for testing, they were filled with gypsum as a binding material. Two identical panels were prepared: one incorporating PCM elements and the other without (Fig. 5). Several thermocouples were embedded into the fabricated panels, which were then exposed to artificial light with a power output of 1,000 W to simulate sunlight.

Figure 5. *Appearance of the experimental setup*
Note: *a – plasterboard panels attached to the measurement station; b – 1,000 W lamps*
Source: *developed by the authors based on research by K. Powała et al. (2022)*

The results of the experiment by K. Powała *et al.* (2022) demonstrated that the panel containing PCM granules with a polymer coating exhibited superior thermal performance. Notably, a phase transition occurred after 3 hours of heating at a temperature of approximately 22°C (Fig. 6). It was also observed that the time at which peak temperature was reached was delayed. This is most evident at 25°C, where the delay in reaching this temperature was about one hour compared to plasterboard without PCM. The peak temperature was also reduced by approximately 3°C.

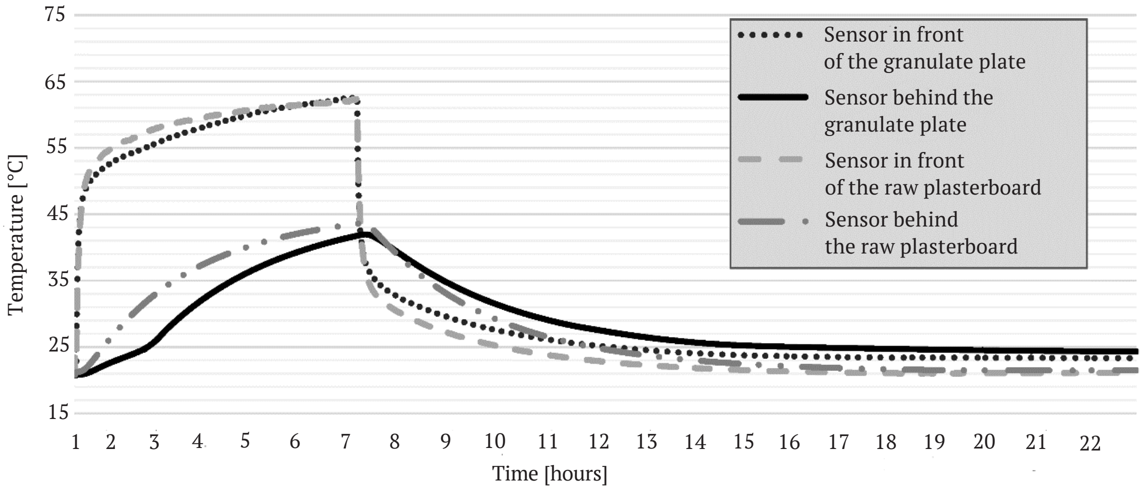

Figure 6. *Temperature variation as a function of time for plasterboard with and without PCM*
Source: *developed by the authors based on research by K. Powała et al. (2022)*

The study by Y. Gao *et al.* (2020) focused on the thermal performance of hollow bricks into which PCM was integrated within the cavities. The aim of the research was to enhance the thermal inertia of lightweight construction materials, which are commonly used in high-rise buildings and can lead to considerable indoor temperature fluctuations. The authors developed a numerical model to simulate the melting-solidification processes of PCM within bricks and validated its accuracy through a full-scale experiment. The results indicated that filling bricks with PCM significantly improved their thermal performance by reducing the rate of heat flux attenuation and increasing the time delay in heat transfer. Specifically, it was found that, with an appropriate phase change temperature, PCM could reduce the attenuation rate from 13.07% to 0.92%-1.93% and extend the delay time from 3.83 hours to 8.83-9.83 hours. In addition, the use of PCM contributed to a reduction in peak heat flux.

The study by M. Saffari *et al.* (2022) focused on exploring methods to enhance the energy flexibility of buildings by integrating PCM into their envelope structures. The authors investigated how PCM could help buildings respond more effectively to variations in energy availability and cost, particularly in the context of an increasing share of renewable sources. The research employed modelling and analysis of the thermal behaviour of buildings with PCM-integrated envelopes. The aim was to demonstrate how such systems can smooth peak loads on the energy grid by storing thermal energy when it is cheap or abundant and releasing it when needed. The results showed that the maximum flexibility efficiency in energy consumption reached 356% in a scenario involving short-term preheating of the building for 30 minutes followed by a long demand response period of four hours.

The study by R. Vanaga *et al.* (2023) focused on a comparative analysis of the effectiveness of two different PCMs – RT21HC and RT28HC – for integration into building envelopes with the aim of thermal energy storage. The research combined experimental and numerical methods, allowing for a comprehensive assessment of their performance. Laboratory tests simulated the conditions of all four seasons using a specialised PASLINK test facility to replicate both indoor and outdoor environments. Based on the experimental data, a numerical model was developed to further explore PCM behaviour under various climatic conditions. The experimental findings demonstrated that RT21HC was more effective at storing and releasing thermal energy into indoor spaces, while numerical simulations indicated that RT28HC performed better in the climate of Southern Europe, where it more effectively prevented indoor overheating.

In summary, the findings confirm that integrating PCM into building envelope structures effectively reduces peak temperatures, heat flux, and energy consumption for cooling. The best outcomes are achieved through the appropriate selection of PCM type, encapsulation method, and placement within the structure. These studies highlight the potential of PCM as a means of enhancing building energy efficiency and flexibility, particularly in the context of increasing reliance on renewable energy sources.

Thermal accumulators based on PCM

A thermal accumulator is a device designed for the accumulation, storage, and gradual release of thermal energy. This article considers the potential application of thermal accumulators based on PCM, taking into account the advantages offered by this type of material. In the context of improving a building's energy efficiency, a thermal accumulator can be integrated into heating systems (Antypov *et al.*, 2022), domestic hot water (DHW) supply, or cooling systems (Bejarano *et al.,* 2018). The charge-discharge cycle is implemented through the circulation of a heat transfer fluid. Depending on the method of heat exchange between the heat transfer fluid and the PCM, accumulators are classified as either contact or non-contact.

In contact-type thermal accumulators, the heat transfer fluid comes into direct contact with the phase change material. Oil is most commonly used as the heat carrier, with water or gas used less frequently. Direct contact enables intense heat exchange, with a heat transfer coefficient ranging from 100 to 1,000 W/m^2·K. The heat carrier is typically injected through nozzles, transferring heat to the PCM primarily via convection, and then exits the accumulator under the influence of gravity. However, contact accumulators present several drawbacks, including the risk of nozzle blockage due to PCM crystallisation (Liu *et al*., 2024), mixing of the heat carrier with the PCM – which is unacceptable for domestic systems – chemical degradation of PCM from prolonged contact with the fluid, and the complexity of the design required to ensure uniform heat transfer, which increases cost and complicates installation. These factors make the use of contact-type accumulators in buildings impractical for enhancing energy efficiency.

Non-contact accumulators separate the heat transfer fluid and the PCM by means of a tubular wall, preventing direct interaction between them. The phase change material is housed within a sealed casing, while one or more tubes of various shapes pass through the accumulator, facilitating heat exchange between the storage medium and the heat carrier. The heat transfer coefficient through the tube walls can reach 50-500 W/m^2·K. Water is most commonly used as the heat transfer fluid due to its affordability, versatility, availability, and high specific heat capacity. This makes such accumulators easy to integrate into even the simplest heating or DHW systems in buildings. Technical-grade paraffins are the most widely used storage materials owing to their physical and chemical stability, low corrosive activity, low cost, and ready availability. During the charging process, hot fluid transfers heat to the PCM through the walls of the tubes, causing it to melt. During discharging, cooler fluid absorbs the stored heat, leading to the crystallisation of the PCM.

The primary function of a thermal accumulator is to store surplus heat and release it during periods of increased demand. When integrated with renewable energy sources (RES), PCM can store excess energy – for instance, from solar panels during daylight hours – and subsequently supply it for heating or DHW at the required time. In systems connected to the traditional electricity grid, night-time charging of the accumulator at reduced tariffs is a viable option.

Enhancing heat transfer in thermal accumulators

The primary drawback of thermal accumulators using paraffins as PCM lies in the inherently low thermal conductivity of paraffins. This significantly prolongs the charging and discharging times and leads to the formation of zones where the storage material does not undergo a phase change and thus does not participate in the heat accumulation process. Another consequence of low thermal conductivity is the emergence of a high temperature gradient, with certain areas containing overheated liquid-phase material and others remaining in a low-temperature solid state. This uneven temperature distribution within the PCM reduces the efficiency of the accumulator and may result in local degradation of the material or a decline in its thermal activity. A substantial body of experimental and theoretical research has focused on addressing this issue through optimisation of the thermal accumulator design and enhancement of heat transfer between the PCM and the heat transfer fluid.

Ye.O. Antipov (2016) proposed an optimised thermal accumulator design featuring a wavy bottom configuration and the addition of electric heating wires as internal heat sources. The temperature fields before and after optimisation are shown in Figure 7. An analysis of the performance of the modified accumulator in comparison to the original model demonstrated that the temperature of the PCM near the lower part of the casing wall was 7%-15% higher than in the previous flat-bottomed design. The introduction of additional electric heating elements enabled an 8%-10% increase in heat removal efficiency, a 10%-15% reduction in the device's mass and overall dimensions, a 36% improvement in the useful mass utilisation coefficient of the storage medium, and an 86% extension of discharge duration (heat release mode), assuming the same thermal output as the baseline model.

In the article by A. Dmitruk *et al.* (2020a), the authors proposed the use of metallic inclusions in the form of honeycomb frameworks (Fig. 8) to optimise heat transfer in paraffin-based thermal accumulators using RT-82. The proposed metal structures present a promising solution for enhancing heat exchange due to their large heat transfer surface area, high thermal conductivity, and compact shape. The aluminium alloy used, containing 13% silicon, has a thermal conductivity of 158 W/m·K, which intensifies heat flow within the PCM during the charging process. An additional design using perforated honeycomb structures was also developed and cast (Fig. 8). Compared to the solid element, this approach allowed for an 18% mass reduction, promoted more active convection, and improved thermal conductivity, while maintaining thermal performance similar to the solid variant.

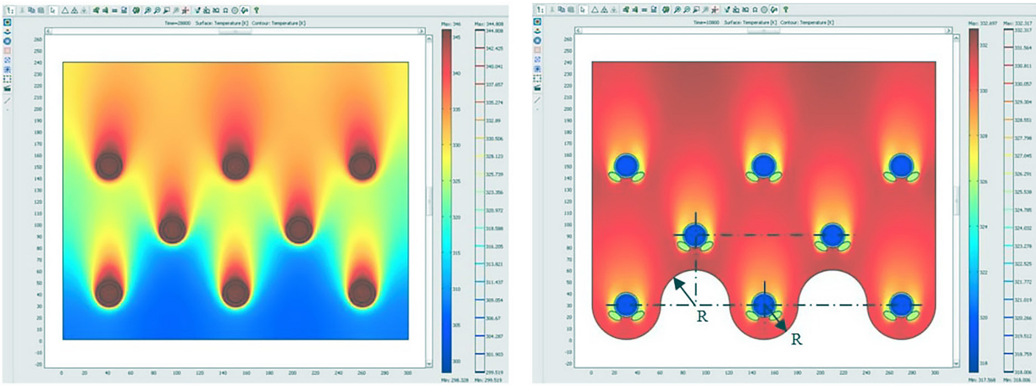

Figure 7. *Temperature fields of the cross-section in the original and optimised accumulator designs*
Source: *developed by the authors based on research by Ye.O. Antipov (2016)*

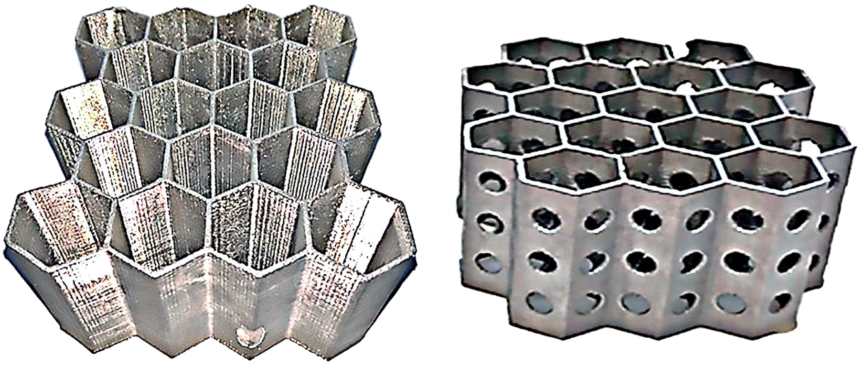

Figure 8. *Cast Al-Si honeycomb structures*
Note: *a – solid honeycomb structures; b – perforated honeycomb structures*
Source:*developed by the authors based on research by A. Dmitruk et al. (2020a)*

Y.O. Hlek (2024), in her study, developed two new paraffin-based thermal storage materials: paraffin/fullerene C_{60} and paraffin/thermally expanded graphite. These materials were produced by introducing carbon-based additives into pure paraffin using nanotechnology. As a result of this combination, the thermal conductivity of the paraffin/thermally expanded graphite composite increased by a factor of 8.9 to 9.6 at 25°C and 8.8 to 10.9 at 65°C, compared to pure paraffin. The findings indicate that the addition of even a small amount of fullerene C_{60} (0.0746 wt%) can enhance the thermal conductivity of the liquid phase from 0.256 to 0.506 $W \cdot m^{-1} \cdot K^{-1}$. L. Constantin *et al.* (2015) based their investigation on a standard PCMbased thermal storage unit incorporating a coil embedded within the PCM volume (Fig. 9), through which the heat transfer fluid (water) circulates. Experimental results showed that a layer of semi-solidified paraffin, approximately 50 mm thick, remained in the lower part of the accumulator.

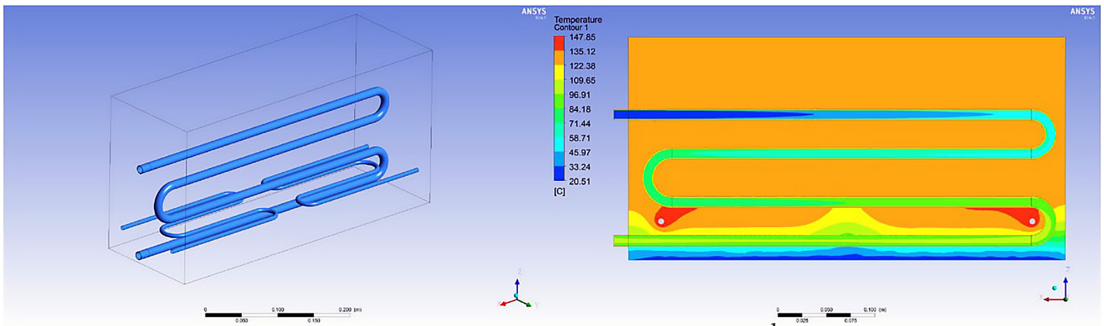

Figure 9. *Reference thermal accumulator model*
Note: *a – base model of the accumulator; b – temperature distribution within the PCM and heat transfer fluid*
Source: *developed by the authors based on research by L. Constantin et al. (2015)*

To improve thermal performance and eliminate heat exchange issues, the original model underwent modernisation. The first optimisation version aimed to homogenise the temperature of the molten paraffin by installing two pipes on either side of the accumulator casing (Fig. 10). The pipes connect the upper and lower parts of the casing, thereby promoting the circulation of paraffin between different layers of the accumulator due to differences in its density.

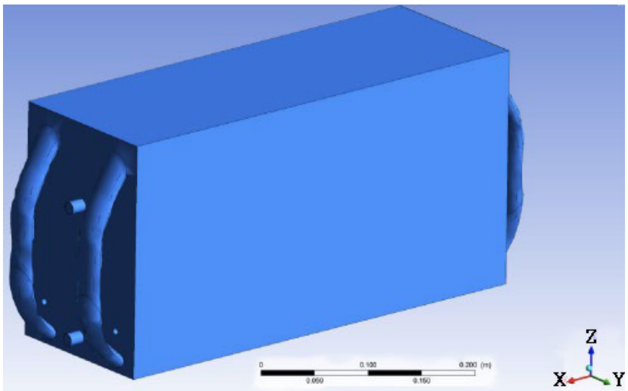

Figure 10. *Thermal accumulator with external pipes*
Source: *developed by the authors based on research by L. Constantin et al. (2015)*

Another modification involved changing the direction of fluid flow to downward, which helps to maintain a high temperature of the heat transfer fluid in the lower part of the PCM volume. As a result of the implementation of these optimisation methods, the thickness of the semi-solidified PCM layer at the bottom of the unit was reduced from 50 mm to 20 mm, thereby increasing the accumulator's storage capacity. A. Dmitruk *et al*. (2020b) investigated the effectiveness of integrating a pin-fin element into the accumulator casing. This element acts as a heat exchange insert in the form of one or several thin rods or pins inserted into the PCM volume to improve heat transfer and stabilise the temperature gradient (Fig. 11). During the experiment, the authors measured temperatures at three points located along the central axis of the accumulator: 1 mm, 18 mm, and 38 mm above the metal base, comparing two accumulator configurations – one with the pin-fin structure and one without it. The results showed that the temperature difference between the measured points was more than twice as low in the PCM with the metallic pin-fin structure compared to the configuration without it. This helped to significantly reduce the temperature drop across the height of the heat accumulator, reduce its recharging time and generally increase the efficiency of the heat storage system.

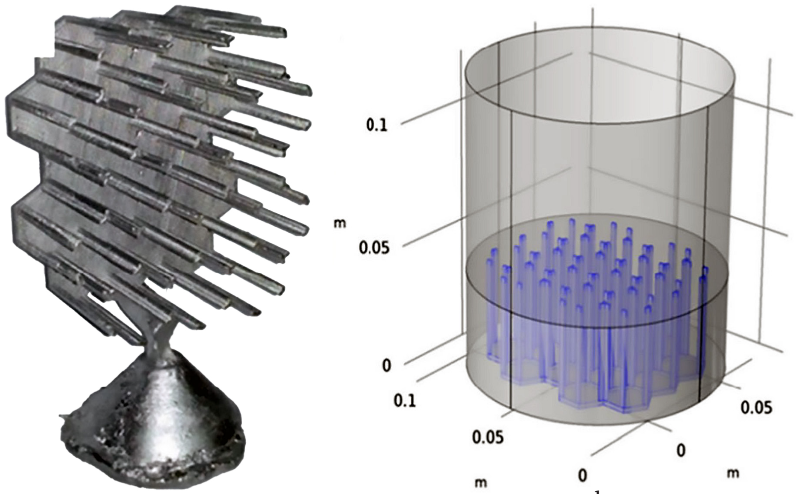

a b

Figure 11. *Pin-fin heat exchange insert*
Note: *a – cast element made from Al-Si AC 44200 alloy;b – pin-fin structure as a separate metal element in a laboratory-scale thermal accumulator model*
Source: *developed by the authors based on research by A. Dmitruk et al. (2020b)*

In the study by Y. Bai *et al*. (2023), the authors examined the effectiveness of using fins to enhance heat transfer between the heat transfer fluid and the PCM, as well as to reduce the charging time of the thermal accumulator. The main aim of this modification was to test fins of different configurations (longitudinal and annular) and to determine their optimal parameters, such as fin length, thickness, and number. The results showed that under heat accumulation conditions, a built-in longitudinal fin was more effective than an annular one (Fig. 12). The length of the fin played a dominant role in the charging/discharging rate of the accumulator. An analysis of the phase change behaviour of the PCM with and without embedded longitudinal fins revealed that in the model with fins measuring 45 mm in length, the PCM fully solidified in 3,200 s, whereas in the model without fins, it solidified in 19,500 s – a difference of 610%. This result indicates that the embedded fins significantly enhanced heat transfer between the heat transfer fluid and the PCM.

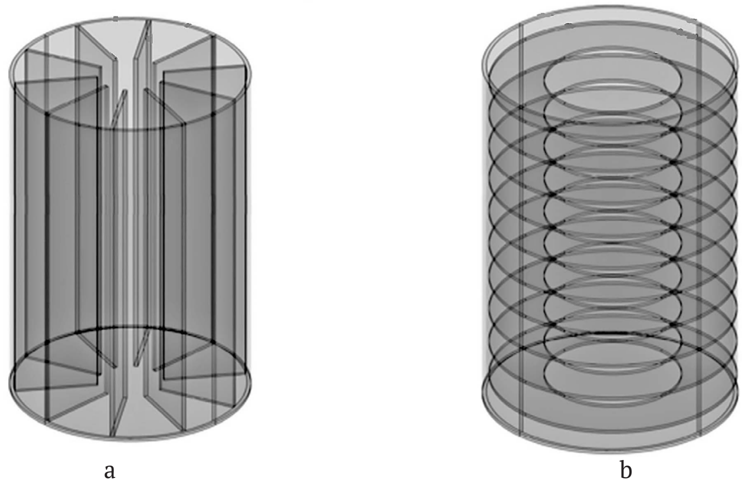

Figure 12. *Configuration of longitudinal and annular fins*
Note: *a – longitudinal fin; b – annular fin*
Source: *developed by the authors based on research by Y. Bai et al. (2023)*

The study by G. Liu *et al.* (2022) focuses on investigating the effect of the position of the internal heating tube on the efficiency of the phase change (melting) process in a shell-andtube type thermal energy storage system. The authors developed a two-dimensional numerical model to simulate the thermal energy accumulation process. The primary objective was to determine the optimal position of the internal tube to minimise the total melting time of the material. The simulation results indicated that displacing the internal tube from the central axis significantly affects the rate of the phase change. In particular, it was found that positioning the tube 12 mm off-centre reduced the total melting time by 13.4% compared to a centrally placed tube. This demonstrates the potential of geometric optimisation to enhance heat transfer efficiency and accelerate energy storage processes in such systems.

The study by C. Liu *et al.* (2020) was dedicated to the experimental investigation of the effectiveness of oscillating heat pipes (OHPs) in improving heat transfer in PCM-based thermal energy storage systems. The article focuses on integrating OHPs into a reservoir containing PCM to accelerate the charging and discharging of thermal energy. During the experiments, the influence of various parameters – such as the working fluid inside the OHP and the heat flux – on the melting and solidification rates of the PCM was measured. The results showed that the thermal energy storage time for a paraffin-based unit combined with OHPs (Dinr = 3 mm, Dout = 4 mm, 4 loops) was 38.45% shorter compared to a unit without such pipes. This makes the use of OHPs effective for enhancing heat transfer, which in turn leads to a reduction in the time required for storing and releasing thermal energy.

In the study by H. Yang *et al.* (2021), an experimental investigation was conducted into the mechanisms of control and improvement of heat transfer efficiency in composite phase change materials (CPCMs). The authors focused on developing and testing innovative approaches to improve thermal energy charging and discharging using CPCMs. The research included an analysis of the impact of various structural components and methods of their integration on the thermophysical properties of the materials. The experimental results demonstrated that copper foam significantly improved the thermal conductivity of CPCMs. The thermal conductivity of the composite material (copper foam/PCM) with 95% porosity and a pore density of 50 pores per inch was 1.34 W/m·K, while for a foam with 85% porosity and the same pore density, it reached 4.35 W/m·K – approximately 20 times higher than the thermal conductivity of PCM without copper foam.

The study by B. Lu *et al.* (2023) was devoted to improving the melting efficiency of PCM in latent heat thermal energy storage systems. The authors focused on the development and analysis of new configurations to enhance heat transfer during the phase change process of PCM. The study examined the impact of fin geometry and the use of additional thermally conductive elements on the melting rate of phase change materials. Numerical methods were applied to assess system performance. The results showed that the total melting time for nonuniformly distributed longitudinal fins was reduced by 31% compared to a traditional fin arrangement. A correlation was found between the PCM melting rate and both the intensity and distribution of natural convection throughout the melting process.

In the study by S.K. Singh *et al.* (2022), an experimental investigation was carried out on a latent heat thermal energy storage system using encapsulated PCM. The authors focused on the integration of multiple types of PCM within a single storage unit to improve overall system efficiency. This research aimed to analyse the thermal characteristics and behaviour of the system under various operating conditions. The findings confirmed that using multiple PCMs with different melting points in a single unit enhances the system's heat storage capacity. As the heat transfer fluid (HTF) flow rate increased from 1 to 5 litres per minute, the melting time decreased by 10%-30%, while the solidification time was reduced by 14%-28%.

Research has shown that the efficiency of PCM-based thermal energy storage systems depends on design geometry, thermal conductivity enhancers, and material type. Optimising the arrangement of heating elements, using heat pipes, copper foam, and multiple PCMs improves heat transfer and shortens the phase transition time. Such approaches hold considerable potential for enhancing the energy efficiency of thermal energy storage systems.

Conclusions

As a result of the analysis of scientific research and experimental findings, it has been established that the use of phase change materials holds significant potential for enhancing the energy efficiency of buildings and ensuring effective thermal energy storage. Incorporating PCM into building envelope structures can considerably increase their thermal inertia, reduce indoor temperature fluctuations, and lower energy consumption for heating and cooling. Various types of energy storage and phase transitions that underpin PCM operation have been reviewed, along with a classification of PCM by composition and methods of integration into construction materials. It has been identified that the correct selection of the material's phase change temperature, as well as its optimal placement within the building envelope, are critical factors in achieving maximum energy-saving effects. Particular attention has been given to the potential integration of PCM in thermal storage units for heating and hot water supply systems, as well as to methods of enhancing heat transfer in such systems to maximise their efficiency. The results indicated that the choice of PCM type should be based on the building's operating temperature conditions and the required level of thermal stability of the indoor environment. The use of encapsulation technologies and shape-stabilised methods significantly enhances the reliability and durability of PCMs when integrated into building structures. Furthermore, PCM-based thermal storage units offer additional opportunities for controlled heat supply, particularly in the context of the widespread adoption of renewable energy sources, thereby contributing to the overall improvement of building energy efficiency.

Future research should focus on conducting experimental and numerical studies on the long-term performance of PCM in building applications under real operating conditions, particularly considering the effects of cyclic phase transitions and material degradation. A key area of development involves the creation of new PCM-based composite materials with improved thermal conductivity, chemical stability and resistance to leakage. Further research is also required to optimise heat transfer processes in PCM thermal storage systems through the use of specialised inserts, fins and other structural elements. Another promising direction is the study of PCM integration in combination with other energy-efficient technologies for buildings, such as heat recovery ventilation systems, solar collectors and heat pumps. Additionally, it is important to analyse the effectiveness of PCM use in construction across different climate zones of Ukraine, taking into account projected climate change over the coming decades. In summary, continued research in this area offers wide-ranging opportunities for the development of innovative building solutions that enhance energy independence, indoor comfort and the reduction of greenhouse gas emissions.

Acknowledgements

None.

Funding

None.

Conflict of Interest

None.

References

[1] Akeiber, H., Nejat, P., Majid, M.Z.A., Wahid, M.A., Jomehzadeh, F., Zeynali Famileh, I., Calautit, J.K., Hughes, B.R., & Zaki, S.A. (2016). A review on phase change material (PCM) for sustainable passive cooling in building envelopes. *Renewable and Sustainable Energy Reviews*, 60, 1470-1497. doi: 10.1016/j.rser.2016.03.036.

[2] Alshuraiaan, B. (2022). Efficient utilization of PCM in building envelope in a hot environment condition. *International Journal of Thermofluids*, 16, article number 100205. doi: 10.1016/j.ijft.2022.100205.

[3] Al-Yasiri, Q., & Szabó, M. (2021). Incorporation of phase change materials into building envelope for thermal comfort and energy saving: A comprehensive analysis. *Journal of Building Engineering*, 36, article number 102122. doi: 10.1016/j.jobe.2020.102122.

[4] Antipov, Ye.O. (2016). *System of comprehensive energy supply for consumers using alternative sources and combined energy storage systems*. (For the degree of Candidate of Technical Sciences, National University of Life and Environmental Sciences of Ukraine, Kyiv, Ukraine).

[5] Antypov, Ie., Mishchenko, A., Shelimanova, O., & Tarasenko, S. (2022). Analysis of the influence of the internal heat capacity of a public building on the thermal comfort parameters of the premises during the operation of the heating system in alternating mode. *Machinery & Energetics*, 13(2), 20-31. doi: 10.31548/machenergy.13(2).2022.20-31.

[6] Bai, Y., Guo, X., Pu, Y., Kang, X., & Wang, H. (2023). Effects of heat transfer medium flow field changes on the heat storage and discharge performance of phase change heat accumulators. *Journal of Energy Storage*, 57, article number 106278. doi: 10.1016/j.est.2022.106278.

[7] Bayraktar, F.S., & Köse, R. (2025). The impact of phase change materials on electricity consumption in prefabricated temporary houses. *Energy Science & Engineering,* 13(5), 2352-2363. doi: 10.1002/ese3.70035.

[8] Bejarano, G., Suffo, J.J., Vargas, M., & Ortega, M.G. (2018). Novel scheme for a PCM-based cold energy storage system. Design, modelling, and simulation. *Applied Thermal Engineering*, 132, 256-274. doi: 10.1016/j.applthermaleng.2017.12.088.
[9] Bodarya, K., & Kaushal, V. (2025). Thermoenergetic performance of phase change materials in building envelopes under future climate scenario. *Applied Sciences*, 15(3), article number 1562. doi: 10.3390/app15031562.
[10] Carlucci, F., Cannavale, A., Triggiano, A.A., Squicciarini, A., & Fiorito, F. (2021). Phase change material integration in building envelopes in different building types and climates: Modeling the benefits of active and passive strategies. *Applied Sciences*, 11(10), article number 4680. doi: 10.3390/app11104680.
[11] Cellat, K., Tezcan, F., Beyhan, B., Kardaş, G., & Paksoy, H. (2017). A comparative study on corrosion behavior of rebar in concrete with fatty acid additive as phase change material. *Construction and Building Materials*, 143, 490-500. doi: 10.1016/j.conbuildmat.2017.03.165.
[12] Constantin, L., Dragomir-Stanciu, D., & Crismaru, I.V. (2015). Optimization of heat exchange in a heat accumulator with latent heat storage. *Procedia Technology*, 19, 737-741. doi: 10.1016/j.protcy.2015.02.104.
[13] de Gracia, A. (2019). Dynamic building envelope with PCM for cooling purposes – proof of concept. *Applied Energy*, 235, 1245-1253. doi: 10.1016/j.apenergy.2018.11.061.
[14] Dmitruk, A., Naplocha, K., Grzęda, J., & Kaczmar, J.W. (2020a). Aluminum inserts for enhancing heat transfer in PCM accumulator. *Materials*, 13(2), article number 415. doi: 10.3390/ma13020415.
[15] Dmitruk, A., Naplocha, K., Kaczmar, J.W., & Smykowski, D. (2020b). Pin-fin metal alloy structures enhancing heat transfer in PCM-based heat storage units. *Heat and Mass Transfer*, 56, 2265-2271. doi: 10.1007/s00231-020-02861-6.
[16] Gao, Y., He, F., Meng, X., Wang, Z., Zhang, M., Yu, H., & Gao, W. (2020). Thermal behavior analysis of hollow bricks filled with phase-change material (PCM). *Journal of Building Engineering*, 31, article number 101447. doi: 10.1016/j.jobe.2020.101447.
[17] Hlek, Y.O. (2024). *Experimental and computational study of thermophysical properties of composite thermal storage nanomaterials based on technical paraffin*. (Doctoral dissertation, Odesa National Technological University, Odesa, Ukraine).
[18] The International Energy Agency. (n.d.). *Buildings*. Retrieved from https://www.iea.org/energy-system/buildings.
[19] Jaradat, M., Al Majali, H., Bendea, C., Bungau, C.C., & Bungau, T. (2023). Enhancing energy efficiency in buildings through PCM integration: A study across different climatic regions. *Buildings*, 14(1), article number 40. doi: 10.3390/buildings14010040.
[20] Khayyaminejad, A., & Fartaj, A. (2024). Unveiling the synergy of passive cooling, efficient ventilation, and indoor air quality through optimal PCM location in building envelopes. *Journal of Energy Storage*, 89, article number 111633. doi: 10.1016/j.est.2024.111633.
[21] Kots, I., Pankevych, O., & Badiaka, O. (2023). Current state and trends of improvement characteristics of main heat accumulating installations and materials. *Modern Technology, Materials and Design in Construction*, 35(2), 159-166. doi: 10.31649/2311-1429-2023-2-159-166.
[22] Kulish, V., Aslfattahi, N., Schmirler, M., & Sláma, P. (2023). New library of phase-change materials with their selection by the Rényi entropy method. *Scientific Reports*, 13, article number 10446. doi: 10.1038/s41598-023-37701-0.
[23] Lei, J., Yang, J., & Yang, E.-H. (2016). Energy performance of building envelopes integrated with phase change materials for cooling load reduction in tropical Singapore. *Applied Energy*, 162, 207-217. doi: 10.1016/j.apenergy.2015.10.031.
[24] Liu, C., Ma, Z., Jiang, R., Qu, J., & Rao, Z. (2020). Experimental study on heat transfer enhancement of phase change material using embedded oscillating heat pipe for thermal energy storage. *ISIJ International*, 60(10), 2157-2164. doi: 10.2355/isijinternational.isijint-2019-507.
[25] Liu, G., Xiao, T., Wang, X., Yang, X., & Li, H. (2022). Numerical analysis of inner heating tube position for improving solid-phase transition in a shell-and-tube heat accumulator. *Alexandria Engineering Journal,* 65, 771-784. doi: 10.1016/j.aej.2022.10.022.
[26] Liu, P., Wang, C., Chen, P., Cheng, X., & Wang, Z. (2024). Research progress of direct contact heat storage based on phase change heat storage. *Energy Storage*, 6(2), article number e585. doi: 10.1002/est2.585.
[27] Lu, B., Zhang, Y., Sun, D., Wang, C., Wang, Z., & Luo, M. (2023). Improving the melting performance of phase change material (PCM) in a latent heat thermal energy storage unit via a non-uniform arrangement of longitudinal fin. *Proceedings of the Institution of Mechanical Engineers, Part A: Journal of Power and Energy*, 237(5), 1100-1112. doi: 10.1177/09576509231156236.
[28] Lu, S., Li, Y., Kong, X., Pang, B., Chen, Y., Zheng, S., & Sun, L. (2016). A review of PCM energy storage technology used in buildings for the global warming solution. In *Energy solutions to combat global warming* (pp. 611-644). Cham: Springer International Publishing. doi: 10.1007/978-3-319-26950-4_31.
[29] Nallusamy, N., Sampath, S., & Velraj, R. (2007). Experimental investigation on a combined sensible and latent heat storage system integrated with constant/varying (solar) heat sources. *Renewable Energy*, 32(7), 1206-1227. doi: 10.1016/j.renene.2006.04.015.

[30] Osterman, E., Del Pero, C., Zavrl, E., Leonforte, F., Aste, N., & Stritih, U. (2023). Phase-change material thermal energy storage for the smart retrofitting of existing buildings. *Energies*, 16(17), article number 6127. doi: 10.3390/en16176127.

[31] Özdemir, M., & Gülten, A. (2024). Effect of phase change materials on building heating and cooling load considering different wall combinations. *Journal of Design for Resilience in Architecture and Planning*, 5(3), 363-377. doi: 10.47818/drarch.2024.v5i3137.

[32] Pfleger, N., Bauer, T., Martin, C., Eck, M., & Wörner, A. (2015). Thermal energy storage – overview and specific insight into nitrate salts for sensible and latent heat storage. *Beilstein Journal of Nanotechnology*, 6, 1487-1497. doi: 10.3762/bjnano.6.154.

[33] Powała, K., Obraniak, A., Heim, D., & Mrowiec, A. (2022). Macroencapsulation of paraffin in a polymer-gypsum composite using granulation technique. *Materials*, 15(11), article number 3783. doi: 10.3390/ma15113783.

[34] Rathore, P.K.S., & Shukla, S.K. (2020). An experimental evaluation of thermal behavior of the building envelope using macroencapsulated PCM for energy savings. *Renewable Energy*, 149, 1300-1313. doi: 10.1016/j.renene.2019.10.130.

[35] Saffari, M., Roe, C., & Finn, D.P. (2022). Improving the building energy flexibility using PCM-enhanced envelopes. *Applied Thermal Engineering*, 217, article number 119092. doi: 10.1016/j.applthermaleng.2022.119092.

[36] Sharma, A., Tyagi, V.V., Chen, C.R., & Buddhi, D. (2009). Review on thermal energy storage with phase change materials and applications. *Renewable and Sustainable Energy Reviews*, 13(2), 318-345. doi: 10.1016/j.rser.2007.10.005.

[37] Singh, S.K., Verma, S.K., Kumar, R., Sharma, A., Singh, R., & Tiwari, N. (2022). Experimental analysis of latent heat thermal energy storage system using encapsulated multiple phase-change materials. *Proceedings of the Institution of Mechanical Engineers, Part E: Journal of Process Mechanical Engineering*, 238(1), 124-133. doi: 10.1177/09544089221110983.

[38] Vanaga, R., Narbuts, J., Freimanis, R., Zundāns, Z., & Blumberga, A. (2023). Performance assessment of two different phase change materials for thermal energy storage in building envelopes. *Energies*, 16(13), article number 5236. doi: 10.3390/en16135236.

[39] Velasco-Carrasco, M., Chen, Z., Aguilar-Santana, J.L., & Riffat, S. (2020). Experimental evaluation of thermal energy storage (TES) with phase change materials (PCM) for ceiling tile applications. *Future Cities and Environment*, 6(1), article number 11. doi: 10.5334/fce.101.

[40] Yang, H., Zhang, G., Liu, Z., Yan, X., Lu, W., & Wang, Z. (2021). An experimental investigation on the control mechanism and heat transfer enhancement of composite phase change materials. *Energy Proceedings*, 16, article number 8390. doi: 10.46855/energy-proceedings-8390.

Аналіз використання фазоперехідних матеріалів для підвищення рівня енергоефективності будівель та акумуляції теплової енергії

Євген Лазарєв

Аспірант
Національний технічний університет України
«Київський політехнічний інститут імені Ігоря Сікорського»
03056, просп. Берестейський, 37, м. Київ, Україна
https://orcid.org/0009-0008-1655-7918

Ірина Суходуб

Кандидат технічних наук, доцент
Національний технічний університет України
«Київський політехнічний інститутімені Ігоря Сікорського»
03056, просп. Берестейський, 37, м. Київ, Україна
https://orcid.org/0000-0002-5895-1306

Анотація. Зростання попиту на енергоефективні будівлі та прагнення до зниження викидів парникових газів вимагають впровадження інноваційних підходів до управління тепловою енергією в будівлях. Одним із таких підходів є використання фазоперехідних матеріалів, які забезпечують акумуляцію теплової енергії та підвищують теплову інерційність будівельних конструкцій, що робить їх ефективним рішенням для оптимізації енергоефективності будівель у різних кліматичних умовах. Метою статті був аналіз існуючих методів використання фазоперехідних матеріалів для підвищення енергоефективності будівель шляхом акумуляції теплової енергії. Зокрема, досліджувалися методи включення таких матеріалів в оболонку будівель та застосування їх у теплових акумуляторах. У статті застосовано методи аналізу та систематизації наукової літератури, зокрема розглянуто результати досліджень щодо впливу фазоперехідних матеріалів на теплову інерційність будівельних конструкцій, ефективність їх використання в теплових акумуляторах та вплив на енергоефективність будівель. Встановлено, що застосування фазоперехідних матеріалів сприяє значному підвищенню теплової інерційності будівель та зниженню втрат теплової енергії. Проаналізовано різні методи включення фазоперехідних матеріалів в оболонку будівель та їх використання у теплових акумуляторах. Виявлено основні переваги та недоліки кожного з методів, а також наведено приклади їх практичного застосування. Висвітлено можливі способи використання теплових акумуляторів з метою підвищення енергоефективності будівель, зокрема їх включення в системи опалення та гарячого водопостачання. Результати дослідження можуть бути використані при проєктуванні енергоефективних будівель, систем опалення та гарячого водопостачання, які використовують фазоперехідні матеріали для акумуляції теплової енергії, що сприятиме зниженню енергоспоживання та підвищенню комфорту проживання

Ключові слова: фазоперехідні матеріали; парафін; огороджувальні конструкції; теплова інерційність; прихована теплота

TECHNOLOGIES AND ENGINEERING

Journal homepage: https://technologies-engineering.com.ua/en
Vol. 26, No. 3, 2025

Received: 27.01.2025
Revised: 19.05.2025
Accepted: 25.06.2025

UDC 504.064:004.942

DOI: 10.30857/2786-5371.2025.3.4

Information and analytical technologies for decision support in environmental monitoring systems of amalgamated territorial communities

Andriy Moshensky

PhD, Associate Professor
National University of Food Technologies
01033, 68 Volodymyrska Str., Kyiv, Ukraine
https://orcid.org/0000-0002-4584-4958

Igor Savchenko*

Postgraduate Student
National University of Food Technologies
01033, 68 Volodymyrska Str., Kyiv, Ukraine
https://orcid.org/0000-0002-5798-7104

Abstract. The relevance of this study is conditioned by the increasing need to improve the effectiveness of environmental monitoring of amalgamated territorial communities in the context of growing anthropogenic and military impacts on the environment. The purpose of the study was to create an integrated decision support system for environmental monitoring, which allows combining data from different sources, continuously monitoring the state of ecosystems, predicting changes, and quickly responding to environmental threats. In the course of the research, a systematic approach, mathematical modelling of ecosystem dynamics, the least squares method for identifying model parameters based on limited data were applied, including cloud technologies, the Internet of Things, crowdsourcing platforms, and sensor networks for collecting and processing information were introduced. Data integration was carried out from government, public and departmental sources, which provided comprehensive coverage of various types of environmental impacts. The main results of the study were: development of a multi-level organisational structure of the monitoring system, construction of discrete and continuous mathematical models for assessing and predicting the state of ecosystems, implementation of recurrent algorithms for adapting models to changes in the environment. The system helped to ensure constant monitoring of industrial, agro-industrial and military-anthropogenic impacts, identify potential threats in a timely manner, assess their impact, and make informed management decisions to reduce environmental risks. The developed decision support system helps to effectively manage environmental risks, contributes to improving environmental safety and sustainable development of amalgamated territorial communities. The integration of advanced information technologies, mathematical models and public involvement in the monitoring process creates a new paradigm of environmental management in crisis conditions

Keywords: Internet of Things; military impact; crowdsourcing; mathematical modelling; anthropogenic load; risk management; cloud technologies

Introduction

Environmental monitoring in amalgamated territorial communities (ATC) defined a key role for sustainable development and environmental protection. The problem of insufficient coordination between the international, state, local, public, and departmental levels was identified, which made it difficult to respond to threats in a timely manner, especially due to the growing anthropogenic and military burden. Public monitoring was recognised as important for the implementation of the right to a safe environment and the detection of violations. The relevance of the study was

Suggested Citation:
Moshensky, A., & Savchenko, I. (2025). Information and analytical technologies for decision support in environmental monitoring systems of amalgamated territorial communities. *Technologies and Engineering,* 26(3), 54-65. doi: 10.30857/2786-5371.2025.3.4.

*Corresponding author

justified by the need to create an integrated decision support system (DSS) for combining information, continuous monitoring, forecasting, and rapid response in ATC. Global experience and current scientific paradigms were used for effective monitoring and implementation of advanced DSS.

A. Popov (2024) focused on the analysis of advanced regional environmental monitoring systems using cloud and Internet of Things technologies. The study examined the level of development of integrated information systems for collecting, processing, and managing eco-data. The advantages are the use of the Internet of Things with multisensory systems for instant collection and processing of large amounts of information in real time. Due to its modular architecture, systems are flexible, scalable, and integrated with other technologies. However, the complexity of integrating heterogeneous data and technologies, and the dependence of model accuracy on information quality, remain problems. It is also important to ensure compatibility and standardisation of components for effective interaction of the system.

The study by A. Bonfante *et al*. (2024) detailed the development of a geospatial DSS to support EU authorities in implementing climate change adaptation policies. The tool combines spatial and non-spatial data, works at various scales from municipality to Europe, and includes advanced climate models for assessing anomalies and crop adaptation. The advantages were openness, free access, flexible architecture, working with large amounts of data, fast visualisation and report generation. The disadvantages were the complexity of implementation due to the need for high-quality information and technical training of users, and significant efforts to standardise and compatibility of system components. S. Xu (2024) combined the development of artificial intelligence-based DSS for sustainable urban planning in smart cities. The system analyses big data, models scenarios, and optimises resources to improve energy and water efficiency, develop public gardens, and transport infrastructure. The advantages were an integrated approach, integration of various data and technologies to improve environmental sustainability, and forecasting long-term impacts and optimising resources. The disadvantages were dependence on data quality, which affects the accuracy of forecasts, the difficulty of integrating with existing infrastructure due to different standards, and the need for significant investment in technology and training of specialists.

The study by J. Haqbeen *et al.* (2021) focused on involving residents, particularly women and minorities, in identifying problems and finding solutions for local authorities. The study demonstrated how digital tools promote equal participation of citizens in urban planning, even in times of crisis. The advantages were the involvement of different segments of the population, reducing bias in discussions, and creating a platform for dialogue between society and the authorities. The system collects and organises proposals, increasing the transparency and effectiveness of strategic planning. The disadvantages were the need to improve digital literacy, ensure confidentiality, and the need to support the authorities and adapt to socio-cultural conditions, which makes it difficult to scale and stability the system.

B. Orlove *et al*. (2020) reviewed climate decision-making processes. The researchers tracked the development of the industry from politics to the analysis of various stakeholders – the private sector, community organisations, and indigenous communities, with a focus on cognitive and deliberative processes. Special attention was paid to the influence of the social environment, scientific knowledge, and conceptual framework. The advantages were an interdisciplinary approach that combined psychological and rational aspects, and the use of non-climatic narratives and the concept of urgency to encourage change. The disadvantages were the complexity of performance assessment due to multidimensional processes, the lack of empirical data, the difficulty of interaction between participants and the limited integration of scientific data into practice, which makes it difficult to achieve climate policy goals.

A. Sadeghi-Niaraki *et al*. (2020) combined information from citizens with geoinformation technologies and multi-criteria analysis to improve pollution monitoring and decision-making in waste management. The researchers highlighted the advantages of the system – improving the accuracy and detail of data due to the participation of local residents as human sensors, and the effectiveness of management decisions and the development of environmental consciousness. The disadvantages were the heterogeneity and subjectivity of data, the complexity of verification and integration, the dependence of performance on the activity of the population, digital technologies, and infrastructure for collecting and analysing information. A.J. Constable *et al*. (2022) conducted an analysis of decision support tools in the field of climate risk management. Systematisation of methods, consideration of the political, social and cultural context, and involvement of interested parties were noted. The lack of a universal tool, complexity of integration in multi-level systems, uncertainty of goals and limited quality data were revealed. The importance of a flexible, context-sensitive approach, and an iterative decision-making process was emphasised.

Recent research in systems ecology and decision support information technologies has shown the effectiveness of mathematical models of ecosystem dynamics, expert systems, the Internet of Things, cloud technologies, and crowdsourcing for integrated environmental monitoring. Despite the numerous systems at different levels, there are problems of interaction between them and modelling the impact of anthropogenic and military factors, which requires further study. The issues of identifying model parameters based on limited data and integrating multi-level monitoring systems were not sufficiently investigated. The purpose of the study was to develop and substantiate an integrated decision support system for environmental monitoring of amalgamated territorial communities using advanced information technologies, modelling ecosystem dynamics, and identifying parameters based on limited data to improve the effectiveness of environmental risk management.

Materials and Methods

The study was conducted in accordance with the principles of scientific correctness, reproducibility, and transparency. The key stages of scientific research were the analysis of current approaches to environmental monitoring and decision support systems; formalisation of necessary requirements for an integrated multi-level monitoring system; development of mathematical models of ecosystem dynamics; identification of model parameters based on a limited amount of data; creation of an organisational and technical structure for information support of the decision support system. To achieve this goal, a systematic approach was applied, focused on the analysis of monitoring levels (state, local, public, departmental), which contributes to the comprehensive consideration of interaction between participants in environmental control. The rationale for choosing modelling methods was explained by the need to recreate complex processes in terrestrial ecosystems under anthropogenic and military pressure. For this purpose, linear and nonlinear differential and difference equations were used to describe the dynamics of organic matter reserves (Chapin *et al.*, 2012), and the least squares method for identifying model parameters based on available environmental data (Lysenko *et al.*, 2017). To improve the accuracy of prediction, recurrent parameter estimation algorithms were used (Slabospytsky, 2008), which ensured the adaptation of models to changes in the environment. Recurrent algorithms for estimating ecosystem parameters are a type of algorithm that uses previous values or the state of the ecosystem to calculate the current value.

The information base of the decision support system was developed based on integrating data from various sources: state and public environmental monitoring networks, crowdsourcing platforms, wireless sensor systems, and open databases (Füller *et al.*, 2021). For data collection, storage and processing, cloud technologies for the development of multidimensional databases, the Internet of Things for the development of intelligent sensors, automated workplaces for conducting expert assessments of the parameters of the impact of anthropogenic and military loads on ecosystems, local area networks and server capacities for decision support systems (Killen *et al.*, 2022). The criteria for developing a sample for the empirical part of the study were based on the representativeness of data on various types of load on ecosystems (anthropogenic, agro-industrial, military) and the availability of high-quality information for modelling. The experimental base of the study covered data from open state and public sources of environmental monitoring (Ecodozor, n.d.; Ecozagroza, n.d.), and simulation results at test sites (dedicated locations for monitoring background monitoring parameters) that reflect typical environmental impact scenarios.

The dynamics of organic matter reserves in the biogeocoenosis was described by a system of discrete equations that consider changes in organic mass reserves in various components of the ecosystem over a certain period of time:

$$\begin{cases} P(i+1) = P(i) + \Delta_P(i,\ i+1) - \Delta_G(i,\ i+1); \\ G(i+1) = G(i) + \Delta_G(i,\ i+1) - \Delta_S(i,\ i+1); \\ S(i+1) = S(i) + \Delta_S(i,\ i+1) - \Delta_S^*(i,\ i+1), \end{cases} \tag{1}$$

where $i \in N$ – discrete time; $\Delta_P(i, i+1)$, $\Delta_G(i, i+1)$, $\Delta_S(i, i+1)$ – respectively, an increase in aboveground phytomass, precipitation, and litter in the time interval from i to $i+1$; $\Delta_S^*(i, i+1)$ – reduction of litter in the time interval from i to $i+1$.

The sampling interval is assumed to be one year, and the countdown began with the period when plants reach their maximum development – this is usually the end of May or the beginning of June. In order to construct a continuous mathematical model, the following dependencies were used:

$$\dot{P}(t) \cong \frac{P(i+1)-P(i)}{1\ year} = P(i+1) - P(i); \tag{2}$$

$$\dot{G}(t) \cong \frac{G(i+1)-G(i)}{1\ year} = G(i+1) - G(i); \tag{3}$$

$$\dot{S}(t) \cong \frac{S(i+1)-S(i)}{1\ year} = S(i+1) - S(i). \tag{4}$$

Given that in the first approximation, the increments $\Delta_P(i, i+1)$, $\Delta_G(i, i+1)$, $\Delta_S(i, i+1)$, $\Delta_S^*(i, i+1)$ are proportional to $P(i) + S(i)$, $P(i)$, $G(i)$, $S(i)$, respectively, a system of equations is derived:

$$\begin{cases} P(i+1) = a_{11}P(i) + 0G(i) + a_{13}S(i); \\ G(i+1) = a_{21}P(i) + a_{22}G(i) + 0S(i); \\ S(i+1) = 0P(i) + a_{32}G(i) + a_{33}S(i); \end{cases} \tag{5}$$

$$a_{11} = 1 + \frac{\Delta_P(i,i+1)}{P(i)+S(i)} - \frac{\Delta_G(i,i+1)}{P(i)} \cong const_1;\ a_{12} = 0; \tag{6}$$

$$a_{13} = 1 + \frac{\Delta_P(i,i+1)}{P(i)+S(i)} \cong const_2; \tag{7}$$

$$a_{21} = \frac{\Delta_G(i,i+1)}{P(i)} \cong const_3; \tag{8}$$

$$a_{22} = 1 - \frac{\Delta_S(i,i+1)}{G(i)} \cong const_4;\ a_{23} = 0;\ a_{31} = 0; \tag{9}$$

$$a_{32} = \frac{\Delta_S(i,i+1)}{G(i)} \cong const_5; \tag{10}$$

$$a_{33} = 1 - \frac{\Delta_S{}^*(i,i+1)}{S(i)} \cong const_6; \tag{11}$$

In matrix form, equation (5), considering external influence, has the following form:

$$\begin{bmatrix} P(i+1) \\ G(i+1) \\ S(i+1) \end{bmatrix} = \begin{bmatrix} a_{11} & 0 & a_{13} \\ a_{21} & a_{22} & 0 \\ 0 & a_{32} & a_{33} \end{bmatrix} \begin{bmatrix} P(i) \\ G(i) \\ S(i) \end{bmatrix} + \begin{bmatrix} W_1(i) \\ W_2(i) \\ W_3(i) \end{bmatrix}, \tag{12}$$

where $W_n(i)$, $(n = \overline{1,\ 3})$ – external influences, including test factors.

Data from open state and public sources of environmental monitoring (Ecodozor, n.d.; Ecozagroza, n.d.) were used to determine the indicators of anthropogenic and military loads $W_n(i)$, $(n = \overline{1,\ 3})$. Vector equation (12) provided a discrete model of the dynamics of organic matter reserves. The continuous model took the form:

$$\begin{bmatrix}\dot{P}(t)\\ \dot{G}(t)\\ \dot{S}(t)\end{bmatrix} = \begin{bmatrix}a_{11}{}^{-1} & 0 & a_{13}\\ a_{21} & a_{22}{}^{-1} & 0\\ 0 & a_{32} & a_{33}{}^{-1}\end{bmatrix}\cdot\begin{bmatrix}P(t)\\ G(t)\\ S(t)\end{bmatrix} + \begin{bmatrix}W_1(t)\\ W_2(t)\\ W_3(t)\end{bmatrix}. \quad (13)$$

The vector of unknown parameters was denoted as $X^T = [a_{11}, a_{13}, a_{21}, a_{22}, a_{32}, a_{33}] = [X_1, X_2, X_3, X_4, X_5, X_6]$ and assumed $W_n(i) \equiv 0$, $(n = 1, 2, 3)$, in which case, a system of equations was obtained to identify these parameters:

$$\begin{cases} P(i+1) = P(i)\cdot X_1 + S(i)\cdot X_2 + 0\cdot X_3 + 0\cdot X_4 + 0\cdot X_5 + 0\cdot X_6;\\ G(i+1) = 0\cdot X_1 + 0\cdot X_2 + G(i)\cdot X_3 + S(i)\cdot X_4 + 0\cdot X_5 + 0\cdot X_6;\\ S(i+1) = 0\cdot X_1 + 0\cdot X_2 + 0\cdot X_3 + 0\cdot X_4 + G(i)\cdot X_5 + S(i)\cdot X_6;\\ P(i+K+1) = P(i+1)\cdot X_1 + S(i+1)\cdot X_2 + 0\cdot X_3 + 0\cdot X_4 + 0\cdot X_5 + 0\cdot X_6;\\ G(i+K+1) = 0\cdot X_1 + 0\cdot X_2 + G(i+1)\cdot X_3 + S(i+1)\cdot X_4 + 0\cdot X_5 + 0\cdot X_6;\\ S(i+K+1) = 0\cdot X_1 + 0\cdot X_2 + 0\cdot X_3 + 0\cdot X_4 + G(i+1)\cdot X_5 + S(i+1)\cdot X_6, \end{cases} \quad (14)$$

where K – time shift, $K \in N$.

Since a limited number of measurements are available at the initial stage of studying the terrestrial ecosystem of the ATC, it is sufficient to solve a system consisting of six linear equations and containing six unknown variables to determine the vector of unknown parameters. In this case, the least squares method was used in the recurrent form (Mokin *et al.*, 2010), but only after the amount of data collected has increased. The obtained values of the parameters of the mathematical model of the ecosystem should be considered as a primary approximation – that is, as an initial condition that will be used in the future for the recurrent application of the least squares algorithm. This approach allows gradually refining the model parameters as the amount of incoming information increases, and increases the accuracy of subsequent calculations. To confirm the correctness of the hypothesis put forward in relation to the mathematical model in the form (5), the following conditions were used: $a_{12} = a_{23} = a_{31} = 0$:

$$\begin{cases} P(i+\tau) - \hat{a}_{11}P(i+\tau) - \hat{a}_{13}G(i+\tau) \cong 0;\\ G(i+\tau) - \hat{a}_{21}P(i+\tau) - \hat{a}_{22}G(i+\tau) \cong 0;\\ S(i+\tau) - \hat{a}_{32}G(i+\tau) - \hat{a}_{33}G(i+\tau) \cong 0, \end{cases} \quad (15)$$

where τ – time shift; $\hat{a}_{11}, \hat{a}_{13}, \hat{a}_{21}, \hat{a}_{22}, \hat{a}_{32}, \hat{a}_{33}$ – estimation of the values of the parameters of the mathematical model (12).

Given the limited number of experimental data available for calculating estimates of model parameters (12), it was necessary to apply the simplest and most efficient algorithm for determining the parameters of the system of difference equations (5). This algorithm was based on relations (6)-(11), which established a relationship between the estimates of system parameters (12) and the increments of the corresponding biomass. First, equation (1) was solved with respect to changes $\Delta_P(i, i+1), \Delta_G(i, i+1), \Delta_S(i, i+1)$, using values *P(i)* and *P(i+1)* known from observations, and it was assumed that the desired values $\Delta_S^*(i, i+1) = K_S S(i)$, $KS \in [0; 1]$ of the system parameters (12) were found. The parameters of this model were calculated based on real experimental data and were shown in Table 1, which ensured its compliance with the actual characteristics of ecosystems.

Table 1. *Model adequacy check*

Data type			1970			1971			1972		
Data on the dynamics of organic matter reserves in the biogeocoenosis of reed grass meadow, [g/m²]			*P*(*i*)	*G*(*i*)	*S*(*i*)	*P*(*i*)	*G*(*i*)	*S*(*i*)	*P*(*i*)	*G*(*i*)	*S*(*i*)
			154	124	121	240	190	145	295	204	245
Simulation modelling: 1970 – initial conditions, 1971, 1972 – forecast	linear model	continuous	154	124	121	234	182	136	318	262	218
		discrete	154	124	121	226	166	150	325	250	200
	nonlinear model	continuous	154	124	121	144	122	144	144	122	150
		discrete	154	124	121	134	130	156	144	110	166

Note: *accuracy of experimental data ±15%*
Source: *V. Smith (1988), F.S. Chapin et al. (2006)*

These experimental results remain relevant and can be used in contemporary research. To identify the parameters, not only data taken from scientific sources were used, but also the results of specially conducted experimental observations. The initial values of the parameters were determined based on the analysis of the first two columns of the corresponding table, and considering the accepted litter loss coefficient, which is shown in Table 2, which allows more accurately reproducing the real conditions of the ecosystem functioning.

Table 2. *Performance improvement indicators*

Natural environment (number of model components)		Conceptual objectivity, score	Pragmatic objectivity (1-10 years), %									
			1	2	3	4	5	6	7	8	9	10
Phytocoenosis	Before	Green phytomass – 1.	K_{ph}	K_{ph}	K_{ph}	1.5 K_{ph}	1.5 K_{ph}	1.5 K_{ph}	2 K_{ph}	2 K_{ph}	2.5 K_{ph}	3 K_{ph}
	After	Green phytomass, litter – forest floor – 3 (prevails).										

Table 2. Continued

Natural environment (number of model components)		Conceptual objectivity, score	Pragmatic objectivity (1-10 years), %									
			1	2	3	4	5	6	7	8	9	10
Zoocoenosis	Before	–	1.5 K_z	1.5 K_z	1.5 K_z	2 K_z	2 K_z	2 K_z	2.5 K_z	2.5 K_z	3 K_z	3 K_z
	After	Divichky target range – 16. Yavoriv military base – 18 (prevails).										

Note: *the level of reduction in the current estimate error – less than 30%. Provided that pollution has led to a decrease in green phytomass growth by reducing the coefficient of organic matter transfer from litter to phytomass by only* K_{ph} *%, or by slowing down the transfer of lower-level consumer biomass to higher-level biomass by* K_z *%*
Source: *A. Lysenko et al. (2017)*

A special observation algorithm based on the Lewinberger observer was used to assess and predict the state of organic matter in the ecosystem. The parameters of this algorithm were optimised using the standard error minimisation criterion, which ensured stable operation of the algorithm even in cases of significant errors in the measurements of green phytomass (Chapin *et al.*, 2012). The parameters of the continuous model were calculated in the same way as for the discrete model, using the same relations. The model parameters were calculated using experimental data and the corresponding equations (17)-(27). Based on the system of balance equations (1), a system of nonlinear difference equations (16) was formed, which describe in detail the dynamic changes in the main components of the ecosystem. This model considered complex interactions between elements of the biogeocoenosis, which helped to more accurately reproduce the processes that occur in the natural environment, especially in conditions where the influence of anthropogenic or other external factors is significant.

$$\begin{cases} P(i+1) = a_1 \cdot P(i) + a_2 \cdot P(i) \cdot S(i) + a_3 \cdot P^2(i) + W_1(i); \\ G(i+1) = b_1 \cdot P(i) + b_2 \cdot G(i) + b_3 \cdot S(i) + b_4 \cdot P^2(i) + b_5 \cdot G^2(i) + W_2(i); \\ S(i+1) = c_1 \cdot P(i) + c_2 \cdot G(i) + c_3 \cdot S(i) + c_4 \cdot G^2(i) + c_5 \cdot S^2(i) + W_3(i); \end{cases} \quad (16)$$

$$a_1 = 1 + \frac{\Delta_P(i,i+1)}{P(i)+P(i)\cdot S(i)} - \frac{\Delta_G(i,i+1)}{P(i)}; \quad (17)$$

$$a_2 = \frac{\Delta_P(i,i+1)}{P(i)+P(i)\cdot S(i)}; \quad (18)$$

$$a_3 = -\left(\frac{\Delta_G(i,i+1)}{P(i)}\right)^2; \quad (19)$$

$$b_1 = \frac{\Delta_G(i,i+1)}{P(i)}; \quad (20)$$

$$b_2 = 1 - \frac{\Delta_S(i,i+1)}{G(i)}; \; b_3 = 0; \quad (21)$$

$$b_4 = \left(\frac{\Delta_G(i,i+1)}{P(i)}\right)^2; \quad (22)$$

$$b_5 = -\left(\frac{\Delta_S(i,i+1)}{G(i)}\right)^2; \; c_1 = 0; \quad (23)$$

$$c_2 = \frac{\Delta_S(i,i+1)}{G(i)}; \quad (24)$$

$$c_3 = 1 - K_S; \quad (25)$$

$$c_4 = \left(\frac{\Delta_S(i,i+1)}{G(i)}\right)^2; \quad (26)$$

$c_5 = -K_S^{\,2}$, $W_n(i)$; $(n = 1, 2, 3)$ – external influence. (27)

To calculate the coefficients in equations (16), the formulas given in the range (17)-(27) were used. In this process, they relied on changes $\Delta_P(i, i+1)$, $\Delta_G(i, i+1)$, $\Delta_S(i, i+1)$, which were obtained by solving the system of equations (1). These changes were calculated based on the observed values of P(i) and P(i + 1), while considering the assumptions that $\Delta^*_S(i, i+1) = K_S S(i)$, $K_S \in [0; 1]$. The continuous model took the form:

$$\begin{cases} \dot{P}(t) = (a_1 - 1) \cdot P(t) + a_2 \cdot P(t) \cdot S(t) + a_3 \cdot P^2(t) + W_1(t); \\ \dot{G}(t) = b_1 \cdot P(t) + (b_2 - 1) \cdot G(t) + b_3 \cdot S(t) + b_4 \cdot P^2(t) + b_5 \cdot G^2(t) + W_2(t); \\ \dot{S}(t) = c_1 \cdot P(t) + c_2 \cdot G(t) + (c_3 - 1) \cdot S(t) + c_4 \cdot G^2(t) + c_5 \cdot S^2(t) + W_3(t). \end{cases} \quad (28)$$

A nonlinear computer simulation model was created based on a discrete model, the parameters of which were calculated using experimental data presented in Table 1. For this purpose, the corresponding dependencies were used, which are defined by equations (17)-(27). Simulation estimation and prediction of the development over time of the state vector of a nonlinear discrete system describing changes in the content of organic matter was carried out on the condition that the initial parameters of the system were unknown, and the components of the model can vary up to 20% of the nominal values. The parameters of the continuous model were calculated based on experimental data using the corresponding dependencies defined by equations (17)-(27).

Results and Discussion

Analysing the work of the territorial community in the field of environmental monitoring, certain doubts arise as to how effectively the coordination and integration of different levels of observation – from international to state, local, public and departmental – is taking place. At the international level, there are systems for assessing the environmental condition specified in the Resolution of the Cabinet of Ministers of Ukraine No. 391 (1998), which operate under the leadership of such organisations as the United Nations, UNESCO, and UNEP. Simultaneously, at the local level, monitoring is carried out by various structures: state bodies, municipal services, specialised divisions of the communities themselves, and industrial and agricultural enterprises that conduct their own departmental environmental control. Special attention should be paid to public monitoring, which plays an important role in the implementation of citizens' right to a safe environment (Morshch & Savchenko, 2018; Alvarez-Risco & Del-Aguila-Arcentales, 2021) and helps to identify violations of environmental laws (Donnelly *et al.*, 2014).

Due to the dispersion and lack of interaction between these different actors, doubts arise whether the existing system is able to respond in a timely and comprehensive manner to environmental threats, especially in the face of growing anthropogenic and military load on the environment. It is these challenges that highlight the urgent need to create a specialised decision support system (Fig. 1), which would be able to combine all information flows, ensure continuous monitoring of sources of industrial, agro-industrial, and military-anthropogenic load, and assess the impact of these factors on the ecosystem, predict possible changes in the natural environment and promote rapid response to emergencies (Morshch & Savchenko, 2018). Special attention was paid to formalising the structure of a multi-level monitoring system, building discrete and continuous models of the dynamics of organic matter reserves in terrestrial ecosystems, and developing recurrent algorithms for estimating parameters to improve the accuracy of scientific forecasts in difficult conditions of anthropogenic and military loads.

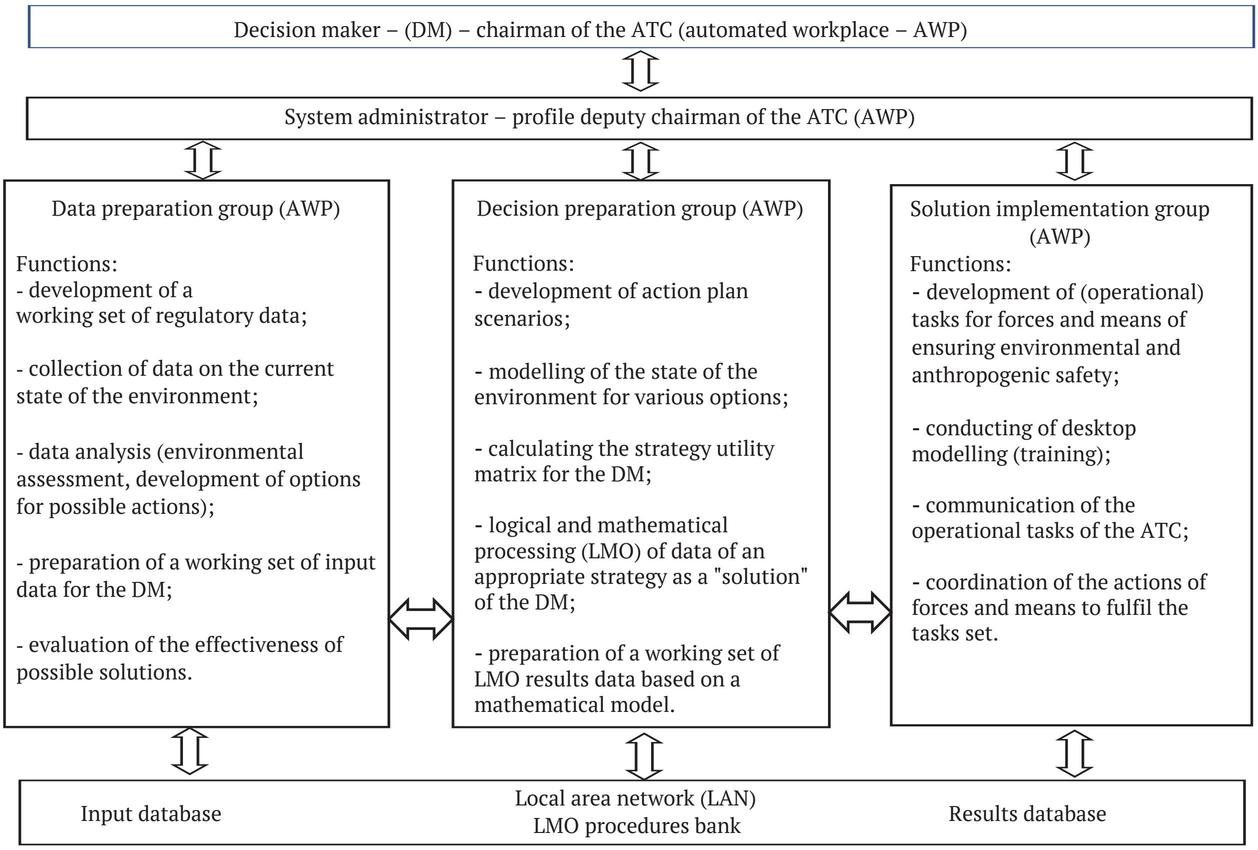

Figure 1. *General block diagram of the DSS for environmental monitoring of the environment*
Source: *developed by the authors*

The main functions of such a decision support system include:

1. Continuous monitoring of industrial anthropogenic load (IAL), agro-industrial anthropogenic load (AIAL) and military anthropogenic load (MAL) (Chumachenko *et al.*, 2022).
2. Assessment of the physical state of the environment and natural processes occurring in it.
3. Forecasting changes in the environmental situation and assessing the potential consequences of these changes.
4. Improving the speed and quality of user information services at various levels of management, in accordance with DSTU 9001:2001 (2001).
5. Support of the adoption of informed and scientifically balanced management decisions aimed at reducing emissions and discharges of harmful substances into the environment.
6. Ensuring safety and comfortable living conditions for residents of amalgamated territorial communities.

The development and further implementation of such an DSS is an extremely necessary step to improve the effectiveness of environmental monitoring in AHS. This will help to identify potential threats that may negatively affect the environment in a timely manner, assess their impact, and take appropriate measures to protect nature and public health. According to advanced approaches to system ecology, for modelling biocoenoses in terrestrial ecosystems, the structure of mathematical models of biotopes can be represented by three main species. Firstly, these are linear scalar equations, which can be either ordinary differential or difference equations. They are used to describe the process of succession – that is, the gradual development and change of communities of organisms over time. Secondly, there are linear multidimensional equations that can also be differential or differential. These models are designed to reflect the dynamics of processes in biotopes where anthropogenic impact is minimal or completely absent, for example, in areas free of external factors, such as zoocoenoses. And thirdly, nonlinear logistic equations are applied, which can be either differential or difference. They are designed specifically for modelling phenomena in biotopes that are exposed to significant anthropogenic or military loads.

These types of models are used not only to estimate the current state of the ecosystem, but also to simulate forecasting, i.e., to analyse the current state of an object and model its behaviour in the future (Ivanyuta & Kachynskyi, 2012). Model parameters were estimated using the least squares method, which is used over a sliding time interval that can last up to 20 years (Dubovoy, 2012). Forecasting, in turn, is possible for a period of 10-12 years ahead, which allows assessing the potential consequences of changes in the system. For discrete models, the sampling period T_0 is taken as one year. At the initial stage, several years are allocated to obtain an initial approximation of the parameters, which ensures the accuracy of further calculations. In order to assess and predict the state of terrestrial ecosystems, a special computer simulation model was created (Fig. 2), which reproduces the key processes of the organic matter cycle in nature.

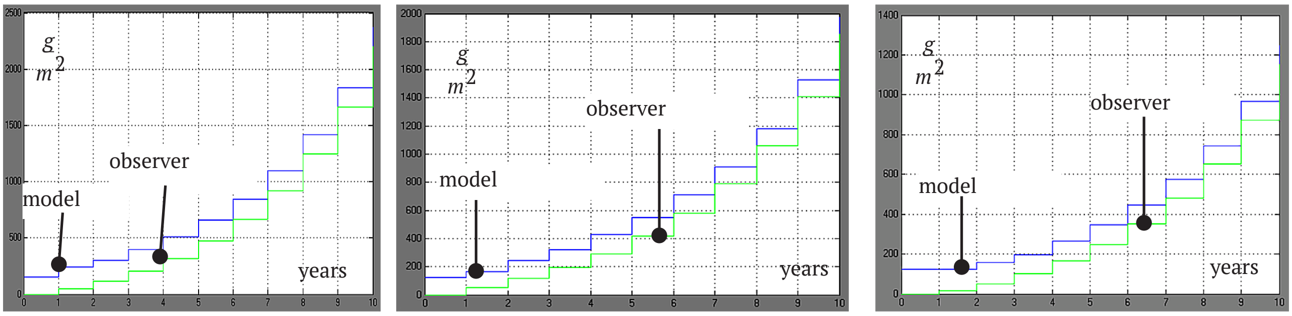

Figure 2. *Results of modelling simulation estimation and forecasting of the dynamics of the state vector of a linear discrete system of organic matter reserves*

Source: *a – green phytomass; b – litter; c – forest floor*

Source: *developed by the authors*

Verification of the model showed that if the initial parameters are the same, the forecast error for the first and second years does not exceed 10% of the actual values obtained during measurements. The conducted modelling showed that even if there are sufficiently large errors in the measurements of green phytomass – up to 30% – after four years, the error in assessing the state of all components of the model does not exceed 10%. This indicates the high ability of the chosen approach to correction and adaptation. In addition, it was found that all components of the model change in a consistent manner, regardless of the type of external perturbations. This result confirmed the expediency of focusing monitoring on green phytomass during its maximum growing season. With this approach, it is possible to obtain representative and reliable information about the overall state of the ecosystem, even if the amount of data available is limited.

It is also worth noting that advanced methods of remote sensing of the Earth greatly facilitate the collection of data on green phytomass. This makes regular monitoring of ecosystems more accessible and efficient, eliminating the need for complex and time-consuming field measurements. Simulation prediction based on a continuous linear model and Lewinberger observers confirmed the conclusions obtained for the discrete case (Fig. 3). This indicates the consistency of both models and the chosen approach as a whole, and their reliability and suitability for long-term forecasting of the state of terrestrial ecosystems. Comparison of the simulation results with actual experimental observations showed that the error can reach approximately ±45%, which is significantly higher than the accuracy shown by the linear model. A nonlinear computer simulation model was created based on a discrete model, the parameters of which are shown in Figure 4.

The results of a simulation experiment conducted using a nonlinear model together with the Lewinberger observer confirmed the same conclusions as previously obtained for the linear model. The initial values of the feedback matrix parameters in the observer were determined based on a linear model, which helped to move smoothly and efficiently to the application of a more complex nonlinear model. The simulation results showed high accuracy and reliability of this approach. Choosing between using a linear or nonlinear model requires a step-by-step and careful approach that considers the length of the observation period (at least 10 years) and the amount of experimental data available (Van Veen & Paul, 1981). This is necessary to ensure reliable identification of model parameters and obtain reliable results. The parameters of the continuous model are illustrated in Figure 5. The results showed that the continuous model confirms the consistency and reliability of the discrete model, which emphasises the effectiveness of both approaches in reflecting the dynamics of the processes under study. This suggests that both models are useful tools for analysing and predicting changes in systems associated with organic matter reserves.

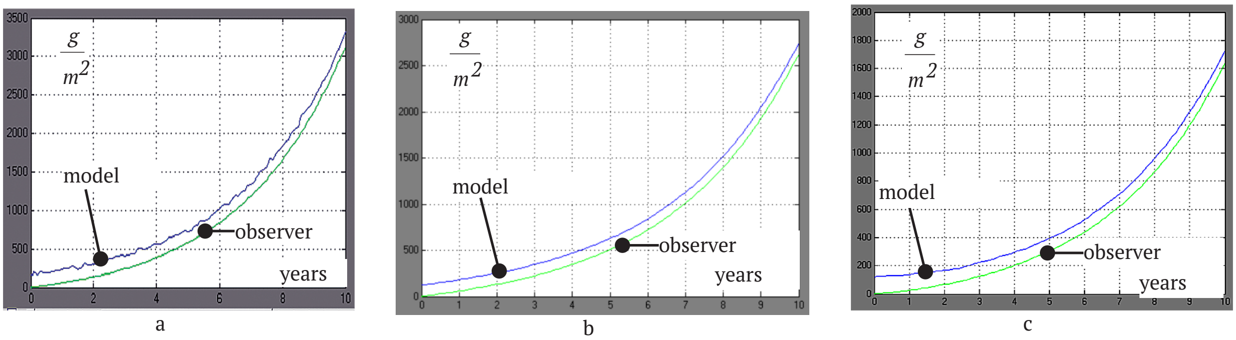

Figure 3. *Results of modelling simulation estimation and forecasting of dynamics of organic matter reserves of a linear continuous system*

Note: *a – green phytomass; b – litter; c – forest floor*

Source: *developed by the authors*

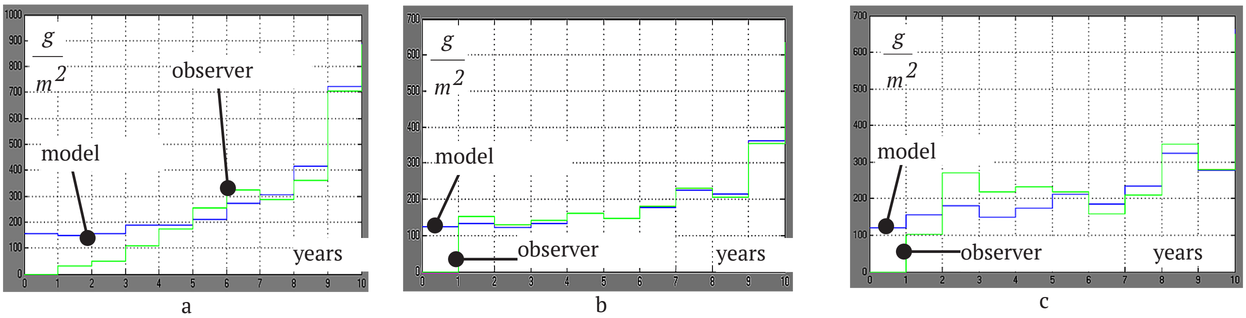

Figure 4. *Results of modelling simulation estimation and forecasting of the dynamics of the state vector of a nonlinear discrete organic matter system*

Note: *a – green phytomass; b – litter; c – forest floor*

Source: *developed by the authors*

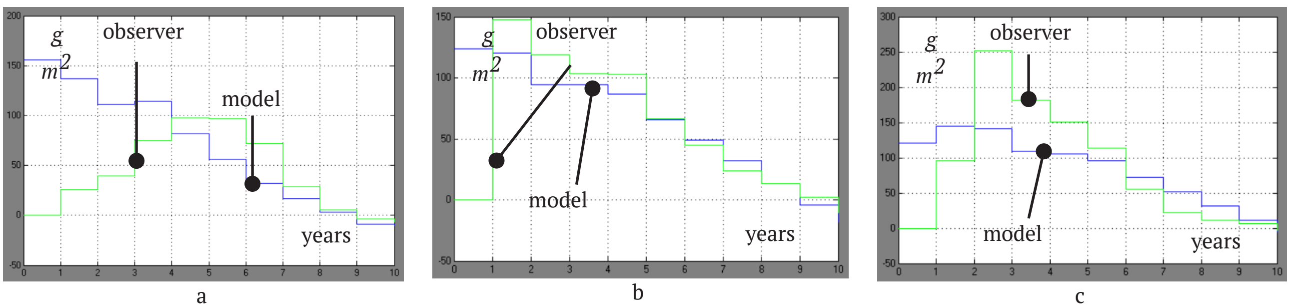

Figure 5. *Results of modelling simulation estimation and forecasting of the dynamics of the state vector of a nonlinear continuous organic matter system*

Note: *– a – green phytomass; b – litter; c – forest floor*

Source: *developed by the authors*

As part of this study, an integrated DSS designed for environmental monitoring in ATC was developed and tested. The key concept was to combine a variety of data sources – from official government resources to public and departmental initiatives – to ensure continuous collection of information on environmental impacts. The main focus was on tracking anthropogenic, agricultural, and military loads, and the ability of the system to quickly respond to environmental risks that arise within the community. Comparing the obtained data with the methods described by E. Levin *et al*. (2023), a significant correlation was observed. Namely, they stressed the importance of implementing cloud platforms, the Internet of Things, and the use of semantic web services. Instead, the study by B. Varer & V. Mokin (2025) focused on artificial intelligence, namely, the use of large language models for building cognitive maps and modelling systems without the participation of experts, that is, on the analytical and predictive part of the DSS, especially in conditions of a lack of high-quality input data. These tools help to improve the flexibility, scalability, and integration capabilities of the system with other advanced solutions. Both in this study and in the paper by E. Levin *et al*., a similar problem was identified: difficulties in integrating different types of data and technologies, and a high dependence of the accuracy of models on the quality of source information. Therefore, the issue of compatibility and standardisation of all components of the system was defined as a key requirement for ensuring its performance.

Paying attention to the study by A. Bonfante *et al.* (2024), similar strategic approaches using geospatial data were observed, and the DSS architecture was designed on a multi-layered basis. In the proposed system, like A. Bonfante *et al.*, used advanced models for predicting the ecological state, in particular climate algorithms. However, if A. Bonfante *et al.* focused on supporting EU authorities in implementing climate change adaptation policies, this study aimed to integrate monitoring at various levels – state, local, public, and departmental – in the context of anthropogenic and military tensions, which is particularly important for Ukraine. S. Xu (2024) considered the use of artificial intelligence in DSS for sustainable urban development, when adaptive models, fuzzy logic, and specialised algorithms were used in this study to improve the accuracy of diagnostics and forecasting of the environmental situation. Similarly to C. Xu, the current study confirmed that the quality of input data and the complexity of integration with the existing infrastructure remain significant obstacles to the widespread use of such systems.

Separately, it is necessary to emphasised the focus on involving ordinary citizens in environmental monitoring as part of the current study. This fully correlated with the approaches outlined by J. Haqbeen *et al*. (2021). The above system, like the current study, contained crowdsourcing mechanisms and the practice of cooperation with public associations. This contributed to the receipt of detailed information, accelerated identification of problems, and the development of environmental consciousness among the population. Simultaneously, certain difficulties have arisen, in particular, those related to the heterogeneity and subjectivity of data, and the need to improve digital literacy and ensure the protection of information.

Comparing the results obtained with the study by G. Anjum & M. Aziz (2025), it was found that both papers emphasised an interdisciplinary approach to environmental strategies. Attention was paid not only to technical aspects, but also to cognitive, social factors, and the importance of scientific data and conceptual frameworks for improving the effectiveness of policy decisions. Similar to G. Anjum & M. Aziz, the problems of comprehensive system performance assessment and the lack of convincing empirical data remained significant obstacles. A.J. Lynch *et al*. (2022) highlighted the key role of a flexible, situation-oriented approach and iterative decision-making process in climate risk management. This approach was also implemented in the present study: systematisation of various methods, considering the political, social, and cultural context, and the involvement of all interested parties became the foundation for the development of an effective DSS.

Summing up, the study showed the effectiveness of the created integrated DSS for environmental supervision of ATC. This is fully consistent with current global practices in this area. To improve the operation of the system, the need to address issues of standardisation, ensuring the quality of information, improving digital awareness of users and adapting models to the specifics of each community was clarified. The experience of Ukrainian and foreign experts has shown that the best results are achieved through a combination of various scientific approaches, the use of advanced information technologies, and the active involvement of the public in the process of environmental monitoring, which will ultimately contribute to the sustainable development of territorial communities.

Conclusions

The present paper offered a scientifically based concept of multi-level DSS for environmental monitoring of ATC. This system considered the current challenges faced as a result of anthropogenic accidents and military operations, which significantly affect the state of the environment. The organisational and technical structure of the DSS was developed, which combined automated workstations, local area networks, cloud services, crowdsourcing platforms, sensor systems, and data from open sources. The use of mathematical models for local monitoring of the dynamics of organic matter reserves with the ability to identify parameters even with limited data is also justified, which allows performing operational analysis of the state of ecosystems and predicting the long-term consequences of anthropogenic and military factors.

Simulation simulations conducted as part of the study demonstrated high accuracy in estimating changes in terrestrial ecosystems. The results also determined the effectiveness of management decisions aimed at reducing the negative impact on the environment. Integrating data from multiple sources – government, public, sensor networks, and crowdsourcing platforms – increases responsiveness to environmental threats. In addition, such integration promotes transparency and accessibility of environmental information to government agencies and the public. An important aspect is the proven possibility of public involvement in environmental control through digital platforms, which, in turn, increases environmental awareness and contributes to the democratisation of the decision-making process.

In the course of the study, the effectiveness of using recurrent algorithms for identifying model parameters was confirmed. This is extremely useful in cases where environmental data is limited or fragmented, which is a typical problem for territorial communities, especially in times of crisis. The proposed methodology allows adapting decision support systems to the specific conditions of each territory, considering local features of the load on ecosystems, and the availability of information resources. Practical testing of the system at test sites has shown its ability to scale and integrate with existing national and international monitoring platforms.

Further research will focus on implementing artificial intelligence techniques to improve the accuracy of predictions. It is also planned to expand the functionality of the decision support system for emergency risk management, integration with national and international monitoring platforms. In addition, it is planned to develop adaptive algorithms for analysing large amounts of environmental data. Further development of this system is aimed at improving the effectiveness of environmental monitoring, ensuring timely response to environmental threats, and promoting scientifically sound management decisions at the local community level.

Acknowledgements

None.

Funding

The study received no funding.

Conflict of Interest

None.

References

[1] Alvarez-Risco, A., & Del-Aguila-Arcentales, S. (2021). Crowdsourcing for sustainability: Case of sustainable development goals. In R. Lenart-Gansiniec & J. Chen (Eds), *Crowdfunding in the public sector* (pp. 187-196). Cham: Springer. doi: 10.1007/978-3-030-77841-5_12.

[2] Anjum, G., & Aziz, M. (2025). Psychological insights and structural solutions: Using community frame (c-frame) in climate action and policy response. *Climate Policy*, 1-11. doi: 10.1080/14693062.2025.2511267.

[3] Bonfante, A., Monaco, E., Vitale, A., Barbato, G., Villani, V., Mercogliano, P., Rianna, G., Mileti, F.A., Manna, P., & Terribile, F. (2024). A geospatial decision support system to support policy implementation on climate change in EU. *Land Degradation & Development*, 35(6), 2046-2057. doi: 10.1002/ldr.5042.

[4] Chapin, F.S., *et al.* (2006). Reconciling carbon-cycle concepts, terminology, and methods. *Ecosystems*, 9, 1041-1050. doi: 10.1007/s10021-005-0105-7.

[5] Chapin, F.S., Matson, P.A., & Vitousek, P. (2012). *Principles of terrestrial ecosystem ecology*. Cham: Springer. doi: 10.1007/978-1-4419-9504-9.

[6] Chumachenko, S.M., Yakovlev, Y.O., Pirikov, O.V., & Partalyan, A.S. (2022). Features of the implementation of the environmental monitoring network of hostilities for the Armed Forces of Ukraine. *Environmental Safety and Nature Resources*, 42(2), 23-34. doi: 10.32347/2411-4049.2022.2.23-34.

[7] Constable, A.J., French, S., Karoblyte, V., & Viner, D. (2022). Decision-making for managing climate-related risks: Unpacking the decision process to avoid “trial-and-error” responses. *Frontiers in Climate*, 4(1), article number 754264. doi: 10.3389/fclim.2022.754264.

[8] DSTU 9001:2001. (2001). *Quality management systems. Requirements*. Retrieved from https://www.zoda.gov.ua/files/WP_Article_File/original/000011/11933.pdf.

[9] Donnelly, A., Crowe, O., Regan, E., Begley, S., & Caffarra, A. (2014). The role of citizen science in monitoring biodiversity in Ireland. *International Journal of Biometeorology*, 58, 1237-1249. doi: 10.1007/s00484-013-0717-0.

[10] Dubovoy, V.M. (2012). *Identification and modeling of technological objects and control systems*. Vinnytsia: Vinnytsia National Technical University.

[11] Ecodozor. (n.d.). *Environmental consequences and risks of the war in Ukraine*. Retrieved from https://ecodozor.org/.

[12] Ecozagroza. (n.d.). Retrieved from https://ecozagroza.gov.ua/.

[13] Füller, J., Hutter, K., & Kröger, N. (2021). Crowdsourcing as a service – from pilot projects to sustainable innovation routines. *International Journal of Project Management*, 39(2), 183-195. doi: 10.1016/j.ijproman.2021.01.005.

[14] Haqbeen, J., Sahab, S., Ito, T., & Rizzi, P. (2021). Using decision support system to enable crowd identify neighborhood issues and its solutions for policy makers: An online experiment at Kabul municipal level. *Sustainability*, 13(10), article number 5453. doi: 10.3390/su13105453.

[15] Ivanyuta, S.P., & Kachynskyi, A.B. (2012). *Environmental and natural-technogenic safety of Ukraine: Regional dimension of threats and risks*. Kyiv: National Institute for Strategic Studies.

[16] Killen, H., Chang, L., Soul, L., & Barclay, R. (2022). Combining physical and digital data collection for citizen science climate research. *Citizen Science: Theory and Practice*, 7(1), article number 10. doi: 10.5334/cstp.422.

[17] Levin, E., Beisekenov, N., Wilson, M., Sadenova, M., Nabaweesi, R., & Nguyen, L. (2023). Empowering climate resilience: Leveraging cloud computing and big data for community climate change impact service (C3IS). *Remote Sensing*, 15(21), article number 5160. doi: 10.3390/rs15215160.

[18] Lynch, A.J., *et al*. (2022). RAD adaptive management for transforming ecosystems. *BioScience*, 72(1), 45-56. doi: 10.1093/biosci/biab091.

[19] Lysenko, A., Chumachenko, S., Bichkov, A., Panayotova, G., Kovacheva, E., Shevchenko, V., & Tureychuk, A. (2017). *Mathematical models and information technologies for assessment and forecasting of environmental state in test polygons*. Kyiv-Sofia: Pro Langs.

[20] Mokin, B.I., Mokin, V.B., & Mokin, O.B. (2010). *Mathematical methods for identification of dynamic systems*. Vinnytsia: Vinnytsia National Technical University.

[21] Morshch, Ye.V., & Savchenko, I.O. (2018). Structural and functional model for the prevention of technogenic emergencies at critical infrastructure facilities. In *Proceedings of the 4th international scientific and practical conference "Problems of hybrid threats assessment, monitoring and protection of critical infrastructure for the prevention of emergencies in the context of globalization"* (pp. 22-27). Kyiv: Tiems Ukraine Chapter.

[22] Orlove, B., Shwom, R., Markowitz, E., & Cheong, S.-M. (2020). Climate decision-making. *Annual Review of Environment and Resources*, 45(1), 271-303. doi: 10.1146/annurev-environ-012320-085130.

[23] Popov, A. (2024). Architecture of regional environmental monitoring. In *Scientific and practical conference dedicated to World Meteorological Day "On guard of climate actions" and World Water Day "Water for peace"* (pp. 211-212). Kyiv: Ukrainian Hydrometeorological Institute. doi: 10.15407/conf_UHMI_CGO_2024.073.

[24] Resolution of the Cabinet of Ministers of Ukraine No. 391 "On Approval of the Regulation on the State Environmental Monitoring System". (1998, March). Retrieved from https://zakononline.com.ua/documents/show/250143___250208.

[25] Sadeghi-Niaraki, A., Jelokhani-Niaraki, M., & Choi, S.-M. (2020). A volunteered geographic information-based environmental decision support system for waste management and decision making. *Sustainability*, 12(15), article number 6012. doi: 10.3390/su12156012.

[26] Slabospytskyi, O.S. (2008). Using additional information in recursive estimation of discrete-time system parameters by least squares method under non-classical assumptions. *Bulletin of Kyiv University. Series: Physical and Mathematical Sciences*, 4, 179-182.

[27] Smith, V. (1988). Production and nutrient dynamics of plant communities on a sub-Antarctic Island. *Polar Biology,* 8, 255-269. doi: 10.1007/BF00263174.

[28] Van Veen, J.A., & Paul, E.A. (1981). Organic carbon dynamics in grassland soils. I. Background information and computer simulation. *Canadian Journal of Soil Science*, 61(2), 185-201. doi: 10.4141/cjss81-024.

[29] Varer, B., & Mokin, V. (2025). Method for constructing a cognitive map of processes in a dynamic system using the cooperation of large language models. *Information Technologies and Computer Engineering*, 22(1), 69-78. doi: 10.63341/vitce/1.2025.69.

[30] Xu, P. (2024). AI-driven decision support system for green and sustainable urban planning in smart cities. *Applied Mathematics and Nonlinear Sciences*, 9(1), 1-14. doi: 10.2478/amns-2024-0736.

Інформаційно-аналітичні технології підтримки прийняття рішень у системах екологічного моніторингу об'єднаних територіальних громад

Андрій Мошенський

Доктор філософії, доцент
Національний університет харчових технологій
01033, вул. Володимирська, 68, м. Київ, Україна
https://orcid.org/0000-0002-4584-4958

Ігор Савченко

Аспірант
Національний університет харчових технологій
01033, вул. Володимирська, 68, м. Київ, Україна
https://orcid.org/0000-0002-5798-7104

Анотація. Актуальність цього дослідження зумовлена дедалі більшою необхідністю покращення ефективності екологічного моніторингу об'єднаних територіальних громад в умовах зростання техногенного та військового впливу на навколишнє середовище. Метою роботи було створення інтегрованої системи підтримки прийняття рішень для екологічного моніторингу, що дозволяє об'єднувати дані з різних джерел, здійснювати безперервний контроль за станом екосистем, прогнозувати зміни та оперативно реагувати на екологічні загрози. У процесі дослідження застосовано системний підхід, математичне моделювання динаміки екосистем, метод найменших квадратів для ідентифікації параметрів моделей на основі обмежених даних, а також впроваджено хмарні технології, Інтернет речей, краудсорсингові платформи та сенсорні мережі для збору й обробки інформації. Інтеграція даних здійснювалася з державних, громадських та відомчих джерел, що забезпечило комплексне охоплення різних типів навантаження на довкілля. Основними результатами дослідження були: розробка багаторівневої організаційної структури системи моніторингу, побудова дискретних і безперервних математичних моделей для оцінки та прогнозування стану екосистем, впровадження рекурентних алгоритмів для адаптації моделей до змін у середовищі. Система дозволила забезпечити постійний моніторинг промислового, агропромислового та військово-техногенного впливу, своєчасно виявляти потенційні загрози, оцінювати їхній вплив і приймати обґрунтовані управлінські рішення для зниження екологічних ризиків. Розроблена система підтримки прийняття рішень дозволяє ефективно управляти екологічними ризиками, сприяє підвищенню екологічної безпеки та сталому розвитку об'єднаних територіальних громад. Інтеграція сучасних інформаційних технологій, математичних моделей та залучення громадськості до процесу моніторингу створює нову парадигму екологічного управління в кризових умовах

Ключові слова: Інтернет речей; воєнний вплив; краудсорсинг; математичне моделювання; техногенне навантаження; управління ризиками; хмарні технології

TECHNOLOGIES AND ENGINEERING

Journal homepage: https://technologies-engineering.com.ua/en
Vol. 26, No. 3, 2025

Received: 13.01.2025
Revised: 16.05.2025
Accepted: 25.06.2025

UDC 621.47:620.9

DOI: 10.30857/2786-5371.2025.3.5

Combined energy production systems with Stirling engines: Analysis of global experience and local prospects

Yevhen Nikitin*

Postgraduate Student
National University of Life and Environmental Sciences
03041, 15 Heroiv Oborony Str., Kyiv, Ukraine
https://orcid.org/0009-0003-4000-3193

Abstract. The study aimed to identify the potential of combined energy production systems with Stirling engines by analysing international experience and assessing the prospects for their adaptation to local conditions. The study used an analytical approach to examine global experience, technical solutions, and conditions for the local implementation of combined energy systems based on Stirling engines. The study analysed global experience in the use of Stirling engines in combined energy systems in Europe (the Netherlands, Germany, the United Kingdom), Asia (Japan), and North America (using the example of the National Aeronautics and Space Administration), where they have demonstrated high energy efficiency and environmental friendliness. The results confirmed the possibility of effective application of these systems in Ukraine for decentralised energy supply using local resources. It has been determined that Stirling engines can be effective for decentralised energy supply to rural communities, medical institutions, educational institutions, and critical infrastructure facilities, especially in regions with access to biomass or household waste. It was established that the main barriers remain the high cost of equipment (from EUR 10,000 to EUR 13,000) and the lack of a production base. The payback period for such systems is 6 to 9 years, with annual energy savings of EUR 500-900. It was concluded that, with appropriate state support and localisation of production, combined systems based on Stirling engines have the potential for widespread use as part of a strategy for energy decentralisation and the transition to sustainable energy. In addition, the engines have a service life of 40,000 to 60,000 hours, and maintenance costs range from EUR 100 to EUR 200 per year. The study provided well-founded technical and economic conclusions on the possibility of adapting and implementing combined systems with Stirling engines in local energy conditions, which can serve as a basis for decision-making in the field of sustainable energy

Keywords: decentralisation; biomass; heat source; cogeneration; environmental friendliness

Introduction

Growing demands for energy efficiency, reduction of carbon dioxide emissions, and transition to renewable energy sources create new opportunities for the introduction of innovative technologies in the energy sector. One promising technology is combined energy production systems based on Stirling engines, which can efficiently convert thermal energy into electricity using various heat sources, such as solar energy, biomass, or industrial waste. The use of Stirling engines in energy systems, particularly in combined installations, is relevant due to the high potential of these technologies to increase energy efficiency and reduce harmful gas emissions. Y.S. Nikitin & V.M. Pavlenko (2024) investigated the possibilities of using Stirling engines to convert heat from biomass into electrical energy, noting their high efficiency in small-scale systems. The prospects for integrating these technologies into renewable energy allowed for a reduction in carbon dioxide emissions. A. Kubule *et al*. (2024) focused on the application of Stirling engines in microgeneration, especially in rural areas where access to centralised energy networks was limited. This was important for improving energy autonomy and reducing energy consumption costs. S. Zhu *et al*. (2021) compared the efficiency of Stirling engines with traditional heat engines, finding them to be significantly more energy efficient with minimal harmful gas emissions. The use of such engines in various sectors, including utilities

Suggested Citation:
Nikitin, Ye. (2025). Combined energy production systems with Stirling engines: Analysis of global experience and local prospects. *Technologies and Engineering,* 26(3), 66-76. doi: 10.30857/2786-5371.2025.3.5.

*Corresponding author

and industrial installations, is promising. M. Sheykhi & M. Mehregan (2024) investigated the economic aspects of introducing Stirling engines, pointing to high initial costs as the main barrier to their widespread use. According to their findings, the long-term economic benefits due to reduced operating costs and energy losses can be significant. B. Shboul *et al*. (2021) studied the role of Stirling engines in bioenergy systems, especially in combination with other renewable energy sources such as solar and geothermal energy. The technical and economic analysis showed that the system achieved Stirling engine efficiency of 37% and a levelised cost of electricity of USD 0.13 to USD 0.15/kWh year, indicating its significant potential for application in bioenergy and small-scale energy projects.

G.T. Udeh *et al*. (2022) focused on the use of Stirling engines to improve energy efficiency in domestic settings. These systems were important for reducing dependence on traditional energy sources in households. E. Gholamian *et al*. (2024) focused on the environmental benefits of Stirling engines, comparing their CO_2 emissions with other types of generators. The environmental potential of these systems in reducing greenhouse gas emissions when using renewable heat sources was significant. J. Kramens *et al*. (2024) investigated the impact of Stirling engine implementation on energy security in remote regions, particularly in Africa and South America. These technologies could significantly improve access to energy in areas where there are no reliable sources of energy supply. M.D. Al-Nimr *et al*. (2023) focused on integrating Stirling engines with renewable energy sources to ensure a sustainable energy supply in the context of climate change. The opportunities for applying such technologies on the scale of small and medium-sized power systems were great. H. Xu *et al*. (2022) focused on the development of Stirling engine production technology, proposing innovative methods to reduce production costs. This had the potential to reduce the cost of the final product and promote its wider use for commercial and industrial purposes.

Despite these studies, some gaps remain that need further investigation: the impact of integrating Stirling engines into large-scale energy networks and the potential for reducing their production costs to enable mass deployment need to be explored in greater depth. In addition, little research has been done on the potential of Stirling engines in combination with other renewable energy sources, such as solar photovoltaic panels, wind turbines, and geothermal systems, especially in the context of climate change. The environmental performance of these combined systems under different climatic and operating conditions has also been insufficiently studied. The aim of the study was to assess the potential of combined energy systems based on Stirling engines, taking into account current requirements for energy efficiency and environmental friendliness.

Materials and Methods

The study included a comprehensive analysis of combined energy systems based on Stirling engines, aimed at identifying their potential in the context of modern energy transformation challenges. First, the principle of operation of the Stirling engine, which is based on the use of an external heat source, was studied in detail. This made it possible to determine the possibilities of using the engine with various types of heat sources, including solar radiation, heat from biomass combustion, as well as household and industrial waste. Particular attention was paid to the technical characteristics of the engine, such as quiet operation, low vibration, high efficiency in low-power systems, and durability with minimal operating costs.

The study included an analysis of global experience in the use of Stirling engine-based systems in various regions – Europe, Asia, and North America, which are distinguished by the active introduction of innovative energy technologies. In particular, examples of micro-cogeneration plants in the Netherlands (WhisperGen) (Power Engineering International, 2007), Germany (Viessmann) (Viessmann Werke GmbH & Co. KG, 2012), and Sweden (M Microgen Engine Corporation, n.d.) were considered. In the United Kingdom, combined heat and power cogeneration systems (Modern Power Systems, 2007) were tested in social housing, while in Japan, considerable attention was paid to the development of home cogeneration plants with increased energy efficiency as part of the ENE-FARM programme (Japan LP Gas Association, n.d.). Separately, initiatives in the United States were analysed, which included the use of Stirling engines in pilot projects on biomass, in solar thermal concentration systems, as well as NASA (National Aeronautics and Space Administration) space projects, in particular the Kilopower reactor using Stirling technology (Gibson *et al*., 2017) and the advanced Stirling radioisotope generator (Lewandowski, 2013).

To determine the practical potential, the main types of combined systems were classified: combined heat and power, concentrated photovoltaic Stirling, and biomass installations, where the engine performed the function of converting thermal energy into electrical energy. A technical and structural analysis of each type of system was carried out, taking into account their functional purpose, operational requirements, and adaptability to local conditions. Particular attention was paid to the prospects for the implementation of such systems in Ukraine. Data on the availability of local resources – wood, agricultural waste, and solid household waste – as potential energy sources for combined systems was collected and analysed. The potential benefits of using such technologies in various energy sectors were investigated, and key challenges that could affect their implementation and development were considered. The possibilities for adapting these systems to the climatic and infrastructural characteristics of Ukraine were taken into account.

At the final stage of the study, a scenario approach was used to model a hypothetical option for the implementation of Stirling engine technologies in the Ukrainian context. The methodology involved building a logical sequence for the implementation of pilot projects in communities with an existing raw material base of bioresources. The analysis included an assessment of the possibilities for integrating energy systems into educational and medical institutions with a focus on improving the energy sustainability of social infrastructure facilities. In addition, international technical assistance tools, grant funding, and sustainable development mechanisms were analysed for potential support.

Results

Stirling engine: Operating principles and advantages. The Stirling engine, which operates on the principle of an external heat source, is one of the most energy-efficient and versatile types of engines used in alternative energy sources. One of its key advantages is that it can run on any type of thermal energy, from solar radiation to heat obtained from burning biomass, household waste, or other organic materials. Thanks to its ability to convert various heat sources into mechanical energy, the Stirling engine is extremely flexible in its application, opening up new horizons for the use of renewable energy sources (Choque Campero *et al.*, 2024). One of the most significant aspects of this engine is its quietness and low vibration level. This is especially important for applications in places where noise and vibration can be a problem, such as residential or medical facilities. Stirling engines operate without explosive processes, making them much quieter than traditional internal combustion engines. As a result, these engines are suitable for use in environments where noise reduction is important for comfort and safety (Arslan & Kocakulak, 2023).

Another significant advantage of Stirling engines is their high heat-to-electricity conversion efficiency, especially at low power. This allows Stirling engines to be used for power generation in cases where high efficiency must be maintained with limited resources or in small energy systems, such as micro-cogeneration plants or autonomous energy sources. Thanks to this efficiency, Stirling engines can be an ideal solution for energy systems powered by renewable sources such as the sun or biomass (Allouhi *et al.*, 2022). Stirling engines are also durable and have low operating costs, making them economically viable in the long term. Due to the absence of internal combustion and mechanical damage characteristic of internal combustion engines, Stirling engines have a significantly longer service life and require minimal maintenance (Laín *et al.*, 2024). This, in turn, reduces maintenance costs and makes them more attractive for a wide range of applications, from small domestic installations to large industrial solutions (Table 1).

Table 1. *Economic indicators of cogeneration plants with Stirling engines*

Parameter	Value
Average installation cost (household)	EUR 10,000-13,000
Payback period	6-9 years
Energy savings (annual)	EUR 500-900
Engine service life	40,000-60,000 hours
Maintenance costs (annual)	EUR 100-200

Source: *compiled by the author based on data from A.B. Awan et al. (2021)*

Thus, Stirling engines represent an extremely promising technology for ensuring energy independence and sustainability. They can run on a variety of energy sources while providing high efficiency, quiet operation, and low maintenance costs, making them attractive for use in a variety of settings, from residential areas to remote locations.

Global experience in the use of Stirling engines in combined energy systems. Thanks to their versatility and high energy efficiency, Stirling engines are actively used around the world to develop innovative combined energy systems. These systems combine heat and electricity production, making them extremely efficient in conditions where energy autonomy is required or there are restrictions on the use of traditional energy sources. Current global experience in the use of Stirling engines in such systems has demonstrated their high potential efficiency in various regions and areas. In the Netherlands, the market for micro-cogeneration systems is showing steady growth. It is expected to reach USD 115.6 million by 2025, with further growth to USD 270.6 million by 2035, corresponding to an average annual growth rate of 8.9%. WhisperGen company has been actively introducing compact units capable of generating electricity and heat for individual households, helping to reduce dependence on centralised heating and power supply systems (Power Engineering International, 2007).

In Germany, the Viessmann company has become one of the key players in the micro-cogeneration market with Stirling engines. Its units, in particular the 1 kW model, enable households to reduce their annual energy costs by 30-40% through optimised fuel use. The implementation of such systems is part of national energy transition programmes aimed at reducing the use of fossil fuels and CO_2 emissions (Viessmann Werke GmbH & Co. KG, 2012). In Sweden, which is known for its environmental awareness and sustainable development policies, Microgen Engine Corporation (n.d.) is actively promoting Stirling engine cogeneration systems for households. For example, in 2023, an autonomous system based on a biomass Stirling engine was installed at a ski resort near Sapporo, Japan, demonstrating the versatility and efficiency of such technologies even in harsh climatic conditions. In the United Kingdom, combined heat and power systems using Stirling engines are being actively implemented for the simultaneous production of heat and electricity in social housing. For example, the Goldsmith Street project was implemented in Norwich, which includes 105 residential units (45 houses and 60 apartments) and received the Stirling Prize for architecture (Fig. 1). This project provides a high level of energy efficiency and reduces energy costs for residents.

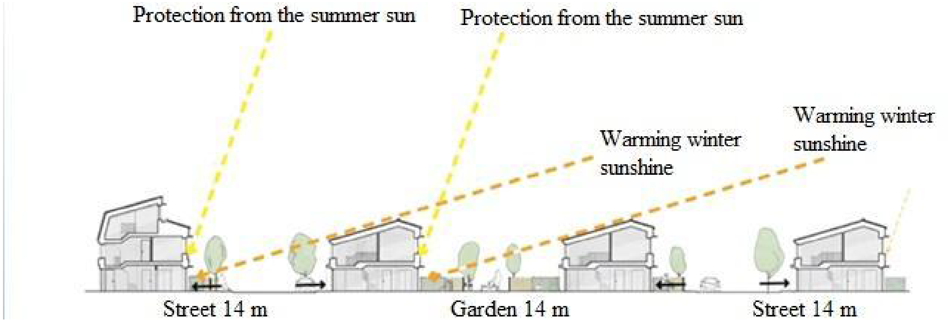

Figure 1. *Goldsmith Street project in Norwich, illustration of natural lighting*
Source: *Modern Power Systems (2007)*

This project demonstrated the effective use of natural lighting thanks to the thoughtful orientation of the buildings and the large window area. This reduces the need for artificial lighting and increases energy efficiency and comfort in the rooms. Japan is actively integrating Stirling engines into energy systems as part of the national ENE-FARM programme, which aims to develop domestic cogeneration systems. As of 2021, approximately 433,200 ENE-FARM systems had been installed in Japan, indicating the widespread adoption of this technology. In 2022, approximately 43,800 new systems running on city gas were sold. These systems allow households to efficiently use local resources to produce heat and electricity, contributing to a reduction in CO_2 emissions and dependence on imported energy sources (Japan LP Gas Association, n.d.).

In the United States, Stirling engines are used in a number of pilot projects aimed at the efficient use of biomass, solar energy, and geothermal sources. In particular, NASA is developing projects such as the Kilopower reactor using Stirling technology (Gibson *et al.*, 2017) and the advanced Stirling radioisotope generator (Lewandowski, 2013), which involve the use of Stirling engines for space power systems. The Kilopower reactor using Stirling technology project successfully passed ground tests in 2018, demonstrating its ability to generate up to 1 kW of electricity, which is an important step in meeting the energy needs of space missions. Global experience in implementing Stirling engines in various regions and energy sectors has demonstrated the significant potential of these systems in achieving high energy efficiency and reducing emissions (Fig. 2).

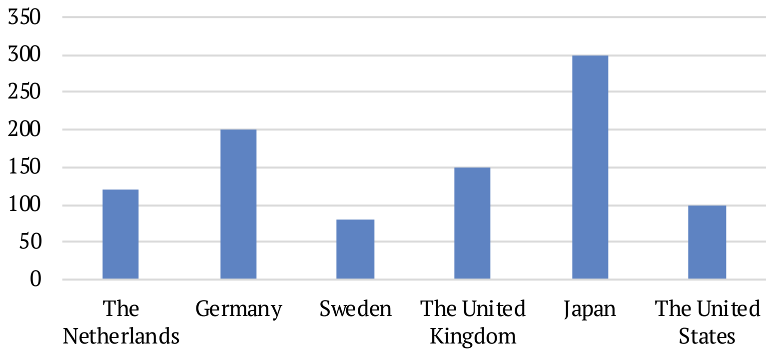

Figure 2. *Global experience in implementing Stirling engine systems: number of projects implemented in leading countries*
Source: *compiled by the author based on data from Power Engineering International (2007), Modern Power Systems (2007), Viessmann Werke GmbH & Co. KG (2012), E.J. Lewandowski (2013), M.A. Gibson et al. (2017), Japan LP Gas Association (n.d.), Microgen Engine Corporation (n.d.)*

Global experience has demonstrated a steady growth in interest in Stirling engine systems, especially in countries with developed energy policies and environmental standards. Japan is the undisputed leader in terms of the number of projects implemented, mainly focused on domestic cogeneration systems. In Europe, Germany, the United Kingdom, and the Netherlands are actively implementing these technologies in the residential sector, using both biomass and natural gas. Sweden stands out for its focus on decentralised heat supply using biofuels, while the United States focuses on industrial and medical facilities. This diverse approach demonstrates the flexibility of Stirling technology and its ability to adapt to different economic and climatic conditions.

Typical combined systems based on Stirling engines. There is growing interest in combined energy systems that combine electricity and heat production. Such technologies are important for ensuring energy efficiency, reducing carbon dioxide emissions, and rational use of local energy resources. One of the most promising solutions is the use of Stirling engines in combined energy systems. There are different types of such systems, each with its own characteristics and applications (Table 2). The combined heat and power system is one of the most common combined energy technologies, which allows simultaneous generation of electricity and heat. It is based on the principle of cogeneration, which ensures high fuel efficiency compared to traditional separate methods of electricity and heat production. Within this technology, Stirling engines run on heat sources of various origins, such as biomass, geothermal energy, solar heat, or even waste. This results in significant energy savings and reduced CO_2 emissions, making the system extremely important for sustainable development. Such systems can be used in industry, municipal services, and residential complexes (Razmi *et al.*, 2021). Another important technology is the concentrated photovoltaic Stirling system, which combines the concentration of sunlight using special concentrators and the conversion of this energy into electricity through a Stirling engine. In this case, the concentration of solar radiation collected using lenses or mirrors is focused on the heating head of the engine, which allows very high temperatures to be achieved and increases the efficiency of converting thermal energy into electricity. Concentrated photovoltaic Stirling systems are capable of producing large amounts of energy, especially in areas with high solar activity. This makes the technology very promising for solar power plants in sunny regions where traditional photovoltaic panels may be less efficient due to limitations in solar insolation (Kandil *et al.*, 2022).

Table 2. *Comparison of the efficiency of systems with Stirling engines*

Fuel type	Electricity generation efficiency (%)	Overall efficiency (including heat) (%)	CO_2 emissions (kg/MWh)
Biomass	15-20	75-85	<100
Natural gas	20-25	80-90	~200
Solar energy	18-22	–	0
Diesel	30-35	50-60	>300

Source: *compiled by the author based on data from A.R. Razmi et al. (2021), A.A. Kandil et al. (2022)*

Bioenergy plants using Stirling engines operate on heat generated from the combustion of biomass or waste. They can use organic materials such as wood, agricultural waste, household waste, and other biological materials to produce energy. Bioenergy plants with Stirling engines are an important part of the strategy for developing renewable energy sources. They not only reduce dependence on fossil fuels, but also help to effectively utilise waste that could otherwise become a source of environmental pollution. These systems are particularly relevant for rural areas where there is access to large amounts of biomass and other renewable resources. Bioenergy plants not only meet local energy needs but also address waste management issues, reducing the negative impact on the environment (Choque Campero & Araoz, 2024).

Combined energy systems based on Stirling engines provide high efficiency and flexibility in the use of various energy sources. They can be adapted to specific conditions and needs, making them extremely promising for a wide range of applications from industry to domestic needs. The choice between different types of combined systems depends on available resources, economic and environmental requirements. Undoubtedly, these technologies play an important role in the future energy landscape, helping to reduce dependence on traditional energy resources and reducing harmful emissions into the atmosphere.

Local prospects for the introduction of Stirling engines in Ukraine. The introduction of the latest energy technologies in Ukraine has significant potential for creating efficient and environmentally friendly energy solutions. One of the most promising areas is the use of Stirling engines in combined energy systems that run on various types of fuel, such as biomass, waste, and even solar heat. One of the main advantages of using Stirling engines in Ukraine is ensuring energy independence. Thanks to the ability to operate on local resources – such as wood, agricultural waste, or household waste – these technologies can significantly reduce dependence on imported energy sources. For example, imported gas accounted for about 30% of Ukraine's energy consumption in 2024, and the introduction of local cogeneration systems could reduce this dependence by 5-10% in the medium term. This not only reduces the cost of energy (up to 20% savings compared to centralised supply) but also supports the development of the local economy, which is an important factor for regions with limited resources for traditional energy supply (Khodakivskyi *et al.*, 2025). In addition, the use of combined energy systems with Stirling engines allows for the implementation of the principle of decentralised energy supply. This is particularly important for rural areas and critical infrastructure facilities, where traditional energy supply methods are often unavailable or unreliable. It is estimated that about 15% of villages in Ukraine have problems with access to a stable electricity supply, and decentralised systems can fully meet their needs (Davydenko *et al.*, 2022). Such decentralisation ensures a stable and efficient energy supply for small settlements, reducing the risks of energy crises. Another important advantage is the use of solid waste as a source of heat. Ukraine generates over 10 million tonnes of solid household waste every year, of which only 4% is recycled, with the rest ending up in landfills. Switching to technologies that allow this waste to be used for energy production not only helps solve environmental problems but also reduces the burden on landfills and waste processing plants. For example, a single 1 kW cogeneration plant fuelled by solid household waste can utilise up to 2 tonnes of waste per year, while generating electricity for one household. In addition, these systems can replace outdated and inefficient boilers and diesel generators used in remote areas. The energy efficiency of modern Stirling engine-based systems reaches up to 85% in combined heat and power mode. Not only are they highly efficient, but they also help reduce CO_2 emissions by 1.5-2 tonnes per year per household (Khalatov & Fialko, 2025).

Despite all the advantages, the introduction of Stirling engines in Ukraine faces several serious challenges. One of the main ones is the high initial cost of the equipment – the cost of a single micro-cogeneration unit ranges from EUR 5,000 to EUR 12,000, depending on the configuration. Such technologies require significant initial investments, which can be a barrier to implementation in small businesses or rural communities without adequate financial support. Another serious challenge is the limited local production base and experience in installing such units. Currently, there are only three companies in Ukraine that assemble or adapt imported micro-cogeneration systems (Luschini *et al.*, 2024). This leads to dependence on foreign technologies and increases transportation and maintenance costs to 20% of the total project cost. To overcome these barriers, government incentives such as "green tariffs", grant programmes and support for technology parks are needed. For example, with a subsidy of 30-50% of the cost of equipment, the payback period for such systems could be reduced from 8-10 to 4-6 years. This would not only reduce the financial burden on users but also promote local production and create up to 1,000 jobs in the renewable energy sector (Klymenko *et al.*, 2023). In the context of ongoing war and the need for large-scale reconstruction in Ukraine, the introduction of Stirling engines is particularly important. These technologies enable fast and efficient energy supply in destroyed or remote regions where centralised networks are often damaged or inaccessible. The use of local resources, such as biomass or solid waste, contributes not only to the restoration of infrastructure but also to the creation of new jobs, which is critical for stabilising the economy in the post-conflict period. Thus, Stirling engines can become a key element in the country's energy security and sustainable development strategy during its reconstruction.

Despite the existing challenges, the introduction of Stirling engines in Ukraine has great potential for the development of a sustainable energy sector. Technologies that allow the use of local resources and ensure energy independence can become a key element in achieving energy stability and environmental security in these regions. To maximise their effectiveness, it is necessary to develop infrastructure, support investment, and stimulate innovation in the field of renewable energy.

Recommendations for the implementation of Stirling engines. Given the great potential for using Stirling engines in energy systems based on renewable energy sources, it is important to formulate recommendations for their implementation in Ukraine. One of the first steps towards the implementation of combined energy systems with Stirling engines should be the implementation of pilot projects in communities with high biomass potential, such as rural areas or agricultural regions. The use of biomass as an energy source has significant environmental and economic benefits, particularly in terms of reducing greenhouse gas emissions and supporting local resources. Pilot projects will not only test the technologies but also demonstrate their effectiveness in practice, involving local communities and businesses in the implementation of renewable energy solutions. The integration of Stirling engine-based systems into educational and medical institutions can significantly improve the reliability of energy supply in these important sectors. This is particularly important for rural or remote areas where access to centralised energy supplies may be limited or unreliable. The use of combined systems will provide not only electricity but also heat, which is especially important for educational and medical institutions, where a stable energy supply is critical for continuous operation. Attracting state support through EU mechanisms is an important step in the development of Stirling engine-based technologies. Grant programmes, technical assistance, and other forms of EU funding can significantly reduce the financial barriers to the implementation of such systems. The EU actively supports innovative projects in the field of renewable energy, which allows countries, including Ukraine, to gain access to modern technologies and expert knowledge. This will help stimulate the development of green technologies and ensure the competitiveness of energy solutions in the region.

Another recommendation is to stimulate the development of local production of technologies based on Stirling engines. The creation of technology clusters in Ukraine will reduce dependence on imported components, reduce transportation and maintenance costs, and create new jobs. Attracting investors to create such clusters will contribute to the development of the industry, ensuring a high level of technological autonomy and reliability. The development of local production will also increase the level of knowledge and experience among specialists, which is critical for the effective application of the latest technologies. Overall, the introduction of Stirling engines in Ukraine has great potential for the development of a sustainable energy sector. For the successful implementation of these technologies, several strategic steps need to be taken, including pilot projects in communities with high biomass potential, integrating systems into medical and educational institutions, attracting support through EU mechanisms, and developing local production. Only with such a comprehensive approach can long-term success be achieved and the energy situation in the region be significantly improved.

Discussion

The study found that Stirling engines have a number of technical advantages that make them effective for use in modern energy systems. Thanks to its ability to operate on any external heat source, this type of engine is versatile in its application, especially in conditions of limited access to the centralised energy supply. Its quietness, low vibration, and long service life make it attractive for use in the residential sector and noise-sensitive facilities. This topic was also explored by C.R. Ghanem *et al*. (2022), whose results confirmed that the Stirling engine is a thermodynamic device that converts heat into mechanical energy through a cycle of gas compression and expansion. It can operate on any external heat source, making it versatile for use in hybrid energy systems that combine different energy sources such as solar, wind or biomass. This significantly increases efficiency and reduces carbon dioxide emissions, which is important for sustainable energy development.

Research by S.M. Vahidhosseini *et al*. (2024) also showed that one of the main advantages of the Stirling engine is the use of an external heat source, which allows it to operate without noise and vibration, which is a big plus for domestic applications. The engine's quietness makes it ideal for use in residential areas, especially in environments where noise tolerance is low, such as homes, offices, or medical facilities. In addition, the efficient use of heat allows the Stirling engine to provide stable and reliable energy without the need for complex or expensive fuel resources. It should be noted that although the Stirling engine has many advantages in the context of hybrid energy systems, its efficiency largely depends on the stability and quality of the heat source. High heat losses or insufficient source power can reduce the overall efficiency and performance of the system. In addition, to ensure optimal operation of the Stirling engine, it is necessary to use high-quality materials and engineering solutions, which can lead to additional costs at the initial stage of introducing such technologies into domestic or industrial energy systems.

International practice has confirmed the effectiveness of using micro-cogeneration systems based on Stirling engines in various regions. In European countries, these technologies have become widespread thanks to government support and favourable renewable energy policies. The results of implementation have demonstrated the possibility of improving energy efficiency and reducing greenhouse gas emissions in the residential sector. G. Battista *et al.* (2023) concluded that the implementation of micro-cogeneration systems in the residential sector in Europe is gaining popularity due to their ability to effectively reduce energy costs and carbon dioxide emissions. Such systems allow households to generate their own energy using a variety of sources, including solar energy, wind energy, and even Stirling engines. This contributes to the decentralisation of energy and reduces dependence on external energy suppliers, which is an important aspect for many European countries focused on sustainable development.

A study by T.A. Minale *et al*. (2024) found that government support is critical to the popularisation of Stirling technologies and micro-cogeneration systems in general. Subsidy programmes, tax breaks, and other incentives can significantly reduce the initial costs of installing such systems and increase interest among households and businesses. In addition, government initiatives can promote the development of infrastructure to support these technologies, which in turn helps attract investment and accelerate the transition to more environmentally friendly and independent energy systems. These results confirmed the above study, as they demonstrated the significant potential of micro-cogeneration systems to reduce energy costs and increase the energy independence of households. The findings indicated that even in the early stages of implementation, these technologies can deliver significant energy savings, which could lead to substantial benefits for both users and national economies in the future. In addition, the data confirmed the effectiveness of state support in promoting such innovations, creating conditions for wider dissemination and adaptation of these technologies at the population level.

The experience of countries with a high level of technological development has demonstrated the feasibility of integrating such systems into national energy modernisation programmes. In some countries, Stirling engines have been actively used as part of an autonomous energy supply in households, with an emphasis on the use of local resources. In some regions, these systems were part of programmes aimed at increasing the energy independence of the population. It is worth noting the work of L. Zhang *et al*. (2023), who also found that the use of Stirling systems as part of national energy policy could be an important element in reducing dependence on traditional energy sources and reducing greenhouse gas emissions. Many European countries are already seeing the gradual integration of such technologies into national energy security strategies, as they allow for greater decentralisation of energy networks. In particular, in countries with high levels of investment in renewable energy sources, Stirling systems can effectively complement other technologies, creating a more flexible and sustainable energy infrastructure.

In turn, Y. He *et al*. (2021) concluded that domestic cogeneration plants are a promising strategy for energy independence, especially in conditions of traditional energy resource shortages. They enabled households to generate their own electricity and heat, reducing their dependence on centralised energy suppliers. With rising energy prices and the need to transition to more sustainable and environmentally friendly solutions, such installations can become an important part of national strategies for energy security and energy system sustainability. These data are consistent with the results presented in the previous section, as they confirm that the integration of Stirling systems into national energy strategies can significantly improve energy stability and reduce greenhouse gas emissions. As the analysis showed, micro-cogeneration plants, particularly those based on Stirling technology, can significantly reduce the load on centralised power grids, which is especially important in times of crisis or energy shortages. Given the trends in Europe and other regions, such technologies are becoming key to achieving energy independence and strengthening national energy security in the long term.

Special attention was paid to promising technological solutions that combine Stirling engines with various heat sources – biomass, household waste, and solar energy. These systems have proven to be particularly effective for small settlements and remote facilities. They are capable of providing a stable energy supply with minimal environmental impact and without the need for significant infrastructure. S. Kallio & M. Siroux (2021) also conducted a study, the results of which confirmed that promoting decentralised energy supply through bioenergy Stirling installations has significant potential for the development of local energy systems, reducing dependence on centralised networks. Such plants can use various types of biomass, providing renewable energy sources for small consumers and reducing carbon emissions. The introduction of such technologies reduces the energy vulnerability of remote and rural areas, where traditional connection to power grids can be expensive or even impossible.

C. Geng *et al*. (2025) also found that integrating Stirling installations with solar and geothermal energy sources provides a stable and reliable power supply for remote consumers where access to traditional energy networks is limited. Solar panels can power the plant on sunny days, while geothermal sources provide stable heat throughout the year, increasing the overall efficiency of the system. Such a hybrid system optimises the use of renewable energy sources, increasing energy independence and sustainability in unstable or remote regions. Comparing these data with those obtained in the study, it can be concluded that bioenergy Stirling installations have significant potential for the development of decentralised energy supply, especially in rural and remote regions. In particular, their ability to use local biomass resources to produce electricity and heat significantly reduces energy supply costs and carbon dioxide emissions. This creates conditions for sustainable development and energy independence, which is an important step in implementing strategies aimed at preserving the environment and optimising energy costs at the local level.

In the context of local conditions, high potential for the use of Stirling engines in decentralised energy supply systems has been identified. The use of local waste and agricultural resources for heat generation opens up new opportunities for regional development. This was consistent with the findings of O. Sadovyi *et al*. (2025), who demonstrated that biogas and biomethane-based cogeneration technologies can ensure stable electricity and heat supply while significantly reducing greenhouse gas emissions and dependence on fossil fuels in Ukraine. At the same time, problems remain related to the high cost of equipment, limited technical base, and insufficient awareness among potential users. Y. Nikitin *et al.* (2024) concluded that the adaptation of Stirling engines into Ukraine's energy infrastructure is feasible given the availability of renewable energy sources, including biomass, solar heat, and geothermal resources. The introduction of these technologies will reduce dependence on imported energy sources and lower CO_2 emissions, which is important for Ukraine's commitments to reduce its environmental footprint. However, the widespread introduction of such systems requires significant investment in infrastructure, as well as support in the form of government programmes and subsidies to stimulate development in this area. R. Torres de Oliveira *et al*. (2022) found that local market constraints, in particular high investment barriers and a lack of technical expertise, are significant obstacles to the implementation of Stirling technologies in Ukraine. High initial costs for equipment and installation, as well as the need to train personnel and develop specialised engineering, may hinder the implementation of such systems. In addition, the lack of broad technical expertise in the country regarding the operation and maintenance of these installations may limit their effective use, requiring additional efforts to train and create conditions for the development of relevant competencies.

When analysing the results of the study, it is clear that, despite the great potential of Stirling engines for Ukraine's energy infrastructure, there are significant challenges to their implementation. This is due to the high initial investment and the need to create a technical base for servicing such systems, which requires both financial and human resources. However, if proper state support is provided in the form of subsidies or tax incentives, as well as investment in training specialists, these technologies can become an important element in the development of the national energy sector, especially in the context of global changes in the energy sector. In order to expand the application of these technologies, it is advisable to focus efforts on developing pilot projects, developing local production, and stimulating investment in this sector. It is also important to provide information support, and training for specialists for the effective installation and maintenance of such systems. A comprehensive approach will make Stirling engine-based technologies more accessible and contribute to the formation of a sustainable energy policy.

Conclusions

The study confirmed that Stirling engines are a promising technology for creating combined energy systems due to their technical characteristics, in particular their ability to operate on various heat sources, high efficiency, quietness, and durability. This versatility allows for the effective use of both traditional and alternative energy sources, including biomass, household waste, and solar heat. Global experience has demonstrated the widespread adaptation of micro-cogeneration systems based on Stirling engines in countries such as the Netherlands, Germany, Japan, and the United States. In Europe and Asia, the main focus has been on application in the residential sector and improving energy efficiency within the framework of government programmes. In the United States, Stirling engines have even found application in high-tech areas, particularly in NASA space missions. Special attention was paid to the possibilities of introducing such systems in Ukraine. It was found that they can significantly contribute to energy independence, reduce environmental impact, and develop decentralised energy networks in rural areas. The average cost of installation for a household is between EUR 10,000 and 13,000, with energy savings of up to EUR 500-900 per year, providing a payback period of 6 to 9 years. The engine has a service life of 40,000-60,000 hours, and annual maintenance costs are EUR 100-200. At the same time, key barriers have been identified: high technology costs, lack of production infrastructure, and insufficient installation experience. Therefore, the successful scaling of such systems in Ukraine is only possible with targeted state support policies, including pilot projects, subsidies, educational initiatives, and incentives for local production. Further research should look into the technical and economic efficiency of integrating Stirling engines into decentralised energy supply systems in Ukraine, taking into account local resource conditions.

Acknowledgements

None.

Funding

None.

Conflict of Interest

None.

References

[1] Allouhi, H., Allouhi, A., Buker, M.S., Zafar, S., & Jamil, A. (2022). Recent advances, challenges, and prospects in solar dish collectors: Designs, applications, and optimization frameworks. *Solar Energy Materials and Solar Cells*, 241, article number 111743. doi: 10.1016/j.solmat.2022.111743.

[2] Al-Nimr, M.D., Khashan, S.A., & Al-Oqla, H. (2023). Novel techniques to enhance the performance of Stirling engines integrated with solar systems. *Renewable Energy*, 202, 894-906. doi: 10.1016/j.renene.2022.11.086.

[3] Arslan, T.A., & Kocakulak, T. (2023). A comprehensive review on Stirling engines. *Engineering Perspective*, 3(3), 42-56. doi: 10.29228/eng.pers.66847.

[4] Awan, A.B., Zubair, M., Memon, Z.A., Ghalleb, N., & Tlili, I. (2021). Comparative analysis of dish Stirling engine and photovoltaic technologies: Energy and economic perspective. *Sustainable Energy Technologies and Assessments*, 44, article number 101028. doi: 10.1016/j.seta.2021.101028.

[5] Battista, G., Vollaro, E.D., Vallati, A., & Vollaro, R.D. (2023). Technical-financial feasibility study of a micro-cogeneration system in the buildings in Italy. *Energies*, 16(14), article number 5512. doi: 10.3390/en16145512.

[6] Choque Campero, L.A., & Araoz, A. (2024). A case study of the development experience of using a prototype Stirling engine in a novel bioenergy driven co-generation plant in Bolivia. *Heat Transfer Engineering*, 45(3), 289-296. doi: 10.1080/01457632.2023.2185492.

[7] Choque Campero, L.A., Wang, W., Cardozo, E., & Martin, A. (2024). Decentralized biomass-based Brayton-Stirling power cycle with an air gap membrane distiller for supplying electricity, heat and clean water in rural areas. *Applied Thermal Engineering*, 254, article number 123889. doi: 10.1016/j.applthermaleng.2024.123889.

[8] Davydenko, N., Wasilewska, N., Boiko, S., & Wasilewski, M. (2022). Development of rural areas in Ukraine in the context of decentralization: An empirical study. *Sustainability*, 14(11), article number 6730. doi: 10.3390/su14116730.

[9] Geng, C., Zhang, T., & Sun, W. (2025). Hybrid solar, wind, and geothermal power generation combined with energy storage for sustainable energy management in remote buildings. *Journal of Energy Storage*, 123, article number 116655. doi: 10.1016/j.est.2025.116655.

[10] Ghanem, C.R., Gereige, E.N., Bou Nader, W.S., & Mansour, C.J. (2022). Stirling system optimization for series hybrid electric vehicles. *Proceedings of the Institution of Mechanical Engineers, Part D: Journal of Automobile Engineering*, 236(2-3), 407-423. doi: 10.1177/09544070211018034.

[11] Gholamian, E., Mahmoudi, S.M., & Balafkandeh, S. (2024). Techno-economic appraisal and machine learning-based gray wolf optimization of enhanced fuel cell integrated with Stirling engine and vanadium-chlorine cycle. *International Journal of Hydrogen Energy*, 51, 1227-1241. doi: 10.1016/j.ijhydene.2023.03.187.

[12] Gibson, M.A., Oleson, S.R., Poston, D.I., & McClure, P. (2017). *NASA's Kilopower reactor development and the path to higher power missions*. Retrieved from https://ntrs.nasa.gov/search?q=Kilopower.

[13] He, Y., Zhou, Y., Yuan, J., Liu, Z., Wang, Z., & Zhang, G. (2021). Transformation towards a carbon-neutral residential community with hydrogen economy and advanced energy management strategies. *Energy Conversion and Management*, 249, article number 114834. doi: 10.1016/j.enconman.2021.114834.

[14] Japan LP Gas Association. (n.d.). *Appliances*. Retrieved from https://www.j-lpgas.gr.jp/en/appliances/.

[15] Kallio, S., & Siroux, M. (2021). A review – renewable energy based micro-cogeneration and hybrid energy systems. *E3S Web of Conferences*, 294, article number 01004. doi: 10.1051/e3sconf/202129401004.

[16] Kandil, A.A., Awad, M.M., Sultan, G.I., & Salem, M.S. (2022). Investigating the performance characteristics of low concentrated photovoltaic systems utilizing a beam splitting device under variable cutoff wavelengths. *Renewable Energy*, 196, 375-389. doi: 10.1016/j.renene.2022.06.129.
[17] Khalatov, A., & Fialko, N. (2025). Gas turbine and gas piston power plants for decentralized energy sector of Ukraine. *System Research in Energy*, 81(1), 4-14. doi: 10.15407/srenergy2025.01.004.
[18] Khodakivskyi, V., Karpenko, D., Bilous, I., & Savickas, R. (2025). Ensuring energy security in Ukraine: The role of cogeneration and sustainable funding for district heating systems. *Rocznik Ochrona Srodowiska*, 27, 196-210. doi: 10.54740/ros.2025.016.
[19] Klymenko, V.V., Soldatenko, V.P., Pleshkov, S.P., Skrypnyk, O.V., & Sachenko, A.I. (2023). *Alternative energy sources and technologies for their use*. Kyiv: Kyiv National Technical University of Ukraine.
[20] Kramens, J., Svedovs, O., Sturmane, A., Vigants, E., Kirsanovs, V., & Blumberga, D. (2024). Exploring energy security and independence for small energy users: A Latvian case study on unleashing Stirling engine potential. *Sustainability*, 16(3), article number 1224. doi: 10.3390/su16031224.
[21] Kubule, A., Kramens, J., Bimbere, M., Pedišius, N., & Blumberga, D. (2024). Trends for Stirling engines in households: A systematic literature review. *Energies*, 17(2), article number 383. doi: 10.3390/en17020383.
[22] Laín, S., Villamil, V., & Vidal, J.R. (2024). CFD simulation of Stirling engines: A review. *Processes*, 12(11), article number 2360. doi: 10.3390/pr12112360.
[23] Lewandowski, E.J. (2013). *Testing of the advanced Stirling radioisotope generator engineering unit at NASA Glenn Research Center*. Retrieved from https://ntrs.nasa.gov/citations/20140003871.
[24] Luschini, A.C., Rego, E.E., & Montebello, N. (2024). How did the Russia-Ukraine war impact energy imports and electricity generation? A comparative analysis between Germany and the United Kingdom. *Electricity Journal*, 37(3), article number 107396. doi: 10.1016/j.tej.2024.107396.
[25] Microgen Engine Corporation. (n.d.). *Technology*. Retrieved from https://www.microgen-engine.com/technology/.
[26] Minale, T.A., Lanzetta, F., Bégot, S., & Getie, M.Z. (2024). Review on the technological advancement of Stirling cycle heat pumps. *Energy Reports*, 12, 3504-3518. doi: 10.1016/j.egyr.2024.09.028.
[27] Modern Power Systems. (2007). *The influence of micro-CHP units on a distribution network*. Retrieved from https://www.modernpowersystems.com/analysis/the-influence-of-micro-chp-units-on-a-distribution-network/.
[28] Nikitin, Y., Pavlenko, V., & Volianyk, O. (2024). Technological integration of Stirling engines in fuel boilers as the basis for high performing micro-CHP with low emissions. *Technical Creativity*, 8, 99-101.
[29] Nikitin, Y.S., & Pavlenko, V.M. (2024). Technological advantages of Stirling engines in the production of electricity from thermal sources. In O.L. Tonkha, V.V. Otchenashko, N.P. Hryshchenko & N.G. Nesterova (Eds.), *Proceedings of the international scientific conference "Education and science in the face of challenges and threats. Contribution of young scientists to sustainable development"* (pp. 380-381). Kyiv: National University of Life Resources and Environmental Management of Ukraine.
[30] Power Engineering International. (2007). *Dutch direction: Integrating micro-CHP into a smart electricity grid*. Retrieved from https://www.powerengineeringint.com/gas-oil-fired/dutch-direction-integrating-micro-chp-into-a-smart-electricity-grid/.
[31] Razmi, A.R., Afshar, H.H., Pourahmadiyan, A., & Torabi, M.J. (2021). Investigation of a combined heat and power (CHP) system based on biomass and compressed air energy storage (CAES). *Sustainable Energy Technologies and Assessments*, 46, article number 101253. doi: 10.1016/j.seta.2021.101253.
[32] Sadovyi, O., Koshkin, D., Martynenko, V., & Sokolik, V. (2025). Electricity generation from biogas: Modern technologies and prospects for Ukraine's energy independence. *Machinery & Energetics*, 16(1), 173-185. doi: 10.31548/machinery/1.2025.173.
[33] Shboul, B., Ismail, A.A., Michailos, S., Ingham, D., AL-Zoubi, O.H., Ma, L., Hughes, K., & Pourkashanian, M. (2021). Design and techno-economic assessment of a new hybrid system of a solar dish Stirling engine instegrated with a horizontal axis wind turbine for microgrid power generation. *Energy Conversion and Management*, 245, article number 114587. doi: 10.1016/j.enconman.2021.114587.
[34] Sheykhi, M., & Mehregan, M. (2024). Comprehensive technical and economic study and optimization of a novel combined cooling heating and power system driven by a four cylinder α type Stirling engine. *Applied Thermal Engineering*, 236, article number 121869. doi: 10.1016/j.applthermaleng.2023.121869.
[35] Torres de Oliveira, R., Gentile-Lüdecke, S., & Figueira, S. (2022). Barriers to innovation and innovation performance: The mediating role of external knowledge search in emerging economies. *Small Business Economics*, 58(4), 1953-1974. doi: 10.1007/s11187-021-00491-8.
[36] Udeh, G.T., Michailos, S., Ingham, D., Hughes, K.J., Ma, L., & Pourkashanian, M. (2022). A modified rule-based energy management scheme for optimal operation of a hybrid PV-wind-Stirling engine integrated multi-carrier energy system. *Applied Energy*, 312, article number 118763. doi: 10.1016/j.apenergy.2022.118763.

[37] Vahidhosseini, S.M., Rashidi, S., Hsu, S.H., Yan, W.M., & Rashidi, A. (2024). Integration of solar thermal collectors and heat pumps with thermal energy storage systems for building energy demand reduction: A comprehensive review. *Journal of Energy Storage*, 95, article number 112568. doi: 10.1016/j.est.2024.112568.
[38] Viessmann Werke GmbH & Co. KG. (2012). *Vitotwin 350-F and 300-W micro CHP units: The boilers that generate power. Viessmann*. Retrieved from http://viessmann.com.ua/images/uploads/pdfs/Vitotwin_Micro_CHP_units.pdf.
[39] Xu, H., Chen, L., Ge, Y., & Feng, H. (2022). Multi-objective optimization of Stirling heat engine with various heat and mechanical losses. *Energy*, 256, article number 124699. doi: 10.1016/j.energy.2022.124699.
[40] Zhang, L., Han, K., Wang, Y., Zhu, Y., Zhong, S., & Zhong, G. (2023). A bibliometric analysis of Stirling engine and in-depth review of its application for energy supply systems. *Energy Reviews*, 2(4), article number 100048. doi: 10.1016/j.enrev.2023.100048.
[41] Zhu, S., Yu, G., Liang, K., Dai, W., & Luo, E. (2021). A review of Stirling-engine-based combined heat and power technology. *Applied Energy*, 294, article number 116965. doi: 10.1016/j.apenergy.2021.116965.

Комбіновані системи енерговиробництва з двигуном Стірлінга: аналіз світового досвіду та локальні перспективи

Євген Нікітін

Аспірант
Національний університет біоресурсів і природокористування
03041, вул. Героїв Оборони, 15, м. Київ, Україна
https://orcid.org/0009-0003-4000-3193

Анотація. Дослідження спрямоване на виявлення потенціалу комбінованих систем енерговиробництва з двигуном Стірлінга шляхом аналізу міжнародного досвіду та оцінки перспектив їх адаптації до локальних умов. У дослідженні застосовано аналітичний підхід до вивчення світового досвіду, технічних рішень і умов локального впровадження комбінованих енергосистем на базі двигуна Стірлінга. У ході дослідження проаналізовано світовий досвід застосування двигунів Стірлінга в комбінованих енергетичних системах у Європі (Нідерланди, Німеччина, Великобританія), Азії (Японія) та Північній Америці (на прикладі Національного управління з аеронавтики і дослідження космічного простору), де вони показали високу енергоефективність і екологічність. Результати підтвердили можливість ефективного застосування цих систем в Україні для децентралізованого енергопостачання з використанням місцевих ресурсів. Визначено, що двигуни Стірлінга можуть бути ефективними для децентралізованого енергозабезпечення сільських громад, медичних установ, освітніх закладів та об'єктів критичної інфраструктури, особливо в регіонах з доступом до біомаси або побутових відходів. Встановлено, що основними бар'єрами залишаються висока вартість обладнання (від 10 000 євро до 13 000 євро) та відсутність виробничої бази. Термін окупності таких систем становить від 6 до 9 років, з річною економією на енергії в межах 500-900 євро. Зроблено висновок, що за умов відповідної державної підтримки та локалізації виробництва комбіновані системи на основі двигуна Стірлінга мають потенціал для широкого застосування як складова стратегії енергетичної децентралізації та переходу до сталої енергетики. Крім того, двигуни мають ресурс роботи від 40 000 до 60 000 годин, а витрати на обслуговування складають від 100 євро до 200 євро на рік. Дослідження надає обґрунтовані техніко-економічні висновки щодо можливості адаптації та впровадження комбінованих систем з двигуном Стірлінга в локальних енергетичних умовах, що може слугувати основою для прийняття рішень у сфері сталої енергетики

Ключові слова: децентралізація; біомаса; теплове джерело; когенерація; екологічність

TECHNOLOGIES AND ENGINEERING

Journal homepage: https://technologies-engineering.com.ua/en
Vol. 26, No. 3, 2025

Received: 30.01.2025
Revised: 26.05.2025
Accepted: 25.06.2025

UDC 697.93:620.92(477)
DOI: 10.30857/2786-5371.2025.3.6

Integration of a solar power plant and a heat pump into a hot water supply system based on a digital twin

Mykola Politykin

Postgraduate Student
National Technical University of Ukraine "Igor Sikorsky Kyiv Polytechnic Institute"
03056, 37 Beresteiskyi Ave., Kyiv, Ukraine
https://orcid.org/0009-0005-5065-6205

Olena Yatsenko*

PhD, Assistant Lecturer
National Technical University of Ukraine "Igor Sikorsky Kyiv Polytechnic Institute"
03056, 37 Beresteiskyi Ave., Kyiv, Ukraine
https://orcid.org/0000-0002-8001-5987

Abstract. In the context of growing threats to Ukraine's energy security and the need to increase the autonomy of the residential sector, the study of the effective combination of heat pumps and solar generation is highly relevant. The aim of the study was to justify the feasibility of integrating an air-to-water heat pump into the hot water supply system of an multi-apartment building equipped with a solar power plant, using a digital twin to improve energy efficiency and autonomy. The following methods were used in the study: analysis of the actual energy consumption database, energy modelling in the PV*SOL programme, instrumental monitoring of temperatures, water and electricity consumption, as well as comparison of system configuration options taking into account seasonal characteristics. A comparison of heat pump operating modes was carried out: full heating (up to 55°C) and bivalent (up to 35°C with reheating). Seasonal efficiency, coverage of needs from the solar power plant and system balancing options were calculated. As a result, it was found that the actual hot water consumption is 21.5 times lower than the standard, and more than 60% of the thermal energy is spent on circulation. Excess generation by the solar array (over 16,000 kWh/year) can be effectively used to heat water through a heat pump. In the heating mode up to 35°C, electricity consumption is reduced by 50.9% compared to the full water heating mode (up to 55°C). The study also proposed a digital twin of a hybrid solar power plant-heat pump system that adapts to changes in load and operating conditions. For the first time, a quantitative assessment of the efficiency of the bivalent mode in real-life conditions has been carried out, taking into account actual consumption. The results can be used for adaptive design of hot water supply systems in residential buildings. The proposed approach allows reducing costs, increasing autonomy, reducing the load on the network, and adapting systems to crisis conditions and changes in consumer behaviour

Keywords: autonomous heat supply; multi-apartment building; renewable energy sources; energy modelling; energy efficiency

Introduction

In the context of the full-scale military aggression against Ukraine, accompanied by regular attacks on critical energy infrastructure, the issue of ensuring the energy independence of the housing stock has acquired not only technical, but also social and national security significance. This challenge is particularly acute in multi-apartment buildings, where stable electricity supply and hot water provision are prerequisites for maintaining the basic living conditions of the population during prolonged or sudden crises.

The problem of improving the energy efficiency of multi-apartment buildings through the use of renewable energy sources is actively studied in the global scientific

Suggested Citation:
Politykin, M., & Yatsenko, O. (2025). Integration of a solar power plant and a heat pump into a hot water supply system based on a digital twin. *Technologies and Engineering,* 26(3), 77-87. doi: 10.30857/2786-5371.2025.3.6.

*Corresponding author

literature (Martorana *et al*., 2021). Special attention is given to the synergistic combination of photovoltaic systems (PV) and heat pumps (HP) for domestic hot water (DHW) supply, which reduces dependence on centralised energy sources and increases the resilience of the residential sector to energy challenges. The work of M. Alhuyi Nazari *et al*. (2023) highlighted the significant potential of hybrid systems that combine PV and HP to reduce fossil fuel consumption and greenhouse gas emissions. The issue of solar energy storage in the context of DHW demand was explored by A. Gagliano *et al*. (2025), who analysed the role of buffer tanks in smoothing out seasonal imbalances between generation and consumption. Research by R. Dumoulin *et al.* (2021) also confirmed the promise of seasonal storage as a strategy for enhancing the autonomy of heat generation systems, demonstrating the effectiveness of combining a heat pump with a building-integrated photovoltaic/thermal system (BIPV/T), capable of adapting to changes in electricity demand profiles and interacting with the grid for real-time energy balancing.

Within the study by C. Zhang *et al*. (2021), the efficiency of air-to-water heat pump systems integrated with PV was experimentally verified. It was shown that with appropriate configuration, the seasonal coefficient of performance (COP) can reach 4.2 even in winter, significantly improving the efficiency of renewable energy use during the heating season. Practical approaches to the design of rooftop PV systems were analysed in the report by A. Borodinecs *et al*. (2024b), which proposed a methodology for assessing the feasibility of installing solar systems considering architectural and insolation constraints, as well as financial payback criteria. In another study by A. Borodinecs *et al*. (2024a), the use of real electricity consumption data in multi-storey residential buildings was examined for optimising the calculated capacity of PV systems. The authors noted that accurate knowledge of daily consumption profiles helps to avoid excessive daytime generation and improve the balance between consumption and generation. In particular, it was proposed to take into account changes in residents' living patterns caused by social circumstances.

Special attention in the literature has also been devoted to dynamic modelling of PV-HP hybrid systems, accounting for climate parameter variations throughout the year. In the context of hybrid system development, a promising approach is the integration of photovoltaic-thermal (PVT) collectors with heat pumps, which, according to A. Miglioli *et al*. (2021), makes it possible to cover all thermal needs of a building with a high share of renewable energy, increasing the efficiency of both solar generation and heat pump equipment. In the studies by R.E. Alden *et al*. (2023) and B. Xiang *et al*. (2021), the authors emphasised the use of decision-making algorithms (such as ELECTRE) for selecting the optimal system configuration, considering climate conditions, consumer behaviour models and the local energy context. Such an interdisciplinary approach enables the consideration of not only technical but also social parameters of hybrid system operation. In the work by I. Sokolovska *et al*. (2024) it was investigated key barriers to the implementation of heat pump technologies in district heating. They also systematised European experience in technical, economic and regulatory support for the transition to low-carbon heat sources. The analysis of proposed measures – ranging from preferential tariffs to professional staff training – may be applied to shape an effective strategy for deploying heat pumps in Ukrainian multi-apartment buildings.

Thus, there was a need to study the techno-economic parameters and energy operating modes of heat pumps in combination with solar power plants to provide hot water supply under real multi-apartment building conditions. In particular, the relevant issue was the proper selection of heat pump parameters, taking into account seasonal load variations, actual consumption profiles, the type of selected water reheating scheme, and the characteristics of local generation. The aim of this study was to determine the optimal conditions for the application of a heat pump in the hot water supply system of a multi-apartment building, considering solar generation parameters, seasonal load fluctuations and real consumption profiles.

Materials and Methods

A comprehensive scientific approach was applied in this study, incorporating instrumental measurements, energy modelling, regulatory framework analysis, and digital system modelling using the PV*SOL premium (n.d.). This approach made it possible to assess the efficiency of heat pump integration under real operating conditions of a multi-apartment building. A range of scientific methods were employed, including: the analytical method – for the analysis of regulatory documentation, literature sources, and studies in the field of renewable energy; the empirical method – for collecting data on actual hot water consumption, supply and return temperatures, circulation volumes, etc.; the comparative method – for comparing normative and actual consumption indicators, as well as the efficiency of different heat pump operating modes. Mathematical modelling was also applied – to calculate thermal loads under various operating modes of the heat pump – alongside computer-based modelling carried out in PV*SOL to assess the annual PV generation, determine electricity surpluses, and evaluate their utilisation efficiency. In a previous study, M.V. Politykin & O.I. Yatsenko (2025) presented the results of PV*SOL-based modelling of a PV system for a multi-apartment building and identified seasonal surpluses of unused electricity, which could be effectively integrated into heat pump operation.

The object of the study was a typical multi-apartment building located in Kyiv, operating under conditions of district heating. The building belongs to the category of high-rise residential development and has characteristic parameters typical of the housing stock of the late 20th – early 21st century. The main technical and operational characteristics of the building are presented in Table 1.

***Table 1.** Parameters of a multi-apartment building*

Parameter	Value
Purpose	multi-apartment building
Number of floors	16 (+ technical floor and basement)
Number of apartments	75
Total number of residents	210
Temporarily not living there due to the war	63
Total area (m²)	9,664
Living area of the building (m²)	3,800.3
Total height of the building (m)	53

***Source:** technical passport and energy performance certificate of the building, provided by the condominium association "Poryadok Sheptytskoho, 12"*

The heating and hot water supply system of the building is centralised. Heat supply is provided through an individual heat substation (IHS) located in the basement. This configuration enables basic modernisation without the need for complete dismantling of the systems, which is an important advantage during reconstruction. A rooftop PV system with a total installed capacity of 30.6 kW has been installed. The system consists of photovoltaic panels mounted on lightweight metal structures, ensuring an optimal tilt angle: 20°-30° towards the north and up to 10° in the east-west plane. The complex is complemented by hybrid inverters, a monitoring system (Leanheat® Monitor, Danfoss), protective equipment, and electricity storage based on battery units. Additionally, data were obtained from an Apator PoWoGaz JS-130-16 cold water flow meter, installed in the building's heat substation, which measures water consumption for the DHW module. Figure 1 presented the exterior view of the residential building and the layout of a typical floor.

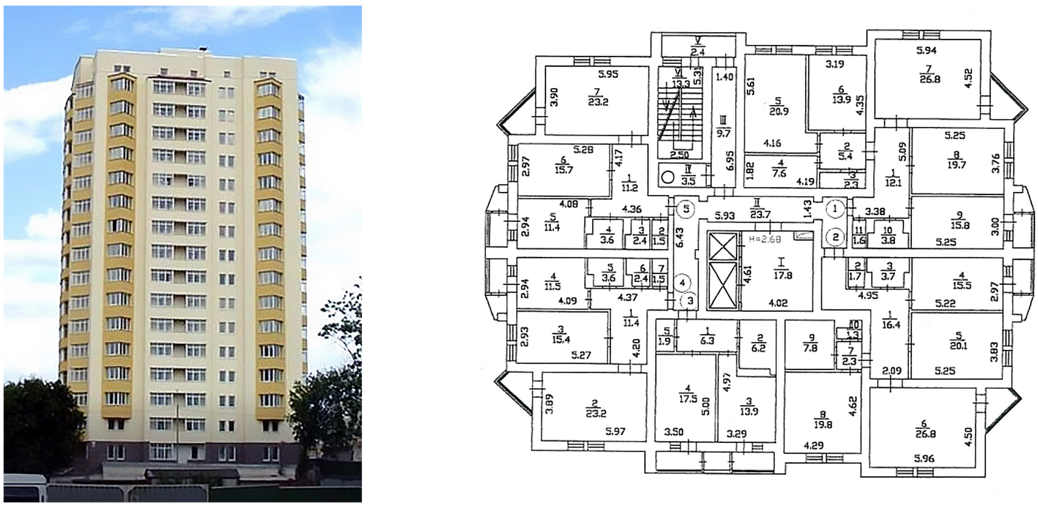

***Figure 1.** General view of the building and floor plan of a typical floor*
***Source:** technical passport and energy performance certificate of the building, provided by the condominium association "Poryadok Sheptytskoho, 12"*

At the beginning of the study, initial data on the apartment building was collected: structural characteristics, number of residents, configuration of existing engineering systems, and parameters of the installed solar power plant. Next, instrumental measurements were taken of actual hot water consumption, supply and return temperatures, circulation losses, and electricity consumption by common building systems. Based on this data, thermal loads for the hot water supply system were modelled and energy modelling of the solar power plant was performed in the PV*SOL software environment to determine annual generation volumes and seasonal surpluses. After that, the operation of the heat pump was modelled using the passport characteristics of the MGSDC-080IIC air-water unit (manufactured in China) with a thermal capacity of 25 kW. The inlet water temperature was assumed to be 5°C during the heating period and 10°C during the non-heating period. Two modes were considered: heating to 35°C (with reheating in the heat exchanger to the standard value) and heating to 55°C without an external source. To compensate for hourly imbalances, two 1 m³ hot water storage tanks were installed. The average COP values of the heat pump depending on the month are summarised in Table 2. Electricity consumption, system balancing options, and a comparison of the standard and actual scenarios were calculated. To determine the energy balance of electricity generation and consumption in the building, measurements of electricity consumption for common building needs (cold water supply pumps, heating circulation, DHW circulation, lighting, elevators – total nominal load 11.92 kW) were taken, as well as measurements of actual electricity generation from the PV station and modelling of the heat pump under real consumption conditions. The final stage was the implementation of the concept of a digital twin of the building's energy system, which allows for hourly load changes, climatic parameters, behavioural aspects of consumption to be taken into account and the system's operating modes to be adapted in real time.

Table 2. *Heat pump parameters depending on the average air temperature and hot water temperature at the heat pump outlet*

Month	Average air temperature 2024, °C	COP (heating to 35°C)	COP (heating to 55°C)
January	-2.6	2.8	2.5
February	2.9	3.5	3.0
March	4.8	3.7	3.2
April	12.8	4.9	4.0
May	16.3	5.4	4.4
June	21.5	5.9	4.7
July	24.3	5.9	4.7
August	23.1	5.9	4.7
September	20.6	5.9	4.7
October	10.9	4.6	3.8
November	2.7	3.5	3.0
December	0.0	3.1	2.7

Source: *compiled based on data from the technical passport of the heat pump and Climatic data for the city of Kyiv (n.d.)*

The assessment of DHW needs was carried out in accordance with design standards. According to DBN V.2.5-64:2012 (2013), daily water consumption in multi-apartment residential buildings with centralised hot water supply for one resident in climate zone I is 250 litres/day, of which 100 litres/day is for hot water supply. Thus: average daily consumption of hot water per resident – 100 litres/day; total daily consumption of hot water for the building – 21,000 litres/day or 21.0 m^3/day; the annual volume of hot water consumed is 7,665 m^3/year; the approximate annual heat consumption for heating water from 10°C to 55°C:

$$Q = 7{,}665{,}000 \cdot 4.19 \cdot 45 = 1{,}445{,}516 \text{ kJ} = 401.5 \text{ MWh/year}.$$

To cover hot water supply loads, options for installing an air-to-water heat pump with a thermal capacity of 30-50 kW were considered. The approximate average annual COP value is assumed to be 3.0. Based on the preliminary calculation of the annual heat energy demand: $Q = 401.5$ MWh, the annual electricity consumption of the heat pump is determined as:

$$E_{HP} = Q / COP = 401.5 \text{ MWh/year} / 3.0 \approx 133.8 \text{ MWh/year}.$$

The solar power plant installed on the roof of the building generates approximately 42 MWh of electricity per year. Therefore, it is theoretically possible to cover HP's energy consumption using the PV:

$$42 / 133.8 \approx 31.4\%.$$

However, it is important to consider the seasonal discrepancy between the PV generation schedule and the actual demand for heat energy for DHW. Without energy storage, the direct use of PV electricity for DHW needs does not exceed 10-15%.

Results and Discussion

In many large cities of Ukraine (Kyiv, Khmelnytskyi, Cherkasy, Lviv, Dnipro, Rivne, Poltava, Sumy, Ternopil), as of 2025, centralised hot water supply systems are still in place, but their efficiency is becoming increasingly difficult to maintain. This is due to the prolonged absence of centralised heat supply in the off-season, as well as the growing number of consumers who are abandoning centralised services in favour of individual hot water preparation using electric boilers. This transition has systemic consequences – an increase in the load on internal electrical networks, which are often not designed for peak loads, especially in the morning and evening hours of consumption (Alden *et al.*, 2023). In addition, this situation is accompanied by an increase in the budgetary burden, in particular due to the need for subsidised regulation of gas prices for the needs of the population. In these conditions, the formation of local autonomous energy supply systems is becoming increasingly relevant – solutions that can provide the residential sector with stable energy even under restrictions imposed by centralised systems. One of the empirical indicators of increased interest in decentralised energy solutions is the rapid growth in the number of purchases of solar power plants in the budget sector. According to the Prozorro system, during 2024 and early 2025, 1,113 lots were recorded relating to the design, supply or installation of PV in state, municipal and educational institutions. The total expected cost of these purchases exceeded UAH 1.1 billion, of which 403 lots were related to design work (architectural and engineering design, development of design and estimate documentation, preparation of energy solutions), which indicates structural planning for modernisation (Prozorro BI module, 2025). Figure 2 illustrated the growth dynamics of the total number of procurements in the field of PV installation in the budget sector, as well as the share of design works, which makes it possible to conclude that there is a systematic increase in the potential of decentralised generation.

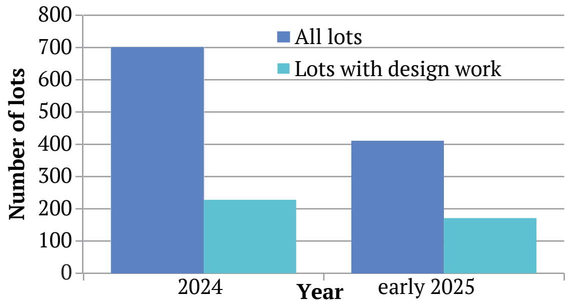

***Figure 2.** Dynamics of procurement by PV in the budgetary sector of Ukraine*
***Source:** developed by the authors based on data from the Prozorro BI module (2025)*

Another important factor stimulating the development of local energy systems is the state program for supporting residential energy efficiency – "GreenDIM". As of early 2025, within this program 188 applications have been submitted, of which 82 projects have already been implemented with full or partial grant disbursement. The total floor area of multi-apartment buildings covered by the projects exceeds 2.78 million m^2, while the number of households amounts to 31,940 (Energy Efficiency Fund of Ukraine, 2025).

The obtained results are based on the analysis of the technical characteristics of a typical multi-apartment residential building in Kyiv, equipped with a centralised heating system and a PV plant. The object of study has an architectural and operational profile typical of the modern housing stock, which allows the findings to be extrapolated to a broader residential sector. The PV plant is designed to supply electricity for common building needs: pumping equipment, lighting of common areas, and elevators. However, results of modelling conducted in PV*SOL in the previous study by M.V. Politykin & O.I. Yatsenko (2025), along with the analysis of actual 2024-2025 production and consumption data from the PV system, demonstrated the presence of a significant daytime generation surplus. In summer, up to 70% of the generated electricity remains unused, while in winter this figure is about 32%. On an annual basis, the unused surplus electricity within the building amounts to 16,529.7 kWh. Thus, it must always be taken into account that the operation of PV plants in the residential sector is characterised by strong seasonal variability, as also emphasised by A. Borodinecs *et al*. (2024a). This creates opportunities for surplus utilisation – either through the "Active Electricity Consumer" mechanism, which allows excess power to be fed into the grid, or by connecting additional loads, as highlighted by the Association of Solar Energy of Ukraine (2024). The most promising direction is the supply of an electric heat pump from the PV system, which can be integrated into the domestic hot water (DHW) system, thereby increasing both the efficiency and autonomy of the building. This approach allows for the effective use of summer surpluses and reduces electricity consumption from external grids (Gagliano *et al*., 2025). Similar conclusions were reached by F. Wang *et al*. (2024), who noted that coupling heat pumps with solar generation ensures high seasonal efficiency even in climates with moderate temperatures. In line with the present study, K. Tomczuk & P. Obstawski (2024) also identified the problem of low PV self-consumption (16.9-19.0%) due to the mismatch between generation and demand. In the current research, several technical and functional measures for system balancing were proposed: installation of DHW storage tanks with a two-day capacity (≈ 42 m^3); installation of electrical storage batteries systems (100 kWh); and optimisation of the heat pump's operational algorithms to maximise daytime operation. Comprehensive implementation of these measures allows the share of PV utilisation to be increased to 50-60%, while reducing dependence on external energy supply.

Instrumental measurements of the building's DHW system confirmed a significant deviation of actual consumption from the design values specified by DBN V.2.5-64:2012 (2013). Actual daily DHW consumption by residents amounted to approximately 1,250 L/day, corresponding to 456.2 m^3/year, which is almost 21.5 times lower than the normative daily consumption. At the same time, daily circulation water volume in the DHW system reached 108,000 L/day, or 39,420 m^3/year, which far exceeds the useful consumption by residents. This indicates low energy efficiency of the circulation loop. Particularly illustrative were the temperature profiles presented in Figure 3, showing the dynamics of supply (T3) and return (T4) water temperatures throughout the day. The average temperature difference between supply and return lines was only 0.79°C, which is an extremely low indicator. This may be attributable to oversized circulation pumps and insufficient hydraulic balancing of the system, resulting in excessive heat losses.

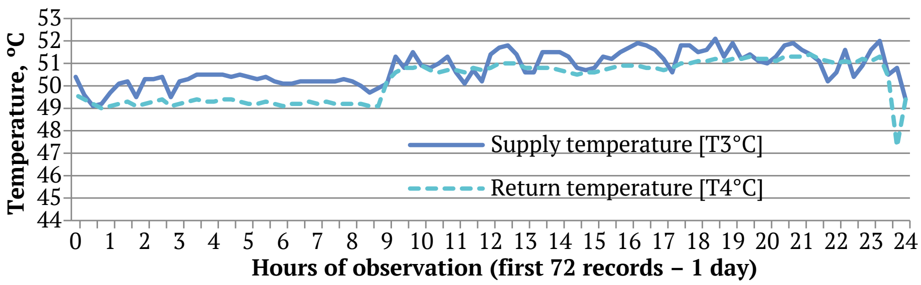

***Figure 3.** Graph showing temperature and hot water circulation over a 24-hour period*
***Source:** developed by the authors based on data from the Leanheat® Monitor (Danfoss) monitoring system*

Calculation of thermal loads on the DHW system based on measurement results allowed determining the following indicators: thermal demand for hot water heating (10 → 55°C) – 23.9 MWh/year; heat demand for maintaining circulation – 36.2 MWh/year; total heat demand of the DHW system – 60.1 MWh/year. It has been demonstrated that more than half of all heat energy consumed is used not to heat water for residents, but to maintain circulation. Additional information on the profile of actual daily consumption is shown in Figure 4, which depicts the average daily dynamics of DHW consumption in the summer period. The highest consumption occurs in the morning and evening hours, which corresponds to the typical behavioural pattern of residents.

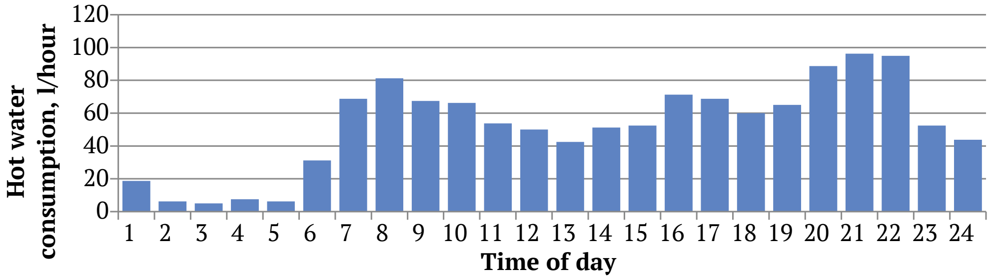

***Figure 4.** Daily hot water consumption graph (residents, without circulation)*
***Source:** developed by the authors based on data from the Apator PoWoGaz JS-130-16 cold water flow meter*

At the same time, Figure 5 illustrated a comparison of the calculated (design), actual, and adjusted heat consumption, the latter corrected according to the current number of residents. Taking into account that, as a result of the war, 63 people are temporarily absent, the actual number of residents has decreased to 147. This necessitated a revision of the energy calculations: DHW consumption – 5,365.5 m^3/year; annual heat demand – 361.0 MWh; electricity consumption of the heat pump (COP = 3.0) – 120.3 MWh; share of demand covered by the PV system – increased to 35% (compared with 31.4% when the DHW demand was assessed according to design standards).

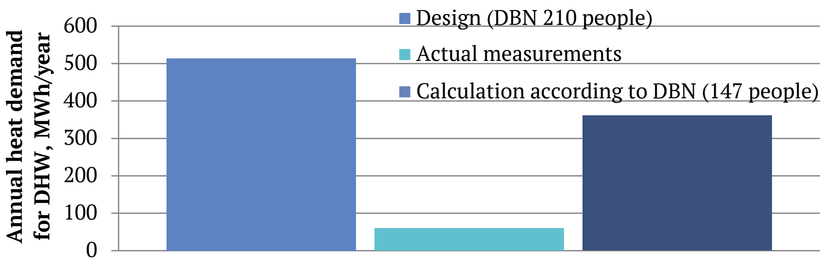

***Figure 5.** Comparison of calculated and actual heat energy requirements for domestic hot water supply in a building*
***Source:** compiled by the authors based on own calculations*

Based on these data, a comparative analysis of the balancing parameters of the hot water supply system was carried out for two scenarios – the standard scenario and the actual one. Table 3 showed the calculation results for the heat pump capacity, the volume of accumulator tanks, and the capacity of electricity accumulators for both options. In addition, the table shows the accepted parameters that were used in this study.

***Table 3.** Comparative parameters of the DHW balancing system*

Indicator	Unit of measurement	Estimate (standard consumption)	Estimate (actual consumption)	Accepted in the pilot project
Heat pump capacity	kW	45.8 kW	10.9 kW	25
Volume of the accumulator tank (2 days)	m^3	42 m^3	2.50	2
Capacity of the electricity accumulator (2 days)	kWh	100 kWh	43.6	75

***Source:** compiled by the authors based on own calculations*

The results obtained confirmed the feasibility of a flexible approach to the design of the domestic hot water (DHW) system based on actual monitoring data. With the help of an adaptive configuration of the elements of a hybrid energy complex, it is possible to significantly reduce the initial costs of equipment and increase the level of autonomy through the optimal use of existing PV generation. In addition, this approach ensures the stability of the temperature regime of consumption and allows for a quick response to changes in weather conditions or user behaviour, which is especially important for improving energy efficiency in decentralised heat supply conditions.

According to the modelling results obtained in PV*SOL premium (n.d.) and presented in the earlier study by M.V. Politykin & O.I. Yatsenko (2025), on a typical summer day around 70% of the electricity generated by the solar array remains unused, while in winter this figure is about 32%. In annual terms, 16,529.7 kWh of electricity produced by the PV system was not consumed within the building. This creates additional opportunities for its effective utilisation, in particular by directing part of the surplus generation to power the heat pump for DHW heating. The COP values obtained, as summarised in Table 2, served as the basis for calculating the building's energy balance. This enabled the determination of electricity consumption volumes and coverage for DHW demand through the integration of the existing solar generation. Based on this modelling, the energy balance presented in Table 4 was developed.

Table 4. *Electricity consumption and generation indicators for a residential building with a PV and heat pump*

Month	Total electricity consumption without HP (kWh)	Total electricity generation by PV (kWh)	Electricity consumption by HP (water heating to +35°C) (kWh)	Electricity consumption by HP (water heating to +55°C) (kWh)	Unused generation (kWh)
January	4,577.9	825.5	161.2	242.3	220.8
February	3,880.4	1,320	145.4	218.5	507.9
March	3,979.2	2,318.2	162.4	243.9	1,048.1
April	1,635.8	2,829.5	135.7	205.2	2,079.2
May	1,690.3	3,421.8	123.2	186.4	2,512.4
June	1,431.3	3,285.8	109.6	165.8	2,471.2
July	2,183.3	3,316.3	111.1	167.9	2,160.5
August	1,619.9	3,146.2	116.2	175.6	2,328.7
September	1,601.7	2,462	121.5	183.7	1,690.4
October	2,570.7	1,821.3	133.8	202.4	1,050.3
November	4,293.9	796.3	146.8	222	257.7
December	5,035.7	525.2	157.4	237.9	116.1
Per year	34,500.1	26,068.1	1,624.3	2,451.6	16,443.3

Note: *total electricity consumption without HP – measurement data; all other data – simulation data*
Source: *compiled by the authors of the study*

As a result of the analysis of Table 4, the annual electricity consumption of the heat pump decreased by 50.9%: from 2,451.6 kWh when heating fully to 55°C, to 1,624.3 kWh in the scenario of partial heating to 35°C. This approach allows for a more rational utilisation of solar generation under its constrained profile. However, the electricity savings were accompanied by an increased demand for thermal energy from external sources to reheat the water from 35°C to the normative level, which complicates a straightforward assessment of the scheme's overall effectiveness. The application of a bivalent heating scheme, whereby the heat pump performs the primary heating only up to 35°C and the final reheating to the normative 55°C is provided by an external thermal energy source (e.g. a district heating network), enables an average increase of 20% in the seasonal coefficient of performance (COP) of the heat pump over the year compared with the full heating mode to 55°C (Fig. 6). This effect is due to the reduced temperature lift at which the heat pump operates, which significantly improves its energy efficiency.

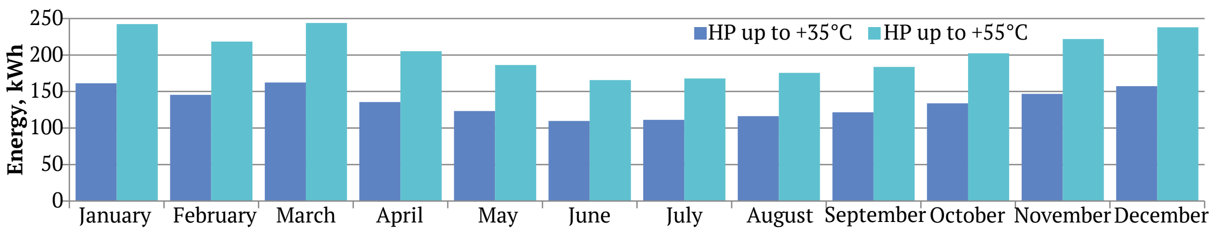

Figure 6. *Monthly energy consumption per heat pump at water heating temperatures of 35°C and 55°C*
Source: *compiled by the authors of the study*

Under standard regulatory conditions, the choice between monovalent and bivalent schemes is typically made on the basis of a techno-economic assessment. However, under the current conditions of martial law in Ukraine, the state's policy of subsidised heat tariffs for households, and the sharp rise in electricity costs driven by increased imports, capacity shortages and the expenses associated with restoring the energy infrastructure, conducting a full techno-economic comparison becomes considerably more challenging. In this context, integrated digital models are increasingly being applied to decision-making, as they enable real-time adjustment of input parameters (tariffs, consumption schedules, source capacities) and allow scenario forecasting that accounts for external factors. This approach was implemented in the present study.

Figure 7 presented a month-by-month comparison of electricity generation from the solar power plant and the total electricity consumption of the residential building, taking into account the operation of the heat pump in reheating mode up to 55°C. As shown in Figure 7a, between April and September a surplus of solar generation was observed: the monthly electricity output exceeded the system's requirements both for common-use building needs and for domestic hot water supply. This creates opportunities for the autonomous operation of the building's energy system during the warmer months, covering hot water demand entirely with solar energy without reliance on the district heating network. By contrast, in the autumn-winter period (October-March), the balance shifted: electricity consumption exceeded PV output, necessitating additional supply sources.

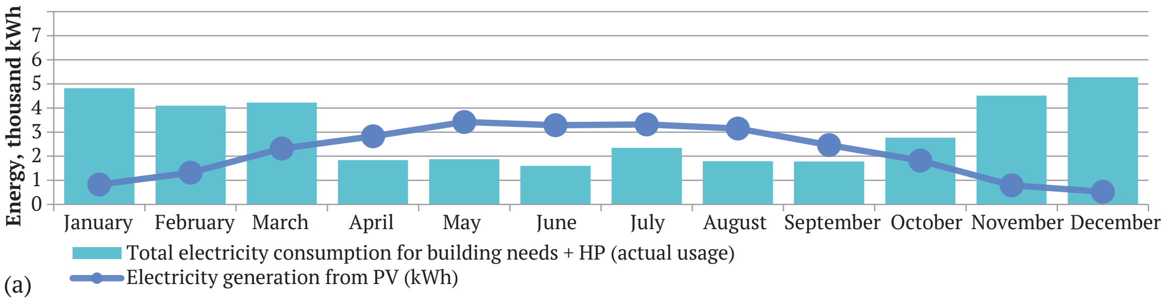

Graph (a)

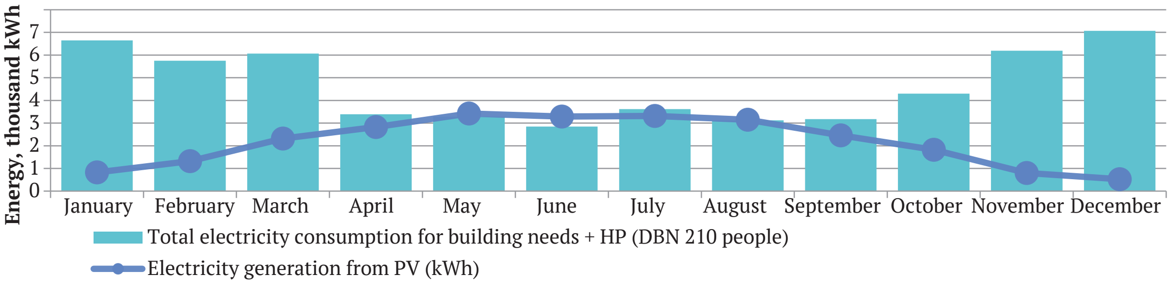

Graph (b)

***Figure 7.** Comparison of electricity generation and consumption by a residential building, taking into account the installation of a heat pump*

***Note:** a – 25 kW and actual hot water consumption; b – 50 kW and estimated hot water consumption according to DBN V.2.5-64:2012 (2013)*

***Source:** compiled by the authors of the study*

A comparison of actual hot water consumption by residents (Fig. 7a) with the calculated standard consumption according to DBN V.2.5-64:2012 (2013) for 210 people (Fig. 7b) showed fundamental differences in the ratio of PV generation and total electricity consumption. The building's real energy consumption, when adjusted for the observed DHW profile and actual occupancy, is significantly lower than the regulatory estimate. This enables a more effective integration of the PV system into the energy supply, achieving a higher share of autonomous coverage, reducing the need for storage, and lowering peak loads. Given the large number of variables and their interaction over time, the optimal approach is to use a digital twin of the building's energy system. Such a digital twin allows not only to simulate the operation of the heat pump, taking into account climatic and behavioural data, but also to perform adaptive optimisation of operating modes in real time.

A schematic diagram of the energy complex with a solar power plant and a heat pump in a bivalent scheme is shown in Figure 8. It includes interaction between power sources (PV, Energy storage, power grid), thermal energy storage devices, heat exchangers and a heat pump that can operate in both mono- and bivalent modes. It also provides for the possibility of automated control of pumps, switches, heat exchangers and energy management modules.

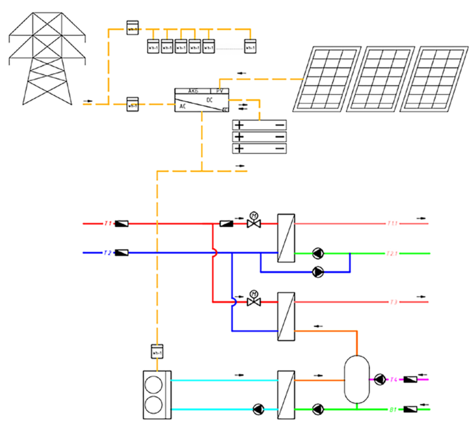

***Figure 8.** Schematic diagram of an energy complex with a solar power plant and a heat pump*

***Source:** compiled by the authors of the study*

For the verification of the digital twin, detailed monitoring of the system parameters is planned. A complete list of key parameters is presented in Table 5, which specifies both physical quantities (energy consumption, temperatures, water volumes) and the frequency of their collection. Particular attention is given to temperature control (T1-T4), PV generation, own consumption, the operation of the heat pump (EHP), as well as individual apartment-level electricity consumption by residents (Eap1…75), which is a key factor for the development of accurate models.

Table 5. *Monitoring parameters for digital twin verification*

Parameter	Designation	Unit	Monitoring period
Total heat energy consumption of the building	Qtotal	Gcal	2 min
Heat energy consumption for heating	Qheat	Gcal	2 min
Heat energy consumption for DHW with circulation	Qdhw	Gcal	2 min (Qgen-Qheat)
Outdoor air temperature	Tout	°C	2 min
Supply temperature from heat network	T1	°C	2 min
Return temperature to heat network	T2	°C	2 min
Supply temperature to DHW	T3	°C	2 min
Return temperature from DHW circulation	T4	°C	2 min
Cold water consumption for DHW	Vmin	m^3/year	2 min
Circulation water consumption	Vcirc	L/hour	2 min
PV generation	Gpv	kWh	1 min
Own PV consumption	Gconsu	kWh	1 min
Heat pump electricity consumption	EHP	kWh	1 min
Apartment-level electricity consumption	Eap1..75	kWh	1 month
Indoor air temperature	Tap1..75	°C	1 hour (sampled flats)

Source: *compiled by the authors of the study*

According to M. Bezrodnyi *et al*. (2017), the combined use of atmospheric air heat and solar energy in heat pump systems can significantly increase the efficiency of heat pumps during the cold season. This was confirmed by the results of the author's research. However, unlike the work of M. Bezrodnyi *et al*., which focused on increasing the air temperature in front of the evaporator using solar collectors, the current study demonstrated the possibility of effectively using excess solar generation to power the heat pump, which is particularly relevant in conditions of energy resource shortages. Unlike the studies by A. Borodinecs *et al*. (2024a), which analysed the potential of rooftop PV for communities under standard operating conditions, this study found significant deviations in actual hot water consumption from standard values (21.5 times lower), which highlighted the need for an adaptive approach to the design of hybrid systems. Although A. Borodinecs *et al*. emphasised the importance of analysing real electricity consumption data to optimise the capacity of PV (covering up to 77% of needs), the authors' results expanded this approach, demonstrating the key role of circulation losses (over 60%), the efficiency of the bivalent mode of the heat pump (50.9% reduction in electricity consumption), and the advantages of digital twins over static models (as in PolySun by A. Borodinecs *et al*.).

Research by F. Wang *et al*. (2024) on hybrid systems demonstrated an increase in COP to 3.92 (+18.7% compared to traditional systems) and a reduction in energy costs. These results are consistent with the findings of the current study on the effectiveness of integrating PV and heat pumps, especially in conditions of unstable solar radiation. In addition, M. Zohri *et al*. (2024) summarised the efficiency of hybrid systems based on collectors, PV and PVT, emphasising the importance of multi-source power supply and mathematical modelling for predicting their performance. However, unlike the proposed approach with parameter optimisation (PVT area, tank volume, etc.), the authors' solution with a digital twin allows the system to be dynamically adapted to real conditions without being rigidly tied to fixed geometric parameters.

The results of the study by Y. Lin *et al*. (2022) showed that research on SAHP (solar-assisted heat pump) systems is intensifying in China, with an emphasis on the efficiency of key components (evaporators, heat exchangers, compressors), but there is a lack of attention to intelligent control algorithms and economic feasibility, taking into account regional climatic characteristics. This study partially addressed these challenges, as the digital twin model took into account both climatic and behavioural consumption factors, as well as scenarios for bivalent heat pump control to improve energy efficiency. These conclusions were consistent with the author's approach to adaptive design and the use of a digital twin, which allows real operating conditions to be taken into account.

J. Uche *et al*. (2024) emphasised the high efficiency of RES-based polygeneration systems designed for multi-apartment buildings. The authors proposed strategies for an optimal energy mix, taking into account local needs and the architecture of the residential sector. The current study confirmed the relevance of such approaches in the context of Ukrainian realities, in particular the need to adapt the hot water supply system to the actual load, seasonal fluctuations and consumption patterns. In this context, it is worth mentioning the model of intelligent decision support for the modernisation of the housing stock proposed by S. Maliar (2024), which provides a comprehensive assessment of economic, technical and operational factors when selecting an effective configuration of energy solutions.

In addition, a study by R. Galvin (2022) highlighted the problem of households in Germany being unwilling to install PV systems that significantly exceed their own consumption due to a lack of economic motivation. The author suggested considering PV systems in combination with heat pumps as a single integrated complex, which allows increasing the share of self-consumption and reducing the payback period. R. Galvin also emphasised the importance of optimal PV system power calculation, taking into account behavioural factors, load profile and energy storage system potential. These conclusions are consistent with the approach implemented in this work, which emphasised the need for accurate modelling and personalised selection of equipment configuration.

Thus, the results obtained indicate the technical and economic feasibility of installing a heat pump in the hot water supply system of an apartment building with a solar power plant. Analysis of system operation scenarios at different times of the year demonstrated significant potential for increasing the autonomy of the building and reducing the load on centralised networks. An important part of the study was the creation of a digital twin of the energy system, which made it possible to take into account variable climatic, behavioural and technical factors when modelling the operation of the equipment. This approach ensures high accuracy of analysis and creates a basis for the development of adaptive control strategies.

Conclusions

This study carried out a comprehensive energy modelling of the domestic hot water (DHW) system for a typical multi-apartment building, taking into account the existing PV installation and the integration of an air-to-water heat pump. A distinctive feature of the approach was the use of both real monitoring data (temperature profiles, hot water consumption volumes, circulation losses) and simulation results obtained with the PV*SOL software environment, considering the climatic conditions of Kyiv. Actual hot water consumption by residents turned out to be significantly lower than the normative design values. This deviation is explained not only by the reduction in the number of residents due to the war, but also by changes in household habits (the replacement of baths with showers, the use of washing machines and dishwashers with autonomous heating, etc.). Such changes necessitate a revision of approaches to the design and justification of loads in DHW systems. The circulation component of the DHW system remained the main source of heat losses, even under conditions of a very small temperature difference between supply and return (0.79°C). This indicated the excessive capacity of circulation pumps and highlights the need to revise control algorithms and hydraulic balancing during the reconstruction of utility networks. The use of the heat pump in bivalent mode, with preliminary water heating to 35°C, makes it possible to increase the average monthly COP to 4.8 during the summer period and reduce annual electricity consumption by more than 50% compared with the scenario of full electric heating to 55°C. At the same time, part of the total thermal load is transferred to the district heating network, which is particularly relevant in the context of high electricity tariffs.

Solar electricity generation exceeds the building's demand for 6-7 months of the year, as confirmed both by PV*SOL modelling results and by analysis of actual measurements. The total unused potential of PV generation per year amounts to more than 16,000 kWh, which creates preconditions for the effective use of excess energy in the heating system through the heat pump and storage. The mathematical model developed on the basis of real data enabled the implementation of the digital twin concept of the building's energy system. Such a twin allows: modelling equipment operating modes depending on weather conditions and load profiles; optimising the choice of heat pump capacity, buffer tank volume and electricity storage; forecasting scenarios of autonomous building operation under conditions of critical shortages of centralised resources. Future research prospects include dynamic modelling of the system with hourly variability, optimisation of control algorithms, integration of real monitoring data, and evaluation of the economic feasibility of implementing hybrid system elements under conditions of unstable tariff policies.

Acknowledgements

The authors express their gratitude to the Sheptytskyi 12 Housing Cooperative for providing information, assisting in organising the study, and actively participating in the data collection process.

Funding

None.

Conflict of Interest

None.

References

[1] Alden, R.E., Gong, H., Rooney, T., Branecky, B., & Ionel, D.M. (2023). Electric water heater modeling for large-scale distribution power systems studies with energy storage CTA-2045 based VPP and CVR. *Energies*, 16(12), article number 4747. doi: 10.3390/en16124747.

[2] Alhuyi Nazari, M., Rungamornrat, J., Prokop, L., Blazek, V., Misak, S., Al-Bahrani, M., & Ahmadi, M.H. (2023). An updated review on integration of solar photovoltaic modules and heat pumps towards decarbonization of buildings. *Energy for Sustainable Development*, 72, 230-242. doi: 10.1016/j.esd.2022.12.018.

[3] Association of Solar Energy of Ukraine. (2024). *The end of the feed-in tariff: How to further develop solar energy in Ukraine.* Retrieved from https://aseu.org.ua/kinets-zelenoho-taryfu-iak-dali-zarobliaty-na-soniachnij-enerhetytsi.

[4] Bezrodnyi, M.K., Prityula, N.O., & Misyura, T.O. (2017). Analysis of the efficiency of heat pump heating schemes using the heat of atmospheric air and solar energy. *Power Engineering: Economics, Technique, Ecology*, 4(50), 47-57. doi: 10.20535/1813-5420.4.2017.127544.

[5] Borodinecs, A., Lebedeva, K., & Odineca, T. (2024a). Evaluation of household electricity consumption in multi-apartment buildings for optimization of rooftop PV systems. *Energy and Buildings*, 325, article number 114971. doi: 10.1016/j.enbuild.2024.114971.

[6] Borodinecs, A., Lebedeva, K., Zajecs, D., & Jacnevs, V. (2024b). Towards a framework for optimizing rooftop pv systems based on household electricity consumption data of multi-apartment buildings. In *ASHRAE international building decarbonization conference*. Washington: ASHRAE. doi: 10.63044/ibd24bor32.

[7] Climatic data for the city of Kyiv. (n.d.). *Central geophysical observatory named after Borys Sreznevsky*. Retrieved from http://cgo-sreznevskyi.kyiv.ua/uk/diialnist/klimatolohichna/klimatychni-dani-po-kyievu.

[8] DBN V.2.5-64:2012. Internal Water Supply and Sewerage. (2013, March). Retrieved from https://dbn.co.ua/load/normativy/dbn/1-1-0-1059.

[9] Dumoulin, R., Rounis, E.D., & Athienitis, A. (2021). Operation and grid interaction modeling of a house with a building integrated photovoltaic thermal (BIPV/T) system coupled to an air-source heat pump. *Science and Technology for the Built Environment*, 27(9), 1311-1329. doi: 10.1080/23744731.2021.1941247.

[10] Energy efficiency fund of Ukraine. (2025). *Monitoring of projects under the "GreenDIM" program*. Retrieved from https://sites.google.com/eefund.org.ua/monitoring.

[11] Gagliano, A., Tina, G.M., & Aneli, S. (2025). Improvement in energy self-sufficiency in residential buildings using photovoltaic thermal plants, heat pumps, and electrical and thermal storage. *Energies*, 18(5), article number 1159. doi: 10.3390/en18051159.

[12] Galvin, R. (2022). Why German households won't cover their roofs in photovoltaic panels: And whether policy interventions, rebound effects and heat pumps might change their minds. *Renewable Energy Focus*, 42, 236-252. doi: 10.1016/j.ref.2022.07.002.

[13] Lin, Y., Bu, Z., Yang, W., Zhang, H., Francis, V., & Li, C.-Q. (2022). A review on the research and development of solar-assisted heat pump for buildings in China. *Buildings*, 12(9), article number 1435. doi: 10.3390/buildings12091435.

[14] Maliar, S. (2022). Model of intellectual decision support for assessment of the housing fund. *Innovation and Sustainability*, 2(2), 177-183. doi: 10.31649/ins.2022.2.177.183.

[15] Martorana, F., Bonomolo, M., Leone, G., Monteleone, F., Zizzo, G., & Beccali, M. (2021). Solar-assisted heat pumps systems for domestic hot water production in small energy communities. *Solar Energy*, 217, 113-133. doi: 10.1016/j.solener.2021.01.020.

[16] Miglioli, A., Aste, N., Del Pero, C., & Leonforte, F. (2021). Photovoltaic-thermal solar-assisted heat pump systems for building applications: Integration and design methods. *Energy and Built Environment*, 4(1), 39-56. doi: 10.1016/j.enbenv.2021.07.002.

[17] Politykin, M.V., & Yatsenko, O.I. (2025). Modeling and analysis of solar PV station for residential infrastructure. In *XXII international scientific and practical conference of young scientists and students "Modern problems of scientific support of power engineering"* (pp. 186-188). Kyiv: Igor Sikorsky Kyiv Polytechnic Institute.

[18] Prozorro BI module. (2025). Retrieved from https://bi.prozorro.org/.

[19] PV*SOL premium. (n.d.). Retrieved from https://valentin-software.com/en/products/pvsol-premium/.

[20] Sokolovska, I., Teslenko, O., & Derii, V. (2024). Obstacles to the introduction of heat pumps in district heating. *System Research in Energy*, 2(77), 16-29. doi: 10.15407/srenergy2024.02.016.

[21] Tomczuk, K., & Obstawski, P. (2024). Analysis of the cooperation of a compressor heat pump with a PV system. *Sustainability*, 16(9), article number 3797. doi: 10.3390/su16093797.

[22] Uche, J., Martínez-Gracia, A., Zabalza, I., & Usón, S. (2024). Renewable energy source (RES)-based polygeneration systems for multi-family houses. *Sustainability*, 16(3), article number 945. doi: 10.3390/su16030945.

[23] Wang, F., Liu, M., Guo, W., Liu, X., Zhang, J., Li, J., Hu, G., & Yin, J. (2024). Photovoltaic/thermal integrated air source heat pump hot water system with phase change tank. *Renewable Energy*, 240, article number 122204. doi: 10.1016/j.renene.2024.122204.

[24] Xiang, B., Ji, Y., Yuan, Y., Wu, D., Zeng, C., & Zhou, J. (2021). 10-year simulation of photovoltaic-thermal road assisted ground source heat pump system for accommodation building heating in expressway service area. *Solar Energy*, 215, 459-472. doi: 10.1016/j.solener.2020.12.056.

[25] Zhang, C., Nielsen, E., Fan, J., Furbo, S., & Li, Q. (2021). Experimental investigation on a combined solar and ground source heat pump system for a single-family house: Energy flow analysis and performance assessment. *Energy and Buildings*, 241, article number 110958. doi: 10.1016/j.enbuild.2021.110958.

[26] Zohri, M., Prabowo, Suwarno, Fudholi, A., Suyono, T., Priandana, E.R., & Utomo, Y.S. (2023). Performance review of solar-assisted heat pump systems using solar collectors, PV, and PVT technologies. *International Journal of Heat and Technology*, 41(3), 657-665. doi: 10.18280/ijht.410318.

Інтеграція сонячної електростанції та теплового насоса в систему гарячого водопостачання на основі цифрового двійника

Микола Політикін

Аспірант
Національний технічний університет України
«Київський політехнічний інститут імені Ігоря Сікорського»
03056, просп. Берестейський, 37, м. Київ, Україна
https://orcid.org/0009-0005-5065-6205

Олена Яценко

Доктор філософії, асистент викладача
Національний технічний університет України
«Київський політехнічний інститут імені Ігоря Сікорського»
03056, просп. Берестейський, 37, м. Київ, Україна
https://orcid.org/0000-0002-8001-5987

Анотація. В умовах зростання загроз енергетичній безпеці України та необхідності підвищення автономності житлового сектору, дослідження ефективного поєднання теплових насосів та сонячної генерації є вкрай актуальним. Метою дослідження було обґрунтування доцільності інтеграції теплового насоса типу «повітря-вода» у систему гарячого водопостачання багатоквартирного будинку, оснащеного сонячною електростанцією, з використанням цифрового двійника задля підвищення енергоефективності та автономності. У дослідженні застосовано наступні методи: аналіз фактичної бази енергоспоживання, енергетичне моделювання в програмі PV*SOL, інструментальний моніторинг температур, витрат води й електроенергії, а також порівняння варіантів конфігурації систем з урахуванням сезонних особливостей. Проведено порівняння режимів роботи теплового насоса: повного нагріву (до 55 °C) і бівалентного (до 35 °C з догрівом). Розраховано сезонну ефективність, покриття потреб від сонячної електростанції та варіанти балансування системи. В результаті встановлено, що фактичне споживання гарячої води у 21,5 раза нижче нормативного, а понад 60 % теплової енергії витрачається на циркуляцію. Надлишкова генерація сонячним масивом (понад 16 000 кВт·год/рік) може бути ефективно використана для нагріву води через тепловий насос. У режимі нагріву до 35 °C електроспоживання знижується на 50,9 % порівняно з режимом повного нагріву води (до 55 °C). Також, в роботі запропоновано цифровий двійник гібридної системи сонячна електростанція-тепловий насос, що адаптується до змін навантаження та умов роботи. Вперше проведено кількісну оцінку ефективності бівалентного режиму в умовах реального будинку з урахуванням фактичного споживання. Результати можуть бути використані для адаптивного проєктування систем гарячого водопостачання у житлових будинках. Запропонований підхід дозволяє знизити витрати, підвищити автономність, зменшити навантаження на мережу й адаптувати системи до кризових умов і змін у поведінці споживачів

Ключові слова: автономне теплозабезпечення; багатоквартирний будинок; відновлювальні джерела енергії; енергетичне моделювання; енергоефективність

TECHNOLOGIES AND ENGINEERING

Journal homepage: https://technologies-engineering.com.ua/en
Vol. 26, No. 3, 2025

Received: 07.02.2025
Revised: 23.05.2025
Accepted: 25.06.2025

UDC 004.056.5:004.8

DOI: 10.30857/2786-5371.2025.3.7

Cyber defence automation: Can AI outperform hackers?

Vitalii Yasenenko*

Master, Senior Software Developer
TP-Link
92618, 36 Technology Str., Irvine, USA
https://orcid.org/0009-0004-4801-9541

Abstract. Growing cyber threats in the context of digital transformation require improved methods of automating cyber defence, in particular, through the use of artificial intelligence to detect and respond to attacks. The purpose of the study was to assess the potential of artificial intelligence in the field of cyber defence automation, and to determine its effectiveness in countering advanced cyber-attacks. The study was based on methods of comparative analysis, a systematic approach, and forecasting of cyber threats using artificial intelligence. For the first time, the effectiveness of using artificial intelligence in automated cyber defence systems was comprehensively considered in the context of the current challenges of the digital environment. An analytical review of the capabilities of artificial intelligence in detecting and predicting cyber threats using neural networks, security information and event management systems, and machine learning algorithms was presented. The potential and limitations of automated response systems were determined, and the risks associated with the possibility of using artificial intelligence by attackers themselves were outlined. Special attention was paid to the analysis of the role of the human factor in interaction with automated systems – it was shown that full automation does not guarantee security without the critical participation of specialists. Based on comparative and predictive analysis, practical approaches to the balanced implementation of artificial intelligence in cyber defence systems were proposed. It was proved that artificial intelligence can be a powerful tool for automating cyber defence, but to ensure a high level of security, it is necessary to consider potential risks and constantly improve systems. The practical significance of the study was to develop recommendations for implementing effective security technologies in various cybersecurity sectors

Keywords: digital security; machine learning; engineering; media literacy; digital threat

Introduction

Since 2020, cyber threats have evolved from isolated attacks by individual hackers to highly coordinated actions by transnational cyber structures that can affect the security of entire states. The globalisation of the information space has created a favourable environment for the spread of malicious software, the organisation of cyber espionage, digital sabotage, and information and psychological operations. Cyberattacks can paralyse energy systems, transportation, financial networks, and medical institutions, creating a chain reaction that goes beyond national borders. Insufficient coordination between states in the field of digital security, lack of uniform response standards and political differences prevent effective countering threats.

Cybersecurity automation using artificial intelligence (AI) has significant potential to improve the effectiveness of protection against cyber threats. The study by O.Yu. Kotlyarov & L.L. Bortnik (2024) included a comparative analysis of modern virtual network protection systems, in particular, methodological approaches to building security mechanisms in a virtualised environment were considered. The researchers described key technologies such as virtual firewalls, network segment isolation, and intrusion detection tools in cloud infrastructure. The paper emphasised that most modern systems required not only a high level of automation, but also adaptability to the latest types of attacks. The researchers also drew attention to the importance of following the principles of multi-level protection and the need to integrate real-time monitoring tools. The conclusions emphasised that effective protection of virtual networks was possible only if technical solutions were combined with a flexible risk management methodology. These results were supported by S. Lysenko *et*

Suggested Citation:

Yasenenko, V. (2025). Cyber defence automation: Can AI outperform hackers? *Technologies and Engineering,* 26(3), 89-99. doi: 10.30857/2786-5371.2025.3.7.

*Corresponding author

al. (2024), who examined the problem of automating protection and threat detection through the integration of AI into cybersecurity infrastructure. Their paper noted that the use of automated monitoring and response systems to threats can significantly reduce the likelihood of successful attacks, but also noted the importance of human supervision for timely intervention in difficult situations.

G.G. Mykhalchenko *et al.* (2023) considered economic aspects of ensuring cybersecurity and challenges related to digitalisation. The researchers noted that effective counteraction to cyber threats required not only technical solutions, but also the development of a comprehensive security strategy that included legal and organisational measures. They stressed that only a systematic approach, which included training, implementation of security standards, and continuous monitoring, can ensure the sustainability of economic infrastructure to threats in the digital environment. In turn, the study conducted by A. Yaseen (2024) emphasised the importance of automating infrastructure management to improve cybersecurity. The researcher emphasised that automated systems that can optimise security measures not only reduce risks, but also allow quickly responding to new threats in real time. This integration of AI with infrastructure management systems is an important step towards ensuring high security reliability in organisations. In turn, the study by S. Tonhauser & J. Ristvej (2023), focused on automating processes in the context of countering cyber-attacks. They noted that automated technologies make it much easier to detect and neutralise threats, which is crucial for reducing the response time to security incidents. However, the researchers stressed the need to integrate such systems with conventional security methods to achieve maximum efficiency.

Analysis by S. Varga *et al.* (2022) supplemented previous research, emphasising that automation in cybersecurity through artificial intelligence allows security systems to adapt to new threats. However, as the researchers noted, such an application of AI should be not only technological, but also strategic, and should consider the context and specifics of organisational structures to maximise efficiency. The integration of AI into enterprise automation and cybersecurity is also the subject of research by S.K. Sundaramurthy *et al.* (2022). They focused on the fact that AI can change approaches to processing large amounts of data and providing cyber defence in the face of rapid changes. However, the researchers stressed the importance of combining technological solutions with human control to achieve an appropriate level of security. The study by M. Khan *et al.* (2024) focused on the latest advances in the application of artificial intelligence in cybersecurity, emphasising the importance of automated systems for detecting threats. The researchers pointed out that the use of AI in combination with other security tools can significantly increase the effectiveness of cyber defence.

An important addition to this topic was the study by S.S. Dasawat & S. Sharma (2023), which examined the integration of cybersecurity in startups and small businesses. The researchers stressed the importance of using AI for risk management and automation, especially in a rapidly changing cyber environment. They noted that the integration of such technologies reduced the vulnerability of businesses to attacks and contributed to more efficient scaling. Research by N.A.D. Sontan & N.S.V. Samuel (2024) highlighted the importance of integrating AI and cybersecurity, focusing on possible challenges and prospects for the development of this technology. The researchers pointed out the need for further developments to minimise the risks associated with ethical and security issues that arise when using AI in cyber defence. They also noted that, despite its significant potential, AI cannot completely replace the human factor, but must complement conventional methods of cyber defence.

Despite the growing interest in using AI in cybersecurity, most research was limited to passive data analysis and threat detection functions. Insufficient attention was paid to the role of AI as an active defender – a tool that can independently respond to attacks, block them in real time, and stay ahead of the actions of intruders. The potential of AI as an autonomous force in the fight against highly dynamic, coordinated cyber threats that go beyond national jurisdictions remains poorly understood. The purpose of the study was to investigate the capabilities of artificial intelligence as an active element of cyber defence, capable not only of detecting threats, but also of autonomously countering attacks in real time, considering the global nature of advanced cyber threats and transnational challenges in the field of digital security.

Materials and Methods

The research was mainly theoretical in nature and was aimed at systematising and generalising knowledge about the use of artificial intelligence to automate cyber defence in a global context. The chronological boundaries covered the period 2020-2025, with a particular focus on 2022-2025 publications. The study was conducted from January to April 2025. The analytical database consisted of secondary data collected from international scientific papers, reviews, preprints, and reports published in leading academic journals and repositories (Springer, Elsevier, arXiv, ResearchGate, ScienceDirect). The focus was on theoretical research and analytical reviews that highlighted the applications of machine learning, deep learning, natural language processing (NLP), generative AI, and the use of artificial intelligence in automated threat detection, risk management, proactive defence, and cyber intelligence. The study used a number of methods that allowed theoretically structuring the material and conducting an in-depth analysis. In particular, the comparative analysis was used to compare conventional and intelligent protection methods based on key criteria: effectiveness, adaptability, and accuracy of cyber threat detection. This approach highlighted the advantages and limitations of each class of methods and helped to assess their potential for use in the conditions of growing cyber threats.

To classify methods for predicting cyber threats, machine learning approaches were systematised by the following types: supervised learning, unsupported learning, and deep learning. This approach allowed theoretically substantiating the functionality of each of the approaches in accordance with the types of threats and data specifics, and determining the feasibility of their use in automated cyber defence systems. This allowed structuring the functionality of various approaches, characterising their areas of application, and determining which algorithms were most effective for specific cybersecurity tasks – from detecting anomalies to predicting potential attacks. A historical and logical method was also applied, which helped to trace the evolution of approaches to the use of AI in cyber defence, identify the main trends and patterns of industry development. An analytical and synthetic approach was used to summarise data from various sources and form a complete picture. Separately, a predictive method was applied, which identified promising areas for the development of automated cyber defence technologies that can effectively counteract new, more complex and adaptive cyber threats. The results obtained were considered from the perspective of efficiency, adaptability, and security of automated cyber defence systems, which was extremely important in the context of the constant increasing complexity of attacks and cybersecurity challenges.

Results

The use of AI to detect cyber threats: Neural networks, SIEM systems, and automated firewalls. The current landscape of cyber threats is becoming increasingly complex, and the growing number and variety of attacks require new approaches to security. In an ever-changing cyber threat environment, conventional defence methods often fail to effectively counter new attacks. That is why AI, in particular, neural networks, security information and event management (SIEM) systems, and automated firewalls, play a crucial role in detecting threats, predicting attacks, and responding quickly to incidents. These technologies not only automate security processes, but also allow systems to adapt to new, unknown threats, making them important tools in modern cybersecurity.

Neural networks have become an important tool in cybersecurity due to their ability to detect anomalies in user behaviour and network traffic. They can learn from large amounts of data and detect when certain user actions or network traffic deviate from normal patterns. This approach allows detecting both known and new types of attacks, especially those that do not yet have predefined signatures in conventional threat detection systems. Neural networks that were used to detect behavioural anomalies can adapt to new conditions and automatically adjust their threat detection algorithms, which is extremely important for dealing with new types of attacks, such as "zero-day" attacks that cannot be detected by signature detection. This technology provides higher detection accuracy and efficiency, reducing the number of false positives and improving the ability to predict attacks.

SIEM systems are the foundation for managing security information because they combine data from multiple sources, such as network devices, servers, applications, and other infrastructure components. These systems use algorithms to correlate events and identify anomalies that may indicate the presence of a threat. They allow quickly detecting security incidents and responding to them in real time, which is critical for timely protection of organisations (Sharma *et al.*, 2024). Integration of AI into SIEM systems allows automating detection and response processes and also predicting possible threats based on historical data. Machine learning algorithms can detect complex relationships between events and detect threats that may not be obvious to the human eye. For example, if some system events indicate the presence of a potential threat, the AI can predict the probability of an attack, which would allow the system to take the necessary measures at an early stage.

Automated firewalls equipped with AI provide a higher level of network protection, as they can adapt to new types of attacks and change their real-time traffic filtering strategies. Conventional firewalls use static rules to block or allow traffic, but they may not always account for new, unknown types of attacks. In turn, AI can detect traffic anomalies and take action without having to manually update security rules. Through the use of machine learning algorithms, automated firewalls can "learn" from new traffic patterns and adapt their algorithms to changes in the network environment. This allows effectively detecting new types of attacks and avoiding outdated signatures or parameters, which makes protection more dynamic and flexible. In addition, AI can use historical data about network threats to predict future attacks, thereby reducing the likelihood of successful penetration into the system. In order to compare conventional and intelligent protection methods, in particular, their effectiveness and adaptability to new threats, Table 1 was presented, which demonstrated the main differences between them.

Table 1. *Comparison of conventional and intelligent security methods*

Technology	Conventional approach	AI-based approach
Neural networks	Detection of threats using fixed signatures.	Detection of anomalies and new types of threats through analysis of user behaviour and network traffic.
SIEM-systems	Analysis of events using simple rules.	Use of machine learning algorithms to correlate events and predict attacks.
Firewalls	Static filtering rules.	Adaptive traffic filtering based on anomaly analysis and machine learning.

Source: *compiled by the author based on E. Aghaei et al. (2022)*

The integration of artificial intelligence into cyber threat detection and protection systems, such as neural networks, SIEM systems, and automated firewalls, provides more effective and adaptive protection for networks and systems. The use of AI can significantly reduce the response time to attacks, reduce the number of false positives, and identify new, unknown threats. The ability of such systems to learn and adapt makes them important tools for maintaining cybersecurity in an ever-changing threat environment. However, to achieve maximum effect, these systems must be constantly improved and adapted to new types of attacks.

Methods for predicting cyber threats based on the analysis of previous attacks using AI. In the light of the rapid evolution of cyber threats, characterised by both high dynamics and increasing complexity, cybersecurity experts face the need to move from conventional reactive protection models to proactive approaches focused on predicting potential attacks. In this context, artificial intelligence, as a set of algorithms capable of self-learning, identifying patterns and making decisions based on large-scale data analysis, becomes of strategic importance. Its use in predicting cyber threats is primarily based on the ability to study historical data on security incidents, model behavioural scenarios, and identify latent patterns inherent in the actions of attackers. As a result of the classification of machine learning methods, the features of each of the approaches were identified in the context of their effectiveness in predicting cyber threats. In particular, supervised learning proved to be suitable for classifying known types of attacks, provided that marked-up data is available, which provides high accuracy, but requires significant resources for preparing datasets. Unsupported learning effectively detects anomalies and new threats in raw data, but may have lower accuracy due to the difficulty of interpreting the results. Deep learning, due to its ability to process complex multidimensional data, has shown high efficiency in detecting hidden and complex threats, in particular, in cases of analysing network traffic or user behavioural patterns.

Analysing previous attacks using machine learning algorithms allows security systems to automatically detect patterns in the actions of cybercriminals. For example, supervised learning models are trained on labelled datasets, where each event is classified as safe or harmful. In the future, these models are used to analyse new data in real time, helping to determine the probability of a threat with high accuracy. Models that work with large sets of network traffic logs, user behavioural logs, security sensor data, etc., were particularly effective. In turn, unsupervised learning methods, in particular, clustering and dimensionality reduction, allow identifying new, previously undetected threats that have no direct analogues in training sets (Iaiani *et al.*, 2021). An important forecasting tool is time series analysis, which is used to identify repetitive patterns in the behaviour of a network or system. The use of such approaches, in particular Arima, Prophet, or recurrent neural networks (RNNs) models, allows predicting periods of increased risk, considering the seasonality of attacks or specific events (for example, large international forums, elections, releases of critical software). In this way, organisations are given the opportunity to take preventive measures in advance, strengthening protection at potentially vulnerable moments.

Special attention should be paid to the concept of threat actor profiling, which is based on the study of characteristic patterns of actions of certain hacker groups or individual attackers. Artificial intelligence analyses attack vectors, penetration methods, typical targets, and tools used to create generalised profiles of attack structures. In the future, such profiles are used to predict future actions of intruders, which allows more accurately configuring attack warning and blocking systems. Systematised forecasting methods, their functional purposes, and examples of practical application in the field of cybersecurity are given in Table 2.

Table 2. *Methods for predicting cyber threats using AI: characteristics and application examples*

Method / algorithm	Type of training	Purpose of the application	Usage examples
Supervised learning	Controlled	Classification of threats based on previous data.	Detection of phishing emails, malicious software.
Unsupervised learning	Uncontrolled	Detection of new threats and anomalies.	Detection of atypical user behaviour on the network.
Time series analysis	Depends on the model	Predicting the frequency of attacks.	Predicting Distributed Denial of Service (DDOS) attacks during peak periods.
Threat profiling (clustering)	Uncontrolled	Defining patterns of activity of hacker groups.	Building attack profiles for Advanced Persistent Threat (APT) groups.
Deep learning (RNN, LSTM)	Deep learning	Behavioural sequence analysis.	Prediction of multi-step attacks in complex systems.

Source: *compiled by the author based on S.S. Dasawat & S. Sharma (2023), R. Kaur et al. (2023)*

The integration of the above methods into integrated cyber defence systems forms a new paradigm, where the key role belongs not only to detecting ex post facto attacks, but also to timely anticipating potential threats. The use of AI in this area provides increased efficiency in detecting complex, hybrid attacks, reducing response time, and improving information security management at the strategic level. Thus, the use of artificial intelligence in predicting cyber threats not only optimises technical processes, but also strengthens the resilience of information systems to future challenges in global cyberspace.

Use of SOAR to quickly respond to cyber-attacks. Modern digital infrastructures are under constant pressure from attackers using increasingly sophisticated attack tools, including sophisticated multi-level intrusions, social engineering, zero-day exploits, and automated botnets. In such conditions, responding to cyber incidents manually loses its effectiveness, as it requires significant time, resources, and highly qualified specialists. This leads to an increasing need for the introduction of SOAR systems – technologies that combine process orchestration, automation of routine actions, and analytical support for responding to security incidents. SOAR platforms perform several key functions. First, they integrate with all elements of enterprise information security: SIEM systems, network traffic monitoring tools, antivirus programmes, cloud services, and threat intelligence sources. Thus, a single incident management point is achieved, which allows quickly responding to threats regardless of their source. Second, SOAR allows automating typical response scenarios. For example, when suspicious activity is detected, the system can automatically block an IP address or user within the corporate network; send a request for verification to the sandbox environment; notify responsible analysts through integrated communication channels; create a ticket in the incident management system and launch an investigation protocol. These actions are performed using built-in playbooks – predefined logical decision chains that can be modified to suit the specifics of the organisation (Li *et al.*, 2023).

A separate role in SOAR systems was played by AI, in particular, machine learning algorithms that are used to prioritise incidents. For example, by analysing the history of attacks, AI can determine that a certain type of traffic has already led to data leaks in the past, and give it a higher level of criticality compared to an inactive threat. AI can also identify false positives, reducing the burden on analysts. An important aspect is the ability to preserve evidence and document actions in SOAR systems. All actions are automatically logged: from the moment the threat is detected until it is completely eliminated. This creates a reliable audit chain that can be used during internal audits or as part of criminal investigations. In practice, the use of SOAR reduces the response time to incidents to several seconds or minutes; increases the level of automation of security processes by up to 80%; reduces the number of false positives due to intelligent analysis; and standardises solutions in accordance with enterprise security policies. In large corporations or government agencies (such as CERT centres), where thousands of security events are recorded daily, SOAR systems (for example, IBM QRadar SOAR, Splunk Phantom, Palo Alto Cortex XSOAR) can reduce the burden on first-level analysts by transmitting only incidents that really require human intervention. The key stages of SOAR systems' automated response to cyber incidents are shown in Figure 1.

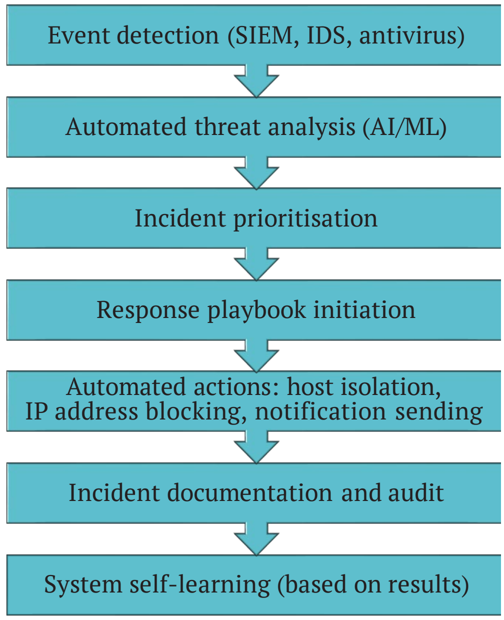

Figure 1. *Key stages of functioning of the SOAR system in the process of responding to cyber incidents*
Source: *compiled by the author based on I.F. Kilincer et al. (2023), R. Kaur et al. (2023)*

Thus, SOAR systems enhanced by AI transform the response to cyber-attacks from a predominantly manual process to a flexible, dynamic, and adaptive security system that can scale according to the level of threats and changes in the cyber environment. In the future, such systems will form the basis of the so-called smart cybersecurity, based on machine analysis, autonomous solutions, and a high degree of self-learning.

Cybersecurity automation risks: Ways for attackers to bypass protection using algorithms. Automation of cyber defence, in particular through the use of AI algorithms, plays a key role in strengthening the effectiveness of security systems against the background of increasing intensity of cyber threats. However, the use of automated security mechanisms introduces a number of risks, including those related to the vulnerability of the algorithms themselves, which are used for both defence and attack. This creates a technological symmetry in which attackers can use the same principles that are used to provide protection to circumvent them or undermine their effectiveness. One of the main problems is the application of adversarial machine learning, which involves targeted modification of input data, which allows attackers to mislead automated detection systems. As a result, adversarial examples are created, which, although they do not look different from normal data, actually carry a hidden threat. Such attack methods allow attackers to manipulate the results of AI algorithms, bypassing security systems, which significantly reduces the effectiveness of conventional methods of detecting threats. They distort behavioural signals, making them impossible to properly interpret within anomaly detection systems.

An important aspect is malware self-learning, which is based on machine learning algorithms that can adapt to changes in the environment and evolve in response to new challenges. In particular, polymorphic viruses can change their signatures as they spread, which allows them to avoid detection by antivirus programmes based on signature analysis. This adaptability makes it difficult to detect malware and significantly increases their ability to avoid conventional cyber defences. In addition, the use of behavioural spoofing allows malware to simulate normal activity, which further complicates the operation of systems based on the analysis of behavioural anomalies. The danger of automated systems also lies in the imperfection of autonomous decisions that are made without human intervention. Despite the potential of automation to ensure prompt response, such systems can lead to false positives that have disastrous consequences for the organisational infrastructure. Excessive aggressiveness of automated mechanisms can lead to blocking legitimate user activity that disrupts the normal activities of organisations, or to missing new threats that were not considered in the system training process. The problem is that many automated systems are unable to adapt to new, unforeseen scenarios, making them vulnerable to evolutionary threats (Alamro *et al.*, 2023).

In addition, algorithms used in cybersecurity systems can become targets of attacks at the training stage, including data poisoning. Attackers, knowing the structure of models, can intentionally enter corrupt or erroneous data at the training stage, which leads to a violation of their ability to correctly interpret information in a real environment. This can have negative consequences for the accuracy of systems, especially at the stages of detecting new or unknown threats, when erroneous training leads to incorrect response to real cyber threats. Table 3 provided a brief overview of the key risks associated with cybersecurity automation, and potential ways to reduce them.

Table 3. *Main risks of cyber defence automation and ways to minimise them*

Type of risk	Essence of the problem	Possible counteraction measures
Reverse machine learning	Deception of AI algorithms using specially prepared input data.	Use of secure models, anomaly detection, regular testing.
Polymorphic malware	Automatic signature change to avoid detection.	Behavioural analysis, combining signature and heuristic approaches.
Excessive system autonomy	Erroneous actions of an automated system without human intervention.	Implementation of manual confirmation for critical actions.
Process disruption due to an error	Automatic blocking of legitimate activity due to false positives.	Multi-level monitoring, hybrid response scenarios.
Data poisoning	Impact on the learning process to distort future decisions.	Verification of data sources, filtering abnormal samples, and monitoring models.

Source: *compiled by the author based on L.F. Sikos (2023)*

As a result, although automation in cyber defence offers significant progress in the speed and efficiency of incident response, its use is accompanied by numerous risks that require careful monitoring and continuous improvement of protection mechanisms. The use of artificial intelligence, combined with flexible security approaches that include the human factor, remains critical to ensuring a reliable and sustainable response to modern cyber threats.

Functions of artificial intelligence in cybersecurity. In the context of the rapid evolution of cyber threats and high requirements for the effectiveness of information system protection, the role of AI in the field of cybersecurity is becoming increasingly important. Advanced technologies allow artificial intelligence to perform functions that previously required significant human resources, and have significant potential to improve the effectiveness of security systems. However, there is a question whether AI can completely replace the human factor, or whether it remains only an auxiliary tool at the disposal of cybersecurity specialists. In this context, it is important to consider the role of AI in automating cybersecurity, its potential to replace humans in threat detection and response processes, and the limitations and challenges that arise from its use Artificial intelligence offers a number of opportunities to automate routine and complex cybersecurity processes, significantly reducing the need for human intervention at the stages of detecting and responding to threats. Machine learning-based systems, such as neural networks, can automatically detect anomalies in user behaviour and network traffic by analysing huge amounts of data in real time. They are able to detect potential threats much faster than humans, which is a critical factor for timely neutralisation of attacks, especially in the case of DDoS or APT attacks. The use of SIEM systems with AI integration allows automating the processes of collecting, analysing, and correlating data from various security sources (network devices, servers, databases). With the help of such technologies, AI can not only detect familiar threats, but also identify new attack patterns that may indicate complex intrusion methods used by attackers. This allows security systems to respond in real time, which is directly important for preventing or minimising damage from attacks. Based on the ability to automatically block suspicious actions, such as unauthorised access attempts or configuration changes, AI-based systems can quickly take countermeasures without human intervention. This allows significantly reducing the response time to incidents, which is important for successful protection of critical infrastructures, where every minute matters (Sharma *et al.*, 2024).

However, despite the power of AI, full automation of cybersecurity is unlikely. AI, even with all its advances in machine learning and data analysis, has significant limitations, especially when it comes to new, unknown, or extremely complex threats. For example, detecting APT attacks or complex phishing attacks using multiphase social engineering techniques requires deep strategic thinking and contextual analysis, which is not always available to automated systems. Cybersecurity professionals can interpret signals coming from systems based on their experience and knowledge of new threats that are not obvious to algorithms. They can consider the context of the event, its priority, and interaction with other incidents, which allows them to make more informed decisions about further actions. In addition, human expertise is needed to adapt and customise AI models, as algorithms require regular training on new data and adjustments to meet changes in the threat environment. It should also be noted that the ethical and legal aspects of using AI in cybersecurity can be important to ensure compliance with national and international security and privacy standards. The human factor is important for developing risk management strategies and ensuring compliance with legal requirements (Kaur *et al.*, 2023).

The most effective approach to cybersecurity is to combine the capabilities of artificial intelligence and human expertise. AI can be used to automate routine tasks such as network monitoring, detecting standard threats, analysing huge amounts of data, and responding to threats in real time. This frees cybersecurity professionals from the need to perform low-level operations, which increases their effectiveness and allows them to focus on more complex tasks, such as developing security strategies, evaluating new vulnerabilities, or analysing new types of attacks. In particular, due to the use of AI, it is possible to significantly reduce the response time to incidents, increase the accuracy of threat detection, and provide more flexible adaptation of security systems to new conditions. However, decisions that require deep strategic analysis should remain in the hands of specialists who can assess the interaction of attacks with other elements of the system, and anticipate possible consequences for the organisation as a whole. Artificial intelligence is an essential tool in modern cybersecurity, allowing automating a number of critical processes, such as threat detection, incident response, and data analysis. However, it cannot completely replace the human factor, because successful detection of complex, unknown, or multiphase attacks requires human intuition, strategic thinking, and the ability to assess the context of events. Therefore, the best approach is to integrate AI into the cybersecurity system, where it acts as a powerful auxiliary tool for specialists, reducing their workload and ensuring a faster and more effective response to threats.

Discussion

An analysis of the literature on the use of AI in cybersecurity has demonstrated various approaches to solving problems of protecting information systems and infrastructures. The study conducted by A. Mohammed (2023) examined the AI paradox in cybersecurity, emphasising that artificial intelligence can act as both a powerful defender and a potential tool for exploiting cyber threats. The researcher focused on the fact that although AI can improve the response to attacks due to the ability to quickly analyse large amounts of data, attackers can also use these technologies to bypass security systems. These results are consistent with current results that highlight the importance of balancing the use of technologies for protection and the risks associated with their possible abuse.

The study by N.P.O. Shoetan *et al.* (2024) presented a conceptual model of the impact of AI on cybersecurity in the telecommunications sector. The researchers stressed that the introduction of AI significantly improves the ability of systems to detect threats, predict attacks, and reduce response time. These results are consistent with data from the current study, which also points to the positive effect of automation and intelligence in the field of cyber defence. The current study looked more broadly at automation as a tool not only for telecommunications security, but also for critical infrastructure in general. W.S. Admass *et al.* (2023) provided an overview of the current state of cybersecurity, the main challenges and areas of its development. The researchers highlighted the complexity of attacks, the lack of qualified personnel, and the limitations of AI adaptation. These findings are partially consistent with current results, especially with regard to the problem of personnel and the importance of automation as a compensatory mechanism in the face of a shortage of specialists. The study added to this the emphasis on reducing the human factor through the introduction of automated tools, which allowed increasing the effectiveness of real-time protection.

V. Švábenský *et al.* (2023) investigated automated feedback in cybersecurity training programmes. Although the researchers focused on the educational field, their findings coincided with the results of the present study, focusing on the use of automated systems to improve the quality of response to incidents. The research reflected a similar idea in the context of production and corporate environments, where training and automation of threat detection processes were critical. S. Vyas *et al.* (2023) proposed a generalised review of automated cyber defence systems, in particular, they analysed technologies that provide early detection of attacks and automatic response. Their findings were fully consistent with the current study, especially in terms of the role of AI in reducing the burden on security analysts, improving response speed, and reducing error rates. N.A. Folorunso *et al.* (2024) focused on the impact of AI on security compliance. They noted that AI-based systems can help not only detect violations, but also ensure compliance with regulations through constant monitoring. This provision correlates with current results, which emphasised that automated systems can maintain a high level of compliance with safety standards through continuous monitoring and flexible response. In this context, S. Ahmadov (2024) emphasised that encryption remains a core tool for securing personal data in cloud environments. The study highlighted the role of effective key management and compliance with data protection laws, reinforcing the importance of a multi-layered approach to cybersecurity.

The study by J. Xu *et al.* (2024) introduced Autoattacker system, which used the capabilities of large language models to automate cyber-attacks. The researchers demonstrated the potential of the Large Language Models (LLM) not only as a security tool, but also as a threat that requires a new level of caution in implementing AI in cybersecurity systems. These findings were consistent with the current study, which also highlighted the twofold nature of AI use – both for protection and as a potential threat in the hands of attackers. This study, however, focused more on the protective aspect and suggested approaches to minimising risks. In turn, the review by J.P. Bharadiya (2023) focused on the future of cybersecurity in the context of Web 3.0, emphasising the role of machine learning in shaping safer digital environments. The researcher noted that machine learning can increase the adaptability of cyber defence systems. The present results also indicated the ability of machine learning systems to quickly learn from new threats and adapt real-time protection methods, which confirmed the relevance of the approaches proposed by J.P. Bharadiya.

N.U. Prince *et al.* (2024) investigated data-driven methods in AI cybersecurity that can improve the accuracy and speed of attack detection. Their emphasised on processing large amounts of data and using predictive analytics directly echoed current approaches, which also emphasised the role of large-scale data processing in creating adaptive protection. F. Mahmud *et al.* (2025) examined the use of AI in IT project management with a focus on threat detection and risk reduction. Their findings demonstrated the effectiveness of AI integration at the planning and risk assessment stages, which was also important for the current study, as it also demonstrated that proactive AI-based risk assessment can reduce the impact of incidents on critical systems. A. Shahana *et al.* (2024) in their paper focused on the balance between implementing AI in cybersecurity and providing safeguards to avoid abuse and technical vulnerabilities. The researchers emphasised the risks of full automation of protection and the need for human control. Similar to the current results, the researchers recognised that an effective system should be hybrid – a combination of AI and the human factor. It was also noted that excessive automation without ethical and legal barriers can lead to threats. In turn, N.A.O. Adewusi *et al.* (2022) considered the specific use of AI for cyber defence in the agricultural sector – "smart farms". AI has been shown to automatically detect threats in Internet of Things (IoT) infrastructures. This study had a broader application, but it also focused on the vulnerability of IoT systems. N.A.O. Adewusi *et al.* supplemented the current study with examples from a specific sector. M. Rizvi (2023) demonstrated the benefits of AI in real-time threat detection, especially through continuous learning and behaviour pattern analysis. The current study also highlighted the adaptability of AI systems that can identify anomalies even before they escalate into full-fledged attacks. The findings of M. Rizvi were fully consistent with these observations.

A.B. Pandey *et al.* (2022) conducted a comprehensive review of general cybersecurity trends, including AI applications, new attack vectors, and security concepts. The current study also highlighted certain trends: the development of threats, the role of artificial intelligence, and a paradigm shift in security. Y. Yigit *et al.* (2024) considered the use of generative AI in cybersecurity – both in defensive and attacking aspects (deepfake, deception of recognition systems, etc.). This was a significant addition to the analysis, which considered AI in a classical context, but generative models created a new level of challenges that deserves further inclusion in this discussion. M. Elsisi & M. Tran (2021) described an IoT architecture that uses deep neural networks to protect automated transport systems from cyber-attacks. The research of scientists is more general, but at the same time it demonstrates the successful application of DNN in real-world cyber-physical systems, which confirms current assumptions about the effectiveness of deep learning in defensive scenarios.

Thus, comparison with other papers showed that the study is consistent with global trends in the investigation of the role of AI in the automation of cyber defence, while contributing to the understanding of how these approaches can be adapted to different sectors and infrastructures. Unlike many reviewed works, it places stronger emphasis on the integration of adaptive mechanisms and blockchain technologies to enhance transparency and resilience. The study also highlights the importance of balancing automation with human oversight, which is crucial for maintaining ethical and secure AI deployment in cybersecurity.

Conclusions

As part of the study of the use of neural networks, SIEM systems, and automated firewalls, it was found that the integration of deep learning significantly increases the accuracy of detecting complex and unknown threats, but simultaneously creates new challenges for controlling algorithms. In the section on methods for predicting cyber threats, it was found out that the most effective systems are those that use historical attack patterns in combination with adaptive algorithms – such approaches allow predicting potential threat vectors with high reliability. SOAR analysis has demonstrated their ability to reduce incident response time to a few seconds, but effectiveness remains dependent on the quality of the initial data and the correct configuration of scenarios. The section on automation risks showed that attackers are already experimenting with using generative models to bypass security and create adaptive malware that requires constant updating of security systems. Ultimately, in the debate about whether AI can replace the human factor, it is concluded that at the moment it is not a replacement, but a symbiosis: artificial intelligence is effective in repetitive tasks and processing large amounts of data, but critical thinking, ethics, and strategic decisions are left to humans. Recommendations for improving the effectiveness of automated cyber defence systems consist in combining AI technologies with the human factor, which will increase the accuracy of threat detection and the effectiveness of responding to them. The key is to improve prediction algorithms to more accurately identify new types of attacks, and develop systems that can detect and neutralise complex threats, including those that use AI to bypass existing defences. Attention should be paid to the ethical and legal aspects of using AI in cybersecurity, which would ensure the safe and responsible use of technologies. Areas for further research include the development of autonomous security systems that can respond independently to new threats, and the creation of security models for new technologies such as IoT and 5G. Investigation of the interaction of AI with other innovative technologies, in particular, blockchain and quantum computing, can lead to more sustainable security systems. It is also important to study adaptive systems that can dynamically adjust their strategies to suit new types of attacks and analyse hybrid attacks that combine cybernetic and physical elements.

Acknowledgements

None.

Funding

None.

Conflict of Interest

None.

References

[1] Adewusi, N.A.O., Chiekezie, N.N.R., & Eyo-Udo, N.N.L. (2022). The role of AI in enhancing cybersecurity for smart farms. *World Journal of Advanced Research and Reviews*, 15(3), 501-512. doi: 10.30574/wjarr.2022.15.3.0889.

[2] Admass, W.S., Munaye, Y.Y., & Diro, A.A. (2023). Cyber security: State of the art, challenges and future directions. *Cyber Security and Applications*, 2, article number 100031. doi: 10.1016/j.csa.2023.100031.

[3] Aghaei, E., Niu, X., Shadid, W., & Al-Shaer, E. (2022). Securebert: A domain-specific language model for cybersecurity. In F. Li, K. Liang, Z. Lin & S.K. Katsikas (Eds.), *Proceedings of the 18th EAI international conference "Security and privacy in communication networks"* (pp. 39-56). Cham: Springer. doi: 10.1007/978-3-031-25538-0_3.

[4] Ahmadov, S. (2024). Data encryption as a method of protecting personal data in a cloud environment. *Bulletin of Cherkasy State Technological University*, 29(3), 31-41. doi: 10.62660/bcstu/3.2024.31.

[5] Alamro, H., Mtouaa, W., Aljameel, S., Salama, A.S., Hamza, M.A., & Othman, A.Y. (2023). Automated Android malware detection using optimal ensemble learning approach for cybersecurity. *IEEE Access*, 11, 72509-72517. doi: 10.1109/access.2023.3294263.

[6] Bharadiya, J.P. (2023). AI-driven security: How machine learning will shape the future of cybersecurity and web 3.0. *American Journal of Neural Networks and Applications*, 9(1), 1-7. doi: 10.11648/j.ajnna.20230901.11.

[7] Dasawat, S.S., & Sharma, S. (2023). Cyber security integration with smart new age sustainable startup business, risk management, automation and scaling system for entrepreneurs: An artificial intelligence approach. In *2023 7th international conference on intelligent computing and control systems (ICICCS)* (pp. 1357-1363). Madurai: Institute of Electrical and Electronics Engineers. doi: 10.1109/ICICCS56967.2023.10142779.

[8] Elsisi, M., & Tran, M. (2021). Development of an IoT architecture based on a deep neural network against cyber attacks for automated guided vehicles. *Sensors*, 21(24), article number 8467. doi: 10.3390/s21248467.

[9] Folorunso, N.A., Adewumi, N.T., Adewa, N.A., Okonkwo, N.R., & Olawumi, N.T.N. (2024). Impact of AI on cybersecurity and security compliance. *Global Journal of Engineering and Technology Advances*, 21(1), 167-184. doi: 10.30574/gjeta.2024.21.1.0193.

[10] Iaiani, M., Tugnoli, A., Bonvicini, S., & Cozzani, V. (2021). Analysis of cybersecurity-related incidents in the process industry. *Reliability Engineering & System Safety*, 209, article number 107485. doi: 10.1016/j.ress.2021.107485.

[11] Kaur, R., Gabrijelčič, D., & Klobučar, T. (2023). Artificial intelligence for cybersecurity: Literature review and future research directions. *Information Fusion*, 97, article number 101804. doi: 10.1016/j.inffus.2023.101804.

[12] Khan, M.I., Arif, A., & Khan, A.R.A. (2024). The most recent advances and uses of AI in cybersecurity. *BULLET: Journal of Multidisciplinary Science*, 3(4), 566-578.

[13] Kilincer, I.F., Ertam, F., Sengur, A., Tan, R., & Acharya, U.R. (2023). Automated detection of cybersecurity attacks in healthcare systems with recursive feature elimination and multilayer perceptron optimization. *Journal of Applied Biomedicine*, 43(1), 30-41. doi: 10.1016/j.bbe.2022.11.005.

[14] Kotlyarov, O.Yu., & Bortnik, L.L. (2024). Comparative analysis of modern virtual network protection systems and their methodologies. *Modern Information Security*, 4(60), 60-72. doi: 10.31673/2409-7292.2024.040007.

[15] Li, G., Ren, L., Fu, Y., Yang, Z., Adetola, V., Wen, J., Zhu, Q., Wu, T., Candan, K., & O'Neill, Z. (2023). A critical review of cyber-physical security for building automation systems. *Annual Reviews in Control*, 55, 237-254. doi: 10.1016/j.arcontrol.2023.02.004.

[16] Lysenko, S., Bobro, N., Korsunova, K., Vasylchyshyn, O., & Tatarchenko, Y. (2024). The role of artificial intelligence in cybersecurity: Automation of protection and detection of threats. *Economic Affairs*, 69, 43-51. doi: 10.46852/0424-2513.1.2024.6.

[17] Mahmud, F., Barikdar, C.R., Hassan, J., Goffer, M.A., Das, N., Orthi, S.M., Kaur, J., Hasan, S.N., & Hasan, R. (2025). AI-driven cybersecurity in IT project management: Enhancing threat detection and risk mitigation. *Journal of Posthumanism*, 5(4), 23-44. doi: 10.63332/joph.v5i4.974.
[18] Mohammed, A. (2023). The paradox of AI in cybersecurity: Protector and potential exploiter. *Baltic Journal of Engineering and Technology*, 2(1), 70-76.
[19] Mykhalchenko, G.G., Snitko, Y.M., & Ivanenko, V.O. (2023). Cyber security in the economy: Protection against cyber threats in a digitalized world. *Scientific Notes of Lviv University of Business and Law*, 38, 377-384.
[20] Pandey, A.B., Tripathi, A., & Vashist, P.C. (2022). A survey of cyber security trends, emerging technologies and threats. In R. Agrawal, J. He, E. Shubhakar Pilli & S. Kumar (Eds.), *Cyber security in intelligent computing and communications* (pp. 19-33). Singapore: Springer. doi: 10.1007/978-981-16-8012-0_2.
[21] Prince, N.U., Faheem, M.A., Khan, O.U., Hossain, K., Alkhayyat, A., Hamdache, A., & Elmouki, I. (2024). AI-powered data-driven cybersecurity techniques: Boosting threat identification and reaction. *Nanotechnology Perceptions*, 20(S10), 332-353. doi: 10.62441/nano-ntp.v20is10.25.
[22] Rizvi, M. (2023). Enhancing cybersecurity: The power of artificial intelligence in threat detection and prevention. *International Journal of Advanced Engineering Research and Science*, 10(5), 55-60. doi: 10.22161/ijaers.105.8.
[23] Shahana, A., Hasan, R., Farabi, S.F., Akter, J., Mahmud, M.A.A., Johora, F.T., & Suzer, G. (2024). AI-driven cybersecurity: Balancing advancements and safeguards. *Journal of Computer Science and Technology Studies*, 6(2), 76-85. doi: 10.32996/jcsts.2024.6.2.9.
[24] Sharma, S., Dutta, N., & Vegesna, V.V. (2024). *Examining ChatGPT's and other models' potential to improve the security environment using generative AI for cybersecurity*. doi: 10.15680/IJMRSET.2024.0709031.
[25] Shoetan, N.P.O., Amoo, N.O.O., Okafor, N.E.S., & Olorunfemi, N.O.L. (2024). Synthesizing AI's impact on cybersecurity in telecommunications: A conceptual framework. *Computer Science & IT Research Journal*, 5(3), 594-605. doi: 10.51594/csitrj.v5i3.908.
[26] Sikos, L.F. (2023). Cybersecurity knowledge graphs. *Knowledge and Information Systems*, 65, 3511-3531. doi: 10.1007/s10115-023-01860-3.
[27] Sontan, N.A.D., & Samuel, N.S.V. (2024). The intersection of artificial intelligence and cybersecurity: Challenges and opportunities. *World Journal of Advanced Research and Reviews*, 21(2), 1720-1736. doi: 10.30574/wjarr.2024.21.2.0607.
[28] Sundaramurthy, S.K., Ravichandran, N., Inaganti, A.C., & Muppalaneni, R. (2022). The future of enterprise automation: Integrating AI in cybersecurity, cloud operations, and workforce analytics. *Artificial Intelligence and Machine Learning Review*, 3(2), 1-15.
[29] Švábenský, V., Vykopal, J., Čeleda, P., & Dovjak, J. (2023). Automated feedback for participants of hands-on cybersecurity training. *Education and Information Technologies*, 29, 11555-11584. doi: 10.1007/s10639-023-12265-8.
[30] Tonhauser, M., & Ristvej, J. (2023). Cybersecurity automation in countering cyberattacks. *Transportation Research Procedia*, 74, 1360-1365. doi: 10.1016/j.trpro.2023.11.283.
[31] Varga, S., Sommestad, T., & Brynielsson, J. (2022). Automation of cybersecurity work. In T. Sipola, T. Kokkonen & M. Karjalainen (Eds.), *Artificial intelligence and cybersecurity: Theory and applications* (pp. 67-101). Cham: Springer. doi: 10.1007/978-3-031-15030-2_4.
[32] Vyas, S., Hannay, J., Bolton, A., & Burnap, P.P. (2023). *Automated cyber defence: A review*. doi: 10.48550/arXiv.2303.04926.
[33] Xu, J., Stokes, J.W., McDonald, G., Bai, X., Marshall, D., Wang, S., Swaminathan, A., & Li, Z. (2024). *AutoAttacker: A large language model guided system to implement automatic cyber-attacks*. doi: 10.48550/arXiv.2403.01038.
[34] Yaseen, A. (2024). Enhancing cybersecurity through automated infrastructure management: A comprehensive study on optimizing security measures. *Quarterly Journal of Emerging Technologies and Innovations*, 9(1), 38-60.
[35] Yigit, Y., Buchanan, W.J., Tehrani, M.G., & Maglaras, L. (2024). *Review of generative AI methods in cybersecurity*. doi: 10.48550/arXiv.2403.08701.

Автоматизація кіберзахисту: чи може ШІ випередити хакерів?

Віталій Ясененко
Магістр, старший розробник програмного забезпечення
TP-Link
92618, вул. Технологій, 36, м. Ірвайн, США
https://orcid.org/0009-0004-4801-9541

Анотація. Зростаючі кіберзагрози в умовах цифрової трансформації вимагають вдосконалення методів автоматизації кіберзахисту, зокрема через використання штучного інтелекту для виявлення і реагування на атаки. Метою дослідження була оцінка потенціалу штучного інтелекту у сфері автоматизації кіберзахисту, а також визначення його ефективності в протидії сучасним кібератакам. Дослідження базувалось на методах порівняльного аналізу, системного підходу та прогнозування кіберзагроз за допомогою штучного інтелекту. Вперше комплексно розглянуто ефективність застосування штучного інтелекту в автоматизованих системах кіберзахисту з урахуванням поточних викликів цифрового середовища. Представлено аналітичний огляд можливостей штучного інтелекту у виявленні та прогнозуванні кіберзагроз за допомогою нейромереж, систем управління інформацією та подіями безпеки і алгоритмів машинного навчання. Визначено потенціал і обмеження систем автоматизованого реагування, а також окреслено ризики, пов'язані з можливістю використання штучного інтелекту самими зловмисниками. Особливу увагу приділено аналізу ролі людського фактора у взаємодії з автоматизованими системами – показано, що повна автоматизація не гарантує безпеку без критичної участі спеціалістів. На основі порівняльного та прогностичного аналізу запропоновано практичні підходи до збалансованого впровадження штучного інтелекту в системи кіберзахисту. Доведено, що штучний інтелект може бути потужним інструментом для автоматизації кіберзахисту, проте для забезпечення високого рівня безпеки необхідно враховувати потенційні ризики та постійно вдосконалювати системи. Практичне значення дослідження полягає в розробці рекомендацій для впровадження ефективних технологій захисту в різних секторах кібербезпеки

Ключові слова: цифрова безпека; машинне навчання; інжиніринг; медіаграмотність; цифрова загроза

ТЕХНОЛОГІЇ
ТА ІНЖИНІРИНГ

Науковий журнал

Том 26, № 3, 2025

Оригінал-макет видання виготовлено
у редакційно-видавничому відділі Київського національного університету технологій та дизайну

Відповідальний редактор:
О. Кривонос

Підписано до друку 25.06.2025 р. Формат 60*84/8
Умовн. друк. арк. 11,8
Наклад 100 примірників

Адреса видавництва:
Київський національний університет технологій та дизайну
01011, вул. Мала Шияновська, 2, м. Київ, Україна
тел/факс: +38 (044) 256-84-27
E-mail: info@technologies-engineering.com.ua
https://technologies-engineering.com.ua/uk

**TECHNOLOGIES
AND ENGINEERING**

Scientific Journal

Vol. 26, No. 3, 2025

The original layout of the publication is made
in the publishing department of Kyiv National University of Technologies and Design

Managing editor:
O. Kryvonos

Signed for print 25.06.2025. Format 60*84/8
Conventional printed pages 11.8
Circulation 100 copies

Publishing Address:
Kyiv National University of Technologies and Design
01011, 2 Mala Shyianovska Str., Kyiv, Ukraine
tel/fax: +38 (044) 256-84-27
E-mail: info@technologies-engineering.com.ua
https://technologies-engineering.com.ua/en